NASA
Contractor Report 195305

Army Research Laboratory
Contractor Report ARL–CR–146

Prediction of Contact Path and Load Sharing in Spiral Bevel Gears

George D. Bibel
University of North Dakota
Grand Forks, North Dakota

Karuna Tiku and Ashok Kumar
University of Akron
Akron, Ohio

April 1994

Prepared for
Lewis Research Center
Under Grant NAG3-1476

National Aeronautics and
Space Administration

U.S. ARMY
RESEARCH LABORATORY

TABLE OF CONTENTS

LIST OF FIGURES

ABSTRACT

A procedure is presented to perform a contact analysis of spiral bevel gears in order to predict the contact path and the load sharing as the gears roll through mesh. The approach utilizes recent advances in automated contact methods for nonlinear finite element analysis. A sector of the pinion and gear is modeled consisting of three pinion teeth and four gear teeth in mesh. Calculation of the contact force and stresses through the gear meshing cycle are demonstrated. Summary of the results are presented using 3-dimensional plots and tables. Issues relating to solution convergence and requirements for running large finite element analysis on a supercomputer are discussed.

CHAPTER I

INTRODUCTION

Spiral bevel gears are important elements for transmitting power between intersecting shafts. They are commonly used in applications that require high load capacity at high operating speeds. One such application is in helicopter transmission systems. Aircraft designers are continually required to improve performance. Reduced weight, size, and cost with increased power, efficiency, and reliability are constantly being sought.

Prior research has focussed on various aspects of spiral bevel gear operation. Much has been done on spiral bevel gear geometry to reduce noise and vibration, kinematic error, improve manufacturability, and inspection. Stress analysis is another important area of ongoing research. Accurate prediction of contact stresses and tooth root/fillet stresses are important to increase reliability and reduce weight.

Much effort has focussed on predicting stresses in gears with the finite element method. Most of this work has involved parallel axis gears with two dimensional models. Only a few researchers have investigated finite element analysis of spiral bevel gears (ref. 1-4). In reference 4, finite element analysis was done on a single spiral bevel gear tooth using an assumed contact stress distribution. In that model, contact stresses were not evaluated.

For parallel axis gears, a closed form solution exists which determines the surface coordinates of a tooth. This is then used as input to finite element methods. For spiral bevel gears there is no closed form solution. Therefore, the kinematics of the cutting or grinding machinery is utilized to numerically describe the surface coordinates of the gear tooth.

The research reported herein is based on the extension of work presented in references 4-7. A model that has three pinion teeth and four gear teeth has been developed based on gear manufacturing kinematics for a single tooth on each the pinion and the gear.

The objective of this research is to study the contact path and load sharing in these gears when contact occurs on multiple teeth in mesh. This is done by performing a static analysis at different incremental rotations. A nonlinear approach is required due to large displacements associated with gear rotation and nonlinear boundary conditions associated with the gear tooth surface contact. Also evaluated are the contact stresses and fillet stresses.

CHAPTER II

GEAR SURFACE GEOMETRY

Briefly described in this chapter are the gear manufacturing process, the kinematics of the manufacturing process, tooth surface coordinates solution technique, surface rotations of the gear and pinion, and different orientations required for the spiral bevel gears to mesh with each other.

2.1 Gear Manufacture

Machinery for the manufacture of spiral bevel gears is provided by the Gleason Works, Rochester, NY. These machines are preferred over gear hobbing machines because they can be used for both milling and grinding operations. Grinding is important in producing hardened high quality aircraft gears.

This machine consists mainly of three parts: the machine frame, the cradle, and the sliding base (ref. 8). The cradle with the head cutter mounted on it, slowly rotates about its axis, as does the gear which is being cut. During this motion the gear surface is generated. As the cutter disengages from the workpiece, the cradle reverses rapidly and the sliding base translates with respect to the cutter to index the workpiece for the next cutting cycle. This sequence is repeated until the last tooth is cut.

The head cutter is mounted on the cradle with an offset from the cradle center. This allows adjustment of the axial distance between the cutter center and the machine center. The adjustment of the angular position between the two axes provides the desired spiral angle. The shape of the blades of the head cutter are typically straight lines that rotate about their own axis at a speed for efficient metal removal. The rotational speed of the cutting head is independent of the cradle or workpiece rotations (ref. 9).

The pinion is typically cut one side at a time, whereas the gear is cut both sides simultaneously. Spiral bevel gears can be either left or right handed. In a left handed spiral bevel gear, the tooth spirals to the left while looking from the apex of cone towards the gear. Whereas, for a right handed spiral bevel gear the tooth spirals to the right.

2.2 Tooth Surface Coordinate Equations

The system of equations, required to define the coordinates of spiral bevel gear tooth surfaces, were derived in reference 4, and are briefly summarized here.

The first equation is the equation of meshing. This equation is based on the kinematics of manufacture and the machine tool settings. The equation of meshing requires that the relative velocity between a point on the cutting surface and the same point on the pinion being cut must be perpendicular to the cutting surface normal (ref. 9).

$$\mathbf{n} \cdot \mathbf{V} = 0$$

where, **n** is the normal vector from the cutter surface and

V is the relative velocity between the cutter and the workpiece surfaces at the specified location.

This equation is developed in terms of machine tool coordinates U, Θ and ϕ_c

$$r_c = \begin{bmatrix} r\cot\psi - U\cos\psi \\ U\sin\psi\sin\theta \\ U\sin\psi\cos\theta \\ 1 \end{bmatrix} \qquad (1)$$

where, U is the generating cone surface coordinate used to locate a point along the length of the cutting head

Θ is the generating cone surface coordinate used for rotational orientation of a point on the cutting head

ϕ_c is the rotated orientation of the cutter as it swings on the cradle

r is the radius of the generating cone surface and is described by the following

equations (ref. 4):

Since the kinematic motion of cutting a gear is equivalent to the cutting head meshing with a simulated crown gear, an equation of meshing can be written in terms of a point on the cutting head i.e in terms of U, Θ and ϕ_c. The equation of meshing for straight sided cutters with a constant ratio of roll between the cutter and the workpiece is given by (ref. 1):

$$\begin{aligned}&(U - r\cot\psi\cos\psi)\cos\gamma\sin\tau\\&+ S(m_{cw} - \sin\gamma)\cos\psi\sin\theta\\&\mp \cos\gamma\sin\gamma\sin(q - \phi_c)\\&\pm E_m(\cos\gamma\sin\gamma + \sin\gamma\cos\gamma\cos\tau)\\&- L_m\sin\gamma\cos\psi\sin\tau = 0\end{aligned} \qquad (2)$$

The upper and lower signs are for left and right hand gears respectively. The following machine tool settings are defined:

τ		$(\Theta \mp q \pm \phi_c)$
q		cradle angle
γ		root angle of workpiece
E_m		machining offset
L_m		vector sum of change of machine center to back and the sliding base
m_{cw}	=	ϕ_c/ϕ_w, the relationship between the cradle and the workpiece for a constant ratio of roll
U		generating cone surface coordinate
S		radial location of cutting head in coordinate system S_m
r		radius of generating cone surface

Equation (2) is equivalent to: $$f_1(U, \theta, \phi_c) = 0 \qquad (3)$$

Because there are three unknowns U, Θ, and ϕ_c; three equations must be developed to solve for the surface coordinates of a spiral bevel gear. The three parameters U, Θ and ϕ_c are defined relative to the cutting head and cradle coordinate systems (S_c and S_s) respectively. These parameters can be transformed through a series of coordinate transformations to a coordinate system attached to the workpiece. Or U, Θ and ϕ_c can be mapped into X_w, Y_w, Z_w

in coordinate system S_w attached to the workpiece. These transformations, used in conjunction with two other geometric requirements, give the two additional equations.

The correct U, Θ and ϕ_c that solves the equation of meshing, must also, upon transformation to the workpiece coordinate system S_w, result in a axial coordinate Z_w that matches with the value of Z found by the projection of the tooth in the XY plane.

$$Z_w - Z = 0 \tag{4}$$

This equation along with the correct coordinate transformations (see Equation 11) result in a second equation of the form:

$$f_2(U, \theta, \phi_c) = 0 \tag{5}$$

A similar requirement for the radial location of a point on the workpiece results in the following:

$$r - \sqrt{(X_w^2 + Y_w^2)} = 0 \tag{6}$$

This is shown in figure 2.1. The appropriate coordinate transformations (see Equation 11) will convert equation 6 into a function of U, Θ and ϕ_c

$$f_3(U, \theta, \phi_c) = 0 \tag{7}$$

Equations (3), (5), (7) form a system of nonlinear equations necessary to define a point on the tooth surface.

2.3 Solution Technique

The three equations discussed earlier to describe the tooth surface coordinates are nonlinear and do not have a closed form solution. They are solved using Newton's method (ref. 10).

An initial guess U_0, Θ_0, ϕ_{c0} is used to the start iterative solution procedure. Newton's method is used to determine subsequent values of the updated vector (U_k, Θ_k, ϕ_{ck}).

$$\begin{bmatrix} U_k \\ \theta_k \\ \phi_k \end{bmatrix} = \begin{bmatrix} U_{k-1} \\ \theta_{k-1} \\ \phi_{k-1} \end{bmatrix} + \begin{bmatrix} Y^1_{k-1} \\ Y^1_{k-1} \\ Y^1_{k-1} \end{bmatrix} \tag{8}$$

where the vector Y is the solution of:

$$\begin{bmatrix} \dfrac{\partial f_1(U^{k-1})}{\partial U} & \dfrac{\partial f_1(\theta^{k-1})}{\partial \theta} & \dfrac{\partial f_2(\theta_c^{k-1})}{\partial \phi_c} \\ \dfrac{\partial f_2(U^{k-1})}{\partial U} & \dfrac{\partial f_2(\theta^{k-1})}{\partial \theta} & \dfrac{\partial f_2(\theta_c^{k-1})}{\partial \phi_c} \\ \dfrac{\partial f_3(U^{k-1})}{\partial U} & \dfrac{\partial f_3(\theta^{k-1})}{\partial \theta} & \dfrac{\partial f_3(\theta_c^{k-1})}{\partial \phi_c} \end{bmatrix} \cdot \begin{Bmatrix} Y_1^{k-1} \\ Y_2^{k-1} \\ Y_3^{k-1} \end{Bmatrix} = \begin{Bmatrix} f_1(U^{k-1}, \theta^{k-1}, \phi_c^{k-1}) \\ f_2(U^{k-1}, \theta^{k-1}, \phi_c^{k-1}) \\ f_3(U^{k-1}, \alpha^{k-1}, \phi_c^{k-1}) \end{Bmatrix} \tag{9}$$

The 3 x 3 matrix in the preceding equation is the Jacobian matrix and must be inverted each iteration to solve for the Y vector. The equation of meshing, function $\mathbf{f_1}$, is numerically differentiated directly to find the terms for the Jacobian matrix. Function $\mathbf{f_2}$ and $\mathbf{f_3}$ cannot be directly differentiated with respect to U, Θ and ϕ_c. After each iteration U^{k-1}, Θ^{k-1}, ϕ_c^{k-1} (in the cutting head coordinate system) are transformed into the workpiece coordinate system) and are transformed into the workpiece coordinate system, S_w, with the series of coordinate transformations as given in Equation 11.

$$\begin{bmatrix} X_w \\ Y_w \\ Z_w \\ 1 \end{bmatrix} = [M_{wc}] \begin{bmatrix} r\cot\psi - U\cos\psi \\ U\sin\psi\sin\theta \\ U\sin\psi\cos\theta \end{bmatrix} \qquad (10)$$

where,

$$[M_{wc}] = [M_{wa} f(\phi_c)\ [M_{ap}]\ [m_{pm}]\ [M_{ms} f(\phi_c)]\ [M\text{-}SC] \qquad (11)$$

Each matrix [M] above represents a transformation from one coordinate system to another (ref. 4).

Functions f_2 and $\mathbf{f_3}$ are evaluated by starting with an initial U_k, Θ_k and ϕ_k, performing the transformations in Equation (11) and evaluating Equations (4) and (6). The numerical differentiation of $\mathbf{f_2}$ and $\mathbf{f_3}$ is performed by transforming U_k+inc, Θ_k+inc, ϕ_k+**inc** (where inc is a small increment appropriate for numerical differentiation) into $\mathbf{X_w}$+**inc**, $\mathbf{Y_w}$+**inc**, $\mathbf{Z_w}$+**inc**. Equations (4) and (6) are then used to evaluate the numerical differentiation. Function $\mathbf{f_1}$, $\mathbf{f_2}$, $\mathbf{f_3}$ and their partial derivatives are required for the Jacobian matrix and are updated each iteration. The iteration procedure continues until the Y vector is less then a predetermined tolerance. This completes the solution technique for a single point on the spiral bevel gear tooth surface. In this way the coordinates of the surface of the tooth are defined. This solution technique is repeated four times for each of the four surfaces; gear convex, gear concave, pinion convex and pinion concave.

Since all four surfaces are generated independently, additional matrix transformations are required to obtain the correct tooth thickness. The concave surfaces are fixed on each tooth. The convex surfaces are rotated as required. The angle of rotation is obtained by matching the tooth top land thickness with the desired value.

2.4 Gear and Pinion Orientations Required for Meshing

After generating the pinion and gear surface as described above, the pinion cone and gear cone apex will meet at the same point (see figure 2.2). This point is the origin of the fixed coordinate system attached to the workpiece being generated. To place the gear and pinion in mesh with each other, rotations described in the following example are required (ref. 5).

1. The gear tooth surface points are rotated by $360/N_t+180$ CW about the global Z_w axis, for this example, the rotation is 190 degrees.
2. The pinion is rotated by 90 deg CCW about the global Y axis.
3. Because the four surfaces are defined independently, their orientation is random with respect to meshing. The physical location of the gear and pinion after rotations described above correspond to the gear and pinion overlapping. To correct this condition the pinion is rotated CW about its axis of rotation Z_w until surface contact occurs. For the example used in this study, the rotation was 3.56 deg.

To make a complete pinion, the generated pinion tooth was copied and rotated 12 times and the generated gear tooth was copied and rotated 36 times with the aid of a solid modelling program as shown in figure 2.3.

CHAPTER III

CONTACT ANALYSIS BY THE FINITE ELEMENT METHOD

The advantages of the Finite Element Analysis (FEA) for accurate deformation and stress analysis of complex forms is well known. This chapter provides a brief outline of the FEA analysis carried out for spiral bevel gears. It also describes the fundamental concepts of non-linearity with emphasis on automated contact analysis. Since the research reported herein is presented using the general purpose finite element code MARC (ref. 11), details of its special features used for the analysis and the description of various blocks of the input deck are also discussed.

3.1 FEA of Spiral Bevel Gears

Only a few researchers have investigated finite element analysis of spiral bevel gears. FEA analysis has been done on a single spiral bevel tooth using an assumed contact stress distribution (ref. 4). More recent FEA spiral bevel gear analysis research has attempted to solve the contact stress distribution in a multi-tooth model (4 gear and 3 pinion teeth) (ref. 3). The tooth pair contact zones in reference 3 were modeled with gap elements. The study here uses software with automated contact options in order to avoid certain limitations in the use of gap elements, such as:

(i) It is difficult to connect the gap elements with proper orientations across the normal from one surface to the other surface parallel to the contact point.

(ii) The orientation of the contact plane remains unchanged during deflection.

(iii) It is difficult to accurately select the properties such as appropriate open/closed

stiffness values, selection of the stiffness matrix update strategy and efficient problem restarts.

New advances in the state of the art for FEA provide deformable body against deformable body penetration algorithms which can be used to establish the nonlinear boundary conditions for contact problems. MARC (ref. 11) is one such FEA package software which uses this algorithm to automatically detect contact.

3.2 Concepts of Nonlinear Analysis

In linear FEA, a simple linear relationship exists between force and deflection (Hooke's law). For a metallic spring under small strain, the force F equals the product of the stiffness K and the deflection U.

Also, the deflection can be obtained by dividing the force with the spring stiffness. This relationship is valid as long as the spring remains linear elastic, and the deflections are such that they do not cause the spring to yield or break. If the spring material is changed, for example, from steel to rubber, the linear force- displacement relation is no longer valid. It becomes a nonlinear problem i.e. $F \neq KU$.

A nonlinear structure is the one for which the force-deflection relationship cannot be directly expressed in terms of a set of linear equations.

The three major types of nonlinearities are:

(i) Geometric nonlinearity (large deformations, large strains, snap through buckling)

(ii) Material nonlinearity (plasticity, creep, viscoelasticity)

(iii) Boundary nonlinearity i.e., a changing status (opening/closing of gaps, contact, follower force)

A nonlinear system cannot be analyzed directly with a linear equation solver. However, it can be analyzed by using a series of linear approximations. Each linear approximation

requires a separate pass or iteration, through the program's linear equation solver. Each new iteration is as expensive, in terms of CPU time, as a single linear analysis solution.

In the preprocessing phase of a nonlinear analysis, everything is quite similar to linear FEA data input except the user is required to specify certain nonlinear analysis controls (i.e., large displacements, "contact" parameters, convergence controls, etc.) and additional material properties required for a nonlinear analysis.

In the solution phase, of nonlinear FEA, the solver must perform the analysis in steps or increments. Within each increment, the code will also iterate as necessary until equilibrium is achieved, before proceeding to the next increment.

In the post processing phase, the user looks at quantities like stress contours, etc. A nonlinear analysis takes tens, hundreds and sometimes, thousands of increments, thus, usually requiring a high speed computer with lots of memory for a reasonable turnaround. The objective in a successful nonlinear analysis is to obtain a converged solution at a reasonable cost.

In large deformation analysis, incremental load ΔF and displacement ΔU is related by the tangent stiffness $\mathbf{K}_T$. In solving this type of problem, the load is increased in small increments, the incremental displacement ΔU is found, and the next value of the tangent stiffness is found and so on. A brief description of the incremental solutions will now be discussed.

FEA is an approximate technique, and there exist many methods to solve the basic equations. In nonlinear FEA, two popular incremental methods used to solve the nonlinear equilibrium equations are: Full Newton-Raphson or the Modified Newton-Raphson.

The Full Newton-Raphson Method (see figure 3.1) assembles and solves the stiffness matrix at every iteration, and is thus expensive for large 3-D problems. It has quadratic convergence properties, which means in subsequent iterations the relative error decreases quadratically. It gives good results for most nonlinear problems.

The Newton-Raphson method iterates using this equation:

$$[K_T]\ \{\Delta U\} = \{F_{app}\} - \{F_{nr}\} \tag{11}$$

where,

$[K_T]$ = the tangent stiffness matrix

$\{\Delta U\}$ = the displacement increment

$\{F_{app}\}$ = the applied nodal force

$\{F_{nr}\}$ = the restoring N-R force (the loads generated by the elemental stresses)

$\{F_{app}\}$-$\{F_o\}$ = the residual force

The program updates the tangent stiffness matrix $[K_T]$ and the residual F_{app}-F_{nr} at each iteration, and then resolves the equation given above. Convergence is achieved once F_{app}-F_{nr} is less then a convergence criterion that is set. If F_{app} is not equal to F_{nr}, the system is not in equilibrium.

As shown in figure 3.1, the 1st iteration yields a displacement ΔU_1, using the initial elastic stiffness and the applied load F_{app}. The nonlinear response yields a force value F_{nr} for this displacement. The 2nd iteration yields ΔU_2, using the updated tangent matrix and the residual load. Subsequent iterations quickly drive the analysis to a convergent solution. This solution guarantees convergence if, and only if, the starting ΔU is "near" the exact solution. This could be obtained by taking smaller load increments.

In solving the convergence problem, one cannot neglect the general FEA conflict of expense versus accuracy. One must balance computational expense against accuracy. Using a finer mesh and multiple load increments can often lead to a more accurate and more robust (less likely to diverge) solution, but usually at increased expense.

The Modified Newton-Raphson method does not reassemble the stiffness matrix during every iteration as shown in figure 3.2. It costs less per iteration, but the number of iterations may increase substantially over that of the full Newton-Raphson method. It is effective for mildly nonlinear problems. In this analysis the full Newton-Raphson method was used.

3.3 Automated Contact Analysis

Many common structural features exhibit nonlinear behavior that is status-dependent. The stiffness of these systems shifts abruptly between different values, depending on the overall status of the item. Status changes might be directly related to load, or they might be determined by some external cause.

Situations in which contact occurs are common to many different nonlinear applications. Contact forms a distinctive and important subset to the category of changing-status nonlinearities (ref. 15). Contact, by its very nature, is a nonlinear problem. During contact, both the forces transmitted across the area and the area of contact change. The force-displacement relationship thus become nonlinear. Usually, the transmitted load is in the normal direction. In this report the method of reference 11 is used to perform the nonlinear analysis.

Reference 11 is a general purpose computer program for linear and nonlinear stress and heat transfer analysis. This program is capable of solving problems with nonlinearities that occur due to material properties, large deformations, or boundary conditions. In general, the solution of nonlinear FEA problems requires incremental solution schemes and sometimes requires iterations within each load/time increment to satisfy equilibrium conditions at the end of each step. The program features relevant to gear meshing are discussed in this section.

The FEA program used has a fully automatic CONTACT option which enables the analysis between finite element bodies without the use of any special gap or contact elements. The procedure is capable of handling the following types of contact:

i) deformable bodies against rigid surfaces

ii) deformable bodies against deformable bodies

iii) a deformable body against itself

The CONTACT option was originally designed for analysis of manufacturing processes such as forging or sheet metal forming, but its capabilities have been expanded to meet other analysis

requirements. The work presented in this document utilized the program of reference 11 running on a supercomputer.

Contact between the bodies is handled by imposing non-penetration constraints (reference 11). The non-penetration constraint, as shown in figure 3.3 and figure 3.4, is

$$U_A \bullet n < D$$

A non-penetration constraint (that the surfaces cannot inter-penetrate) is usually handled in FEA codes by one of three techniques: Lagrange multipliers (used in several FEA codes that offer "gap" elements); penalty functions (one application being the use of stiff or rigid connecting members to approximate the constraint); or solver constraints. In some FEA codes which offer explicit dynamics capabilities, a fourth technique is the direct application of contact forces. Use of a "gap element" means node to node contact. The CONTACT features uses the solver constraints approach.

Solver constraints are used to impose the non-penetration constraint, and a very efficient surface contact algorithm which allows the user to simulate general 2 and 3D multibody contact. Both "deformable-to-rigid" and deformable-to-deformable" contact situations are allowed. The user needs to only identify which bodies might come in contact during the analysis. Self-contact, which is common in rubber problems, is permitted. The bodies can be either rigid or deformable, and the algorithm tracks variable contact conditions automatically. Thus the user no longer needs to worry about the location and open/close status checks of "gap elements". Automatic, in this context, means that user interaction is not required in treating multibody contact and friction, and the program has automated the imposition of non-penetration constraints. Also, coupled thermo-mechanical contact problems (e.g rolling, casting, forging) and dynamic contact problems can be handled.

Real world contact problems between rigid and/or deformable bodies are actually 3D in nature. To solve such contact problems, one needs to define bodies and their boundary

surfaces. The definition of bodies is the key concept in analyzing 3D contact automatically. For rigid bodies, one can define such surfaces as: 4-point patch; ruled surface; plane; tabulated cylinder; surface of revolution; and Bezier surfaces.

Deformable bodies are defined by the elements of which they are made. Once all the boundary nodes for a deformable body are determined, 4 point patches are automatically created, which are constantly updated with the body deformation. Contact is determined between a node and all body profiles, deformable or rigid. A body may fold upon itself, but the contact will still be automatically detected, thus preventing self penetration.

The user must define bodies so that their boundary surfaces can be established. Deformable bodies are defined by a list of finite elements, and rigid bodies are defined by geometrical entities. Because the contact boundary conditions are a function of the applied load, the analysis must be carried out incrementally. Within each load or time increment of an analysis, additional iterations may be required to stabilize the contact zone. Contact problems involve two important aspects:

i) the opening and closing of the gap between bodies

ii) friction between the contacting surfaces.

The MARC program establishes a hierarchy between the bodies so that at a given contact interface, one body is the contactor and the other body is the contacted. The set of nodes on the boundary surface of a contactor are candidate nodes for contact. The boundary surface of a contacted body is defined by a set of geometrical entities. A user specified contact tolerance is used to determine the body separation distance which determines whether two bodies are considered to be in contact with each other. The contactor's boundary nodes are prevented from penetrating the surface of the contacted body by imposing solver constraints. For contact between a deformable body and a rigid body, a displacement constraint is applied. For contact between two deformable bodies MARC applies multipoint constraints in the form of ties. The

ties link the motion of one node on the contactor body to two adjacent nodes on the contacted body. During each iteration as nodes enter and leave contact or slide between adjacent node segments on contacted bodies, a bandwidth optimization is performed to reduce the computer processing time required.

During contact, it is possible to move bodies around during an analysis; however, the user must make sure that deformable bodies do not have rigid body modes. A minimum number of boundary conditions or spring element attachments must be applied to prevent rigid body motion.

A static analysis of two (or) more bodies that are not initially connected poses special problems with a finite element analysis, if one of the bodies has a rigid body motion component. If, at any time, the two bodies are disconnected then the stiffness matrix would become singular and unsolvable (in a static analyses). This is because finite elements require at least some stiffness connecting all the elements together along with sufficient displacement constraints to prevent rigid body motion. In order to overcome this difficulty, weak springs have been added to connect the bodies. The spring stiffness is very low. This stiffness is there only to supply some stiffness to the system. The stiffness should be negligible compared to the material stiffness, so that it has no effect on the solution.

CHAPTER IV

FINITE ELEMENT MODEL AND ANALYSIS

This chapter describes the procedure for assembling a finite element gear pair model for analysis with reference 11 software. Two different models are analyzed. These models are generated in the geometric modelling program of reference 14 (FEA pre and post-processor). The first model is a two tooth segment and the second model is a seven tooth segment of a gearset. Different programs used to create these FEA models and the boundary conditions imposed on them are described. Various sets of rotations carried out in the gearsets for the analysis to determine the contact path and the load sharing across the tooth are then discussed. A detailed report of the problems faced during the course of the analysis for convergence to take place and memory and CPU requirements of the system used are described. Different parameters of the finite element analysis input commands, which have been studied to reduce the CPU and memory requirements of the system, are also reported in this chapter.

4.1 Model Descriptions

To model spiral bevel gears, the machine settings and the gear and pinion design data as given in Tables I and II are necessary. The equation of meshing and the kinematics of gear cutting are incorporated in the computer programs to generate the spiral bevel gear model in the geometric modeling program (ref 14). The input data (for the geometric modeling program) for the seven tooth model is obtained from references 16, 17. This is a 10 x 10 mesh input to generate 4 gear teeth and 3 pinion teeth in mesh to simulate contact on multiple teeth of a spiral bevel gearset. The input also includes the hub attached to the gear. The input data (for the geometric modeling program) for the two tooth model is obtained from reference 6 and 7. The

programs generate a NxM mesh on the tooth profile of a spiral bevel gearset.

TABLE I: PINION AND GEAR DESIGN DATA

	PINION	GEAR
Number of teeth pinion	12	36
Dedundum angle, degree	1.5666	3.8833
Addendum angle, degree	3.8833	1.5666
Pitch angle, degree	18.4333	71.566
Shaft angle, degree	90.0	90.0
Mean spiral angle, degree	35.0	35.0
Face width, mm (in)	25.4 (1.0)	25.4 (1.0)
Mean cone distance, mm (in)	81.05 (3.19)	81.05 (3.19)
Inside radius of blank, mm (in)	5.3 (0.6094)	3.0 (.3449)
Top land thickness, mm (in)	2.032 (0.080)	2.489 (0.098)
Clearance, mm (in)	0.762 (0.030)	0.92964 (0.0366)

TABLE II: GENERATION MACHINE SETTINGS

	CONCAVE	CONVEX	CONCAVE	CONVEX
Radius of cutter, r, in	2.9656	3.0713	3.0325	2.9675
Blade angle, ψ, degree	161.9543	24.33741	58.0	22.0
Vector sum, L_w	0.038499	-0.051814	0.0	0.0
Machine offset, E_m	0.154576	-0.1742616	0.0	0.0
Cradle to cutter distance, s, in	2.947802	2.8010495	2.285995	2.285995
Cradle angle, q, degree	63.94	53.926	59.234203	59.234203
Ratio of roll, M_{cw}	0.30838513	0.32204285	0.950864	0.950864
Initial cutter length, u, in	9.59703	7.42534	8.12602	7.89156
Initial cutter orientation, θ, degree	126.83544	124.43689	223.9899	234.9545
Initial cutter orientation, ϕ_c, degree	-0.85813	-11.38663	-0.35063	-12.3384

A 24 x 12 mesh was used to create the two tooth model. Eight noded, isoparametric HEX elements were used. The seven tooth model and the two tooth model are as shown in figures 4.1 and 4.2. The seven tooth model consisted of 8793 elements and 11261 nodes and the two tooth model consisted of 3116 elements and 4452 nodes.

4.2 Loading and Boundary Conditions

The boundary conditions for the seven teeth and two teeth models are as shown in figures 4.1 and 4.2. The boundary conditions are applied such that the gear teeth are made to pivot about a fixed point at node number 7872 for the seven tooth model and at a node number 4448 for the two tooth model. In both models, the axis of rotation for the gear is the Z axis. The nodes where the forces are applied are in the gear hub of the models. Fixed displacement boundary conditions are applied at 8 nodal points in the Z direction only for the gear and in all directions for the pinion as shown in the figures. Since this is a static problem involving two bodies (the pinion and the gear) in contact, as described in a previous chapter, weak springs are added to prevent the rotational rigid body modes for the gear. Eight springs are added away from the contact region. The springs connect the corner nodes of the pinion with the corner nodes of the gear on the faces where contact occurs. The stiffness of the springs are 100 lbs/in. This is insignificant when compared to the tooth contact stiffness and therefore does not effect the overall solution.

The maximum torque for the gear mesh studied was 9508 in.• lbs. on the gear. This torque is applied as a concentrated force with a moment arm on the gear hub. This concentrated force for the seven tooth model was 4714 lbs. with a moment arm of 2.017 inches. For the two tooth model, the force is 3392 lbs. applied at a radius of 2.798 inches. The force is applied in different increments for convergence to occur. The details of the incremental loading are discussed later in this chapter.

4.3 Model Generation to Predict the Contact Path

To predict the contact path of the spiral bevel gears as they roll in and out of mesh, several rotations have been carried out on the preliminary model. The rotation of the gear and the pinion should be in the same directions, i.e., both positive.[1] For the model being analyzed, the gear has 36 teeth and the pinion has 12 teeth. Therefore, for each degree of gear rotation the pinion has to be rotate three degrees to avoid interference during meshing. For the seven tooth model, seven such rotations were carried out. For the two tooth model, three such rotations have been carried out. From the positioning of the preliminary model, the rotations were carried out in both positive and negative directions to determine the contact path. In the seven tooth model the pinion was rotated by +6,0,-6,-12,-18,-24,-30 degrees and in the two tooth model the pinion was rotated by +6,0,-6 degrees. The corresponding rotation of the gear were -2,0,+2,+4,+6,+8,+10 degrees for the seven tooth model and -2,0,+2 degrees for the two tooth model. (Zero degrees corresponds to the initial position for the gearset based on solving the equation of meshing.)

While generating the models, care must be taken not to change the node numbers and the element numbers. This eliminates a great deal of editing in the FEA input file. The command used in the geometric modeling program to do this with the gear and pinion part names is as follows:

Name, (partname), rot,rotation axis data, (partname)

Care must also be taken to rotate the gear about the Z axis and pinion about the X axis directions to avoid interference of the gears in mesh.

---

[1]NOTE: Although all gearsets must rotate in the opposite sense, (i.e., if the gear rotates CW, the pinion must rotate CCW) this gearset does in fact rotate in the same direction (i.e., both gear and pinion have positive rotation) based on the right hand rule and the defined coordinate system. This occurs because the gear rotates about the Z axis, with the positive Z axis pointing from the toe of the gear to the heel. However, the pinion rotates about the X axis with the positive X axis pointing from the heel of the pinion to the toe. The result is both gear and pinion have positive rotation.

4.4 Assembling the Spiral Bevel Gear Pair for FEA Analysis

The procedure to assemble a spiral bevel gear pair to perform FEA analysis is as follows:

STEP 1. Initially the gear model is generated in the geometric modelling program, from the input file obtained after executing the computer codes from references 6 and 7 as discussed earlier. The model is optimized and the node and the element id's are compacted. The load and the boundary conditions are applied to the model.

STEP 2. A neutral file is created for translation. This creates a preliminary data input file. This data file needs to be edited for the non-linear analysis. Certain commands and controls are added which are not available in the geometric modelling program. These changes are discussed in detail later in the chapter.

STEP 3. After editing the preliminary data input file, it is ready to be submitted for the analysis. (A sample input file is given in appendix A. Appendix B gives a description of specific MARC commands.) To submit the job to a supercompter, a job control language (JCL) file needs to be prepared. (The JCL file is given in appendix C.) This file contains the workspace required and the CPU time required as well as other related details which are discussed later. Also a user subroutine file should be present in the same directory as the input file. This file suppresses the printing of input in the output file generated after a run.

After the job has run, four files are created which are as follows:

1. List file (job.lst) - the output file which gives listing of the results.
2. Post file (job.post) - the post processing file is used as input to the geometric modeling translator. (MARPAT)
3. Restart File (job.restart) - written if this option is included in the input deck. Useful for continuing a run from the last complete run or any complete run for which the post data is asked to be written.

4. Log File (user.0#) - gives details of the job run on the supercompter, giving CPU time used and other data. It also gives any SYSTEM errors encountered while the job is running.

If there are any errors the job ends and the list file exists with an EXIT number depending on the error.

STEP 4. The geometric modelling program translator is used to convert the FEA results file into readable format. The post file is translated into three files for each increment of the analysis which is stored in the post file. These are as follows:

1. Element File (i#s0.els) - gives the elemental stress values.
2. Nodal File (i#s0.nod) - gives the nodal stress values.
3. Displacement File (i#s0.dis) - gives the displacement values.
4. Log files (marpat.msg and marpat.crd)

STEP 5. To view the results in the postprocessor, the original neutral file is read to create the model. Then results are checked and the files are read as required for elemental, nodal or displacement results.

The flow diagram to show the steps undergone to finally prepare the model for the analysis is shown in figure 4.3. A typical MARC input deck is shown in figure 4.4.

4.5 Changes Made in Preliminary MARC File for Nonlinear Analysis

Since all of the features available in the MARC program are not available in the geometric modeling program, the MARC input file created by the geometric modeling translator must be edited to add the following commands and controls for the gear analysis:

1. SIZING - This value is set to meet the greatest workspace requirement for a given problem. The estimate of the greatest workspace requirement is usually based on experience. If the SIZING value is not enough for the analysis, the FEA program

automatically switches to an out of core solution mode. The out of core solution mode is usually not preferred and should be avoided as out of core disk space is required and CPU time increases. Initially, when the preliminary FEA input file is obtained SIZING has a value of 400,000 words. In this analysis SIZING is changed to 26 Mega words (Mw) for the two tooth model and to 28.5 Mw for the seven tooth model. With this values the analysis solutions were obtained in-core. Care should be taken in specifying this value. This value should be 1.7 Mw less than that specified in the JCL for the memory requirement. This accounts for the loading and running of the FEA program. This value specified could be 1.7 Mw less than the JCL value, but should never be more than the JCL value.

2. SETNAME - This gives the number of items in defined sets for elements and nodes. It usually allots 50 items per set. Since the geometric modeling translator converts each named component into a set, a lot of sets are defined with elements and nodes in separate sets. This results in excessive name sets being defined. These defined sets are not required unless it is necessary to define the nodes and elements, which are difficult to identify from the model but are easily defined in these named sets. In that case, only the desired name sets are kept and the others are deleted. This not only reduces the input file size but also reduces the memory requirements to run the job. Because with an increase in name sets, the workspace memory requirement is increased. It is always better to reduce the workspace required to permit the job to run within core. Since the models used have numerous named components, the preliminary FEA input file has many name sets with element and node sets defined separately. The SETNAME has a value of 901 initially which is changed to 200 with 50 items per name set i.e., only 4 name sets are then kept. This change resulted in the reduction of memory requirements for the seven tooth model run.

3. DEFINE SETS - These are kept to the minimum and only used if required as is discussed in SETNAME change. The only four name sets GEARE, PINIONE, PROJ2E and RIME, which define the elements for the respective regions, are used for defining individual material properties.
4. PRINT - This parameter is specified with option 5 to provide output of nodal contact information as nodes contact and separate from surfaces during the analysis.
5. POST - Post processed data is controlled by this option. The type of post process data and the rate at which it is recorded is specified. The post codes given are changed to 17, 131 and 133 which represent VON MISES, MAXIMUM PRINCIPAL and MINIMUM PRINCIPAL stresses. The number of increments at which the data is recorded is added in column 45. Also 0 in column 20 is changed to 1 to write formatted post data.
6. POINT LOAD - This option, which is given in the beginning of model definition cards, is deleted as loads specified in zero (null) increment are ignored.
7. CONNECTIVITY - In column 15 to suppress element connectivity being printed in the output listing a numerical number 1 is added.
8. COORDINATES - In column 20 to suppress the nodal coordinates being printed in the output listing a numerical number 1 is added.

Additional MARC commands are described in appendix B.

4.6 Running Large Finite Element Analysis

Initially, many trial runs were submitted to study how each of the options behaved. The variables in the cards for each option were changed a number of times until an appropriate one was found. Considerable effort was spent debugging and optimizing the finite element code running on the supercomputer. Because this problem utilized significant computer resources, much specialized computer knowledge was needed. This section attempts to document some of this experience.

In the OPTIMIZE option, the method used was changed from 4, the Wave front method followed by Grooms, to use option 2, the Cuthill Mckee method. This new method was less expensive and saved considerable memory requirements. Also, the ELSTO option has been added for this analysis. This reduces the in-core memory requirements below the 28 Mega word (Mw) limit defined on the SIZING card. This option was added after a lot of memory shortage requirements were faced. Before this problem was resolved more memory was required than what could be given in the SIZING card running on the supercomputer. The problem finally ran with much less than 200,000 blocks.

Much experimentation was done on the CONTROL option variables. This option sets limits on the number of increments and recycles which may be performed during a nonlinear analysis.

As discussed earlier, spring elements are used to prevent rigid body modes. The SPRINGS option is a list of nodes and their degrees of freedom which are connected by spring elements. Nodes were identified on the two bodies where SPRINGS were to be connected. A number of trial runs were performed to check the effect of the stiffness value given to the springs.

The RESTART option is used to save and retrieve analysis data so that the analysis can be restarted for additional increments. The variables were adjusted to determine how the loading could be continued for the next restart. While performing the initial runs, the restart option was used frequently. This was because the number of increments in which the load was applied to

reach the final torque in the gears was not appropriate for the solution to converge. However, the option was not used in the final analysis, since an efficient the number of load increments was eventually found for efficient convergence.

The loading was specified incrementally with the AUTO LOAD option. AUTO LOAD will cause the current load vector to be repeatedly applied (additively) for the number of increments requested. The number of increments to be specified in the AUTO LOAD and also the CONTROL card sets posed another problem. The actual number of increments to be run were specified in the AUTO LOAD card set. The number of increments in the CONTROL card were set to the upper limit for the total number of increments allowed for an analysis. This can be left blank and let the program take the default maximum allowed. The POINT LOAD option is used to apply the load per increment. The FEA program uses incremental values of the load which are summed to give the total value that is used in that increment. The last value of the incremental load that was input will be used until the new incremental value is read in to replace it.

For contact analysis with AUTO LOAD, a TIME STEP history definition card set must be included. Although the time step for each increment is arbitrary for this research analysis, it must be included. When rigid bodies are included in a contact analysis, displacements, velocities or accelerations are specified and therefore a time step is essential. This problem has deformable bodies, not rigid bodies, but the FEA program code still requires a TIME STEP card set. An arbitrary time step of 10 units per increment was specified.

In the CONTACT option, the number of entities present in body 1 and body 2 have to be given appropriately depending on the mesh density of the contacting surface. Care has to be taken to define the two bodies as body 1 and body 2. Identifying elements present on the contacting surface of the bodies becomes complicated for complex models like the spiral bevel gears. Many times during this research, the model was optimized in the solid modeler due to

some small modifications on the model which caused element numbering to change. This necessitated the element numbers to be identified all over again.

4.7 Convergence Problems

For a nonlinear analysis, many load steps or increments must be used to reach the final or fully loaded state. In the process, one can encounter some convergence problems.

A torque of 9508 in. lbs. was applied to the gear. This torque was input as a series of point loads. Since this is a nonlinear problem, the entire torque should not be applied in one increment. Several analysis (about 60) were run to determine the sensitivity of the structure meeting the convergence criteria as a function of the size of the applied load.

The FEA program solves the non-linear problem on an incremental basis and iterates within each increment until the convergence criteria are met. These criteria are specified in the CONTROL data block. Too many iterations within an increment, is an indication that too much loading is being attempted for that load step. Initially the gears are separated by a small gap. At this point the total structure has very little stiffness. Applying any torque causes the gear to rotate and contact the adjoining pinion. Very small load increments should be applied otherwise the matrix updated for this soft structure will not converge. After the gear contacts the stiffness of the structure increases drastically. The amount of loading can then be increased until the required amount of torque is achieved. For the seven tooth model, a total of 8 increments were used to reach the desired torque, while for the two tooth model a total of 10 increments were used.

While performing the trial analysis some increments kept repeating as the convergence criteria was not met. Also it was observed that load was automatically decreased by the program. The conclusion was drawn that the load applied was too high for the solution to converge, which was seemed correct as the program itself was decreasing the load values. This

gave an indication that the load step needed to be reduced.

To determine the correct load to be applied many trial analysis were performed. The load was reduced from about 100 lbs. to 5 lbs. but the solution was still not converging. Each time different nodes kept coming into contact and disturbed the convergence requirement. The nodes in contact were found to lie on the border of the defined contact region. Since nodes other than those defined as contact region nodes were trying to contact, convergence was affected.

The next step taken was to define more surface nodes on the contact region (CONTACT CARD). After this the convergence criteria was changed from displacement to force residuals (CONTROL CARD). This eventually led to the convergence of the analysis.

A summary table of the computer runs and the incremental loads given to the seven tooth model and two tooth model is given in Table III.

TABLE III: SUMMARY OF LOADING AND CPU TIME

SEVEN TOOTH MODEL			
Increment Number	Total CPU time (sec)	Load increment (lbs.)	Total Load (lbs.)
1	437.5	12	12
2	1403.37	2	14
3	1968.24	785	799
4	2541.77	785	1584
5	3115.01	785	2369
6	4287.06	785	3939
7	4886.40	785	4274

TWO TOOTH MODEL			
Increment Number	Total CPU time (sec)	Load Increment (lbs.)	Total Load (lbs.)
1	121.11	2	2
2	150.38	2	4
3	181.13	2	6
4	212.98	2	8
5	309.7	2	10
6	405.28	2	12
7	775.31	845	857
8	856.49	845	1702
9	939.53	845	2547
10	1097.90	845	3392

4.8 Supercomputer Requirements

Supercomputers have various queues with different memory and CPU time requirements as shown in Table IV. Each of the queues has either 1 or 2 jobs running. A small job with SIZING of around 400,000 words usually takes less than 300 secs of CPU time and can be in the smallest queue called debug. But as the size of a problem increases the CPU requirements increase which necessitates a job to be submitted in a higher queue. The 2 jobs analyzed in this research required 26 Mw and 28.5 Mw of memory space and about 20 - 80 minutes of CPU time. The turnaround from each job was very slow. A job on an average would take a day and a half in the queue before running. After a lot of experimentation, the job was first submitted in the 300 second slot. Because of this, errors if any would show up in 10 minutes rather than in 2 days.

TABLE IV: TYPICAL INPUT QUEUES FOR SUPERCOMPUTER

Queue Name	CPU Limit (s)	Memory Limit (Mw)	Day Queue Limits		Night Queue Limits		Weekend Queue Limits		Flood Limit
			Max Jobs Running		Max Jobs Running		Max Jobs Running		
			Class	User	Class	User	Class	User	
debug	300	30.2	3	1	2	1	1	1	2
q^3	1,200	4.2	2	1	2	1	1	1	2
q^4	3,600	4.2	2	1	2	1	1	1	2
q^5	7,200	4.2	2	1	2	1	1	1	1
q^6	3,600	8.2	2	1	2	1	1	1	2
q^7	7,200	8.2	2	1	2	1	1	1	1
q^8	10,800	8.2	2	1	1	1	1	1	1
q^9	7,200	16.2	1	1	1	1	1	1	1
q^{10}	14,400	16.2	1	1	1	1	1	1	1
q^{11}	21,600	16.2	1	1	1	1	1	1	1
q^{12}	10,800	30.2	1	1	1	1	1	1	1
q^{13}	21,600	30.2	-	-	1	1	1	1	1
q^{14}	21,600	60.2	-	-	-	-	1	1	1

Day Queues: 0800-1700 Mon. thru Thurs. & 0800-2200 Fri.
Night Queues: 1700-0800 Mon. thru Fri.
Weekend Queues: 2200 Fri. thru 0800 Mon.

Allow 0.7 Mw for System Memory Overhead

As mentioned earlier, the space requested in the job control data (JCL) set should be 1.7 Mw higher than that given in the SIZING card. This is required for the FEA program to be loaded. A detailed listing of the JCL is given in appendix C.

If the job is required to be restarted, the input and output RESTART files should be mentioned in the correct format. This option was utilized in this research since the turnaround was very slow. Only a few increments were requested for the analysis and were saved in the restart file. By reading the restart file, the job could be restarted from the previous increment.

Computing the amount of workspace required by the FEA program is a complex function

of many variables. The most efficient method is to select a large enough workspace to handle a variety of runs, without sacrificing efficiency or wasting core space.

Both in-core and out-of-core data storage schemes are available in the FEA program. Elements may also be stored out-of-core if the ELSTO option is used. The FEA program chooses the solution type automatically.

The in-core solution technique is used when the workspace size specified in the SIZING card is larger than the total workspace needed in the in-core matrix. When the workspace required is too large, program uses the out-of-core solution techniques and show how much space each nodal row requires, the number of nodal rows per buffer and how large each auxiliary file would be. The buffer size can be increased only by changing allocation on the SIZING card. The amount of size to be given is based on experience. For large problems, the exact workspace requirements can be determined without actually running the job by inserting a STOP parameter card after the workspace is allocated.

The frequency for writing restarts and POST data should be low to avoid disk space problems since these files are very large. Initially these files were written after every 10 iterations. Finally they were written for every 2 iterations when the number of increments to apply the load was reduced for the job to run.

CHAPTER V

RESULTS

Various jobs were successfully run to predict the contact path and the load sharing for the double tooth contact region as the gears roll through mesh.

5.1 Elliptical Stress Distribution

The stress distribution in the contact region was found to be elliptical. Figure 5.1 shows a typical elliptical contour obtained using elemental stress values on the pinion surface. Figure 5.2 shows typical pinion contact stresses with nodal values. Because of the large nodal stress gradient, the nodal stress ellipse is slightly distorted when compared to the ellipse contour with elemental stresses. Note that only the pinion contours and the stress values are discussed in this research, since the gear teeth share a similar load distribution. Also note that only the minimum principal stresses are recorded at the contact region for the study.

5.2 Gap Element and Automated Contact Analysis Comparison

Contact stresses on spiral bevel gears were studied by researchers with gap elements in references 16 and 17 on a similar seven tooth model. Comparison of the results with automated contact analysis will now be presented. Both models contained the same mesh density, boundary conditions, material properties and loading. The nodal stress results of pinion tooth #1 obtained from gap elements and automated contact analysis are as shown in figures 5.3 and 5.4. Note that both the contours show the highest concentrated stress value at the same node. A comparison of the results of these two runs are as follows:

	Gap Element	Automated Contact Analysis
Max Nodal stress	-296,410 (psi)	-291503 (psi)
CPU time (approx)	30 min	80 min
Elemental stress	-84,761 (psi)	-113,577 (psi)
Gap elements closed or (nodal points with contact)	4	8
No. of increments	4	8

The number of contact nodes at the contact region in the automated contact FEA program was higher than identified by the gap element FEA program. With the pinion considered body 1 (contactor body) and the gear considered body 2 (contacted body), eight nodes contacted as shown above. With body 1 and body 2 switched, 16 nodes were found to have contact. Presumably this sort of discrepancy occurred because the mesh was too coarse.

5.3 Seven Tooth Model Results

As discussed earlier, the seven tooth model pinion was rotated from +6 degrees to -30 degrees about the X axis and the gear was rotated from +2 to -12 degrees about the Z axis. As these gears were rolled there was a shift in the contact region. It was observed that as one pinion tooth goes out of mesh and the load on it reduces, the other pinion tooth shares more load and as it starts coming into contact. The elliptical stress contours for pinion tooth #1 and pinion tooth #2 while they are rotated in mesh with the respective gear teeth (for all the rotations stated above) are shown in figure 5.5.

Figures 5.6 to 5.19 show plots of nodal stresses for pinion tooth #1 and #2 for all positions. Shift in the contact nodes while the gearset rolls through mesh are shown in figures 5.20 and 5.21. These nodes are obtained from the output file. The contact forces on the pinion and the

gear nodes which are listed at the end of the last increment are studied to identify the nodes in contact. The contact node density, or all the nodes that contact during meshing, is as shown in figure 5.22.

5.4 Two Tooth Model Results

The two tooth model was generated with a finer mesh with 24 nodes along the length of the tooth and 12 along the height of the tooth.

As discussed earlier, the two tooth pinion is rotated in six degree increments to the following positions: +6, 0, and -6 degrees to observe the shift in the contact ellipse. The direction of rotations were similar to that of the seven tooth model. The element and nodal stress results for the model rotated by -6 degrees are shown in figures 5.23 and 5.24. In this model due to the flexible hub, the gear started sliding over the pinion by a large amount resulting in more nodes in contact. For this reason the contact ellipse was sliding towards the edge of the pinion and the ellipse contour became distorted. A summary of the seven tooth and two tooth models with reference to modeling and analysis are given in Table V.

TABLE V: SUMMARY OF FEA ANALYSIS

FEATURES	7 - TOOTH MODEL	2 - TOOTH MODEL
No. of elements	8793	3116
No. of nodes	11261	4452
No. of degrees of freedom	33748	13321
"In-core" Memory required (Mw)	28.5	26
CPU time (seconds)	4886.40	1092.90
No. of increments	8	10
Contact tolerance (in.)	0.0002	0.0002
Torque applied lbs. in.	9508	9508

5.5 Contact Path

The contact path is defined as the path of the point of maximum force on the gear tooth while it rolls in and out of mesh. These values are determined for the pinion using the output listing which gives the contact force in the final increment before converging. Referring to Figure 5.5, it should be noted that while the contact ellipse in pinion tooth #2 shifts from the toe of the tooth to the center of the tooth, the contact ellipse in pinion tooth #1 shifts from the center of the tooth to the heel of the tooth. The contact path for pinion tooth #1 and pinion tooth #2 are plotted in figure 5.25. The two curves of pinion tooth #1 and pinion tooth #2 do not overlap because the mesh density is too coarse and also the rotations are not small enough.

The force at a particular node is taken to be the square root of the sum of the squares of the forces in the X,Y and Z directions. The maximum force is obtained for all the rotations of the model and are plotted on the pinion. The two tooth model showed a shift in the contact path due to flexibility effects. The hub region for this model was very flexible and had deformed a lot before the gear pair came into contact.

5.6 Load Sharing in Spiral Bevel Gears

The load sharing was analyzed in the double tooth contact region of the seven tooth model. The total forces on pinion tooth #1 and pinion tooth #2 at each of the rotations from +6 degrees to -30 degrees for the seven tooth model are calculated. This is done using the contact table obtained from the output listing of any run. The total contact force on each pinion is determined by

$$\sqrt{(\Sigma F_x)^{+2} + (\Sigma F_y)^2 + (\Sigma F_z)^2} = F_{contact} \qquad (14)$$

Table VI shows the load on pinion tooth #1 and pinion tooth #2 calculated from various runs while the gears were rotated. The load on the tooth as a function of rotation is also plotted as

shown in figure 5.26.

TABLE VI: MAGNITUDE OF CONTACT FORCES
IN PINION1 AND PINION2 ACROSS THE CONTACT REGION

Degree of Rotation of Pinion	PINION TOOTH #1				PINION TOOTH #2			
	F_x	F_y	F_z	F_{t1}	F_x	F_y	F_z	F_{t2}
+6	2870	3294.4	473.6	4397.4	0	0	0	0
0	2710.4	2759.0	447.0	3893.0	154.8	164.9	29.9	226
-6	2323.7	2032.0	391.17	3110.98	513.0	515.0	83.5	767.7
-12	1655.0	1908.4	295.3	2542.9	1008.9	1093.4	164.5	1495.91
-18	1114.0	1267.1	240.5	1704.07	1582.2	1655.1	175.5	2296.16
-24	646.3	763.2	135.7	848.2	1873.3	2019.4	343.68	2775.2
-30	200.91	252.6	45.8	324.8	2156.0	2326.0	450.4	3203.33

5.7 Fillet Stresses

The fillet stresses are plotted for the seven tooth model with load sharing. A typical contour of these stresses for one particular rotation is shown in figure 5.28. Table VII gives the maximum principal nodal stresses at various nodes and at various roll angles. The location of these nodes are given in figure 5.27. These values are plotted as a function of roll angle as shown in figure 5.29.

TABLE VII: FILLET STRESSES AS A FUNCTION OF ROTATION FOR DIFFERENT NODES

PINION1						
Nodes-->	883	871	856	1745	1733	1718
Rotations						
+6	75966.13	138493.3	32738.5	39224	18491	15248
0	44804.1	109165.1	37978.5	45357.8	16021.8	12918.5
-6	24030.4	66600.7	29362.4	67333.4	17878.6	10812.1
-12	10272.5	21690.6	12490.4	74458.8	28887.1	9505.6
-18	3721.5	1312.2	5926.3	81997	55723	11607.1
-24	414.4	15953.0	13148.4	90294.8	67987.5	14639.2
-30	1806.3	29486.5	16799	37915.3	81093.5	27288.9

CHAPTER VI

SUMMARY AND CONCLUSIONS

A procedure for predicting the contact path, load sharing, contact stresses and fillet stresses of spiral bevel gears is presented. The method incorporates the following steps:

1. A model was developed using the kinematics of the manufacturing process, the machine settings, and the design data for the gearset. The model was generated in a geometric modeling program.
2. Automated contact analysis option in a nonlinear finite element analysis program was used to perform the analysis.
3. Two different models were analyzed. Model I consisted of three gear teeth and four pinion teeth in mesh. The nodal mesh density on the tooth surface was 10 by 10. Model II consisted of one pinion and one gear tooth in mesh with a nodal tooth surface mesh density of 24 by 12.
4. These models were analyzed by rotating the gears in angular increments to predict the contact path. Model I was rotated a total of 36 degrees and Model II was rotated a total of 12 degrees.
5. The load sharing was determined from the contact forces on the nodes at the end of the converged solution for each rotational position.

The initial FEA results for Model I at the contact region compared favorably with the results by earlier researchers using gap elements. It was observed that in the double contact zone, when the contact ellipse in the (i)th pinion shifted from the center of the gear tooth to the heel of the gear tooth, the contact ellipse in the (i+1)th pinion shifted from the toe of the gear tooth to the center. The load for each tooth was calculated as the sum of the contact forces on

various nodes in the contact region. The number of nodes in contact changes as the gear rolls through mesh.

There was a large stress gradient between adjacent nodes in the contact region. This indicates a need for mesh refinement.

BIBLIOGRAPHY

1. Handschuh, R., "Thermal Behavior of Spiral Bevel Gears," Ph.D. Dissertation submitted to Case Western Reserve University, July 1993.

2. Choa, H.C., Baxter, M., Cheng, H.S., "A Computer Solution for the Dynamic Load, Lubricant Film Thickness, and Surface Temperatures in Spiral Bevel Gears," Advances Power Transmission Technology, NASA CP-2210, AVRODCOM TR-82-C-16, Fisher, G.K., ed., 1981, pp 345-346.

3. Drago, R.J., Uppaluri, B.R., "Large Rotorcraft Transmission Technology Development Program, vol. I, Tech Report, (D210-11972-1-vol-1, Boeing Vetrol Co., NASA Contract NAS3-22143) NASA CR-168116, 1983.

4. Handschuh, Robert F., Litvin, Fador L., "A Method for Determining Spiral-Bevel Gear Tooth Geometry for Finite Element Analysis," NASA TP-3096 AVSCOM TR-91-C-020, August 1991.

5. Bibel, G.D., Kumar, A., Reddy S., Handschuh R., "Contact Stress Analysis of Spiral Bevel Gears Using Nonlinear Finite Element Analysis," 29th Joint Propulsion Conference by AIAA, SAE, ASME, ASEE, June 1993.

6. Kumar, A., Bibel, G.D., "A Procedure for Finite Element Analysis of Spiral Bevel Gears," NASA Contractor report (in press).

7. Bibel, G.D., Reddy, S., Kumar, A., "Manual for Automated Generation of Spiral Bevel Gears," NASA Contractor Report (in press).

8. Litvin, F.L., et al., "Method for Generation of Spiral Bevel Gears with Conjugate Gear Tooth Surfaces," J. Mech. Trans. Automat. Des., vol. 109, no. 2, June 1987, pp. 163-170.

9. Litvin, F.L., "Theory of Gearing," NASA RP-1212, 1989.

10. Burden, R.L., Fairies, D.J., Numerical Analysis, 3rd Edition, PWS Publishers, 1985..

11. MARC K-5.1 User Manual, MARC Analysis Research Corporation, Palo Alto, California, 1981.

12. Litvin, F.L., Tsung, W.J., Lee, H.T., "Generation of Spiral Bevel Gears with Conjugate Tooth Surfaces and Tooth Contact Analysis," NASA CR-4259, AVSCOM TR 87-C-22, 1987.

13. Litvin, F.L., Lee, H.T., "Generation and Tooth Contact Analysis of Spiral Bevel Gears with Predesigned Parabolic Functions of Transmission Errors," NASA CR-4259, AVSCOM TR 89-C-014, 1989.

14. PATRAN Users Manual, PDA Engineering, Costa Mesa, CA., July 1987.

15. Valco, M.J., "Planetary Gear Train Ring Gear and Support Structure Investigation," Ph.D. Dissertation submitted to Cleveland State University, April 1992.

16. Reddy, S., "Finite Element Analysis and Tooth Contact Analysis of Spiral Bevel Gear," Master's Thesis, submitted to the University of Akron, December 1992.

17. Kumar A., "Spiral Bevel Gear Contact 'Simulation and Stress Analysis' Using Finite Element Analysis," Master's Thesis submitted to the University of Akron, May 1993.

18. Huston, R., Coy, J., "A Basis for Analysis of Surface Geometry of Spiral Bevel Gears," Advanced Power Transmission Technology, NASA CP-2210, AVRADCOM TR 82-c-16, Fischer, G. K., ed., 1981, pp 317-334.

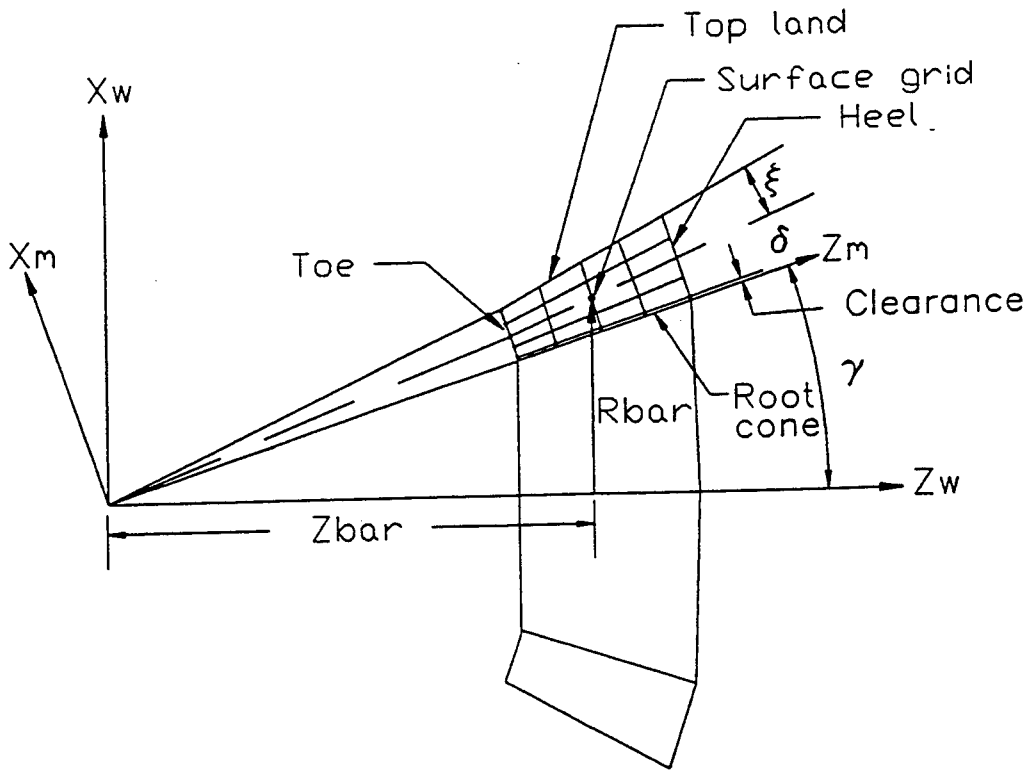

Figure 2.1 Projection of gear teeth over XZ plane

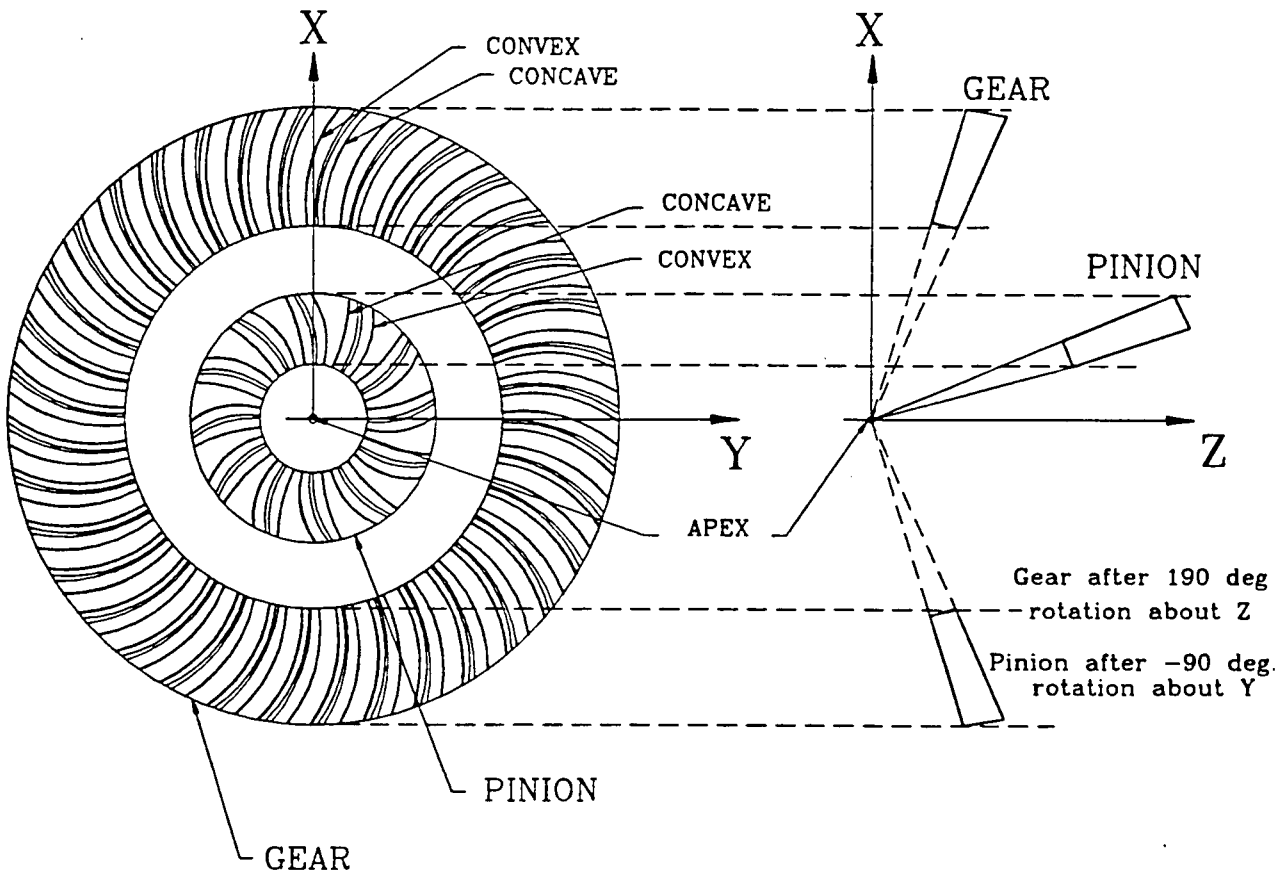

Figure 2.2 Gear and Pinion Orientations to Mesh with Each Other

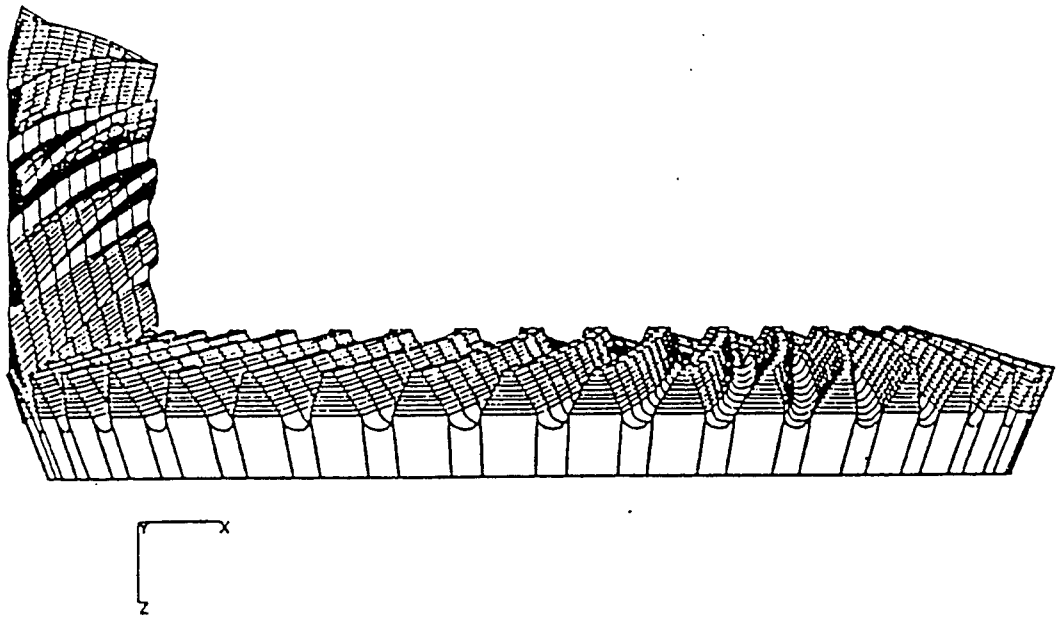

Figure 2.3 3-D Model of the Spiral Bevel Gears

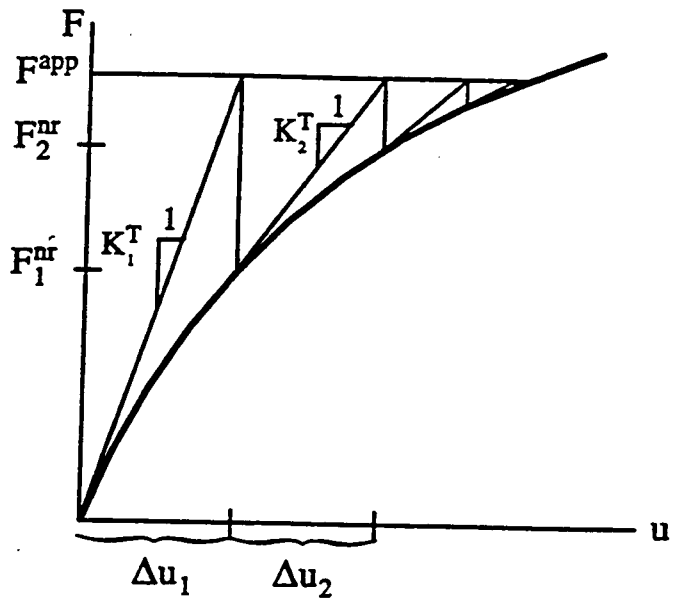

Figure 3.1 The Full Newton-Raphson (N-R) Method

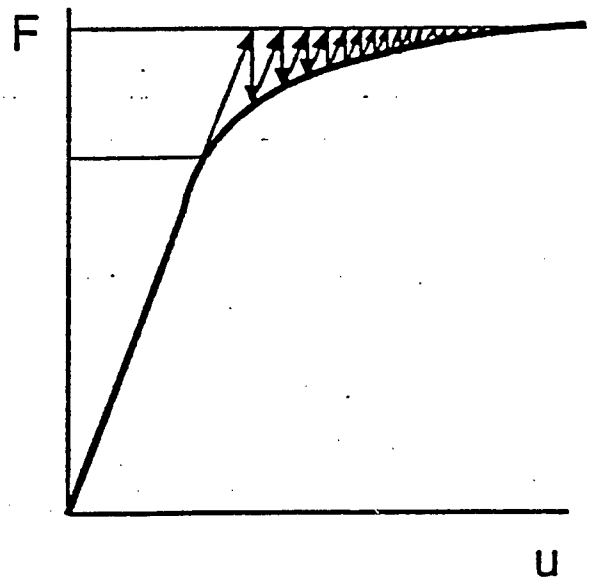

Figure 3.2 The Modified Newton-Raphson Method

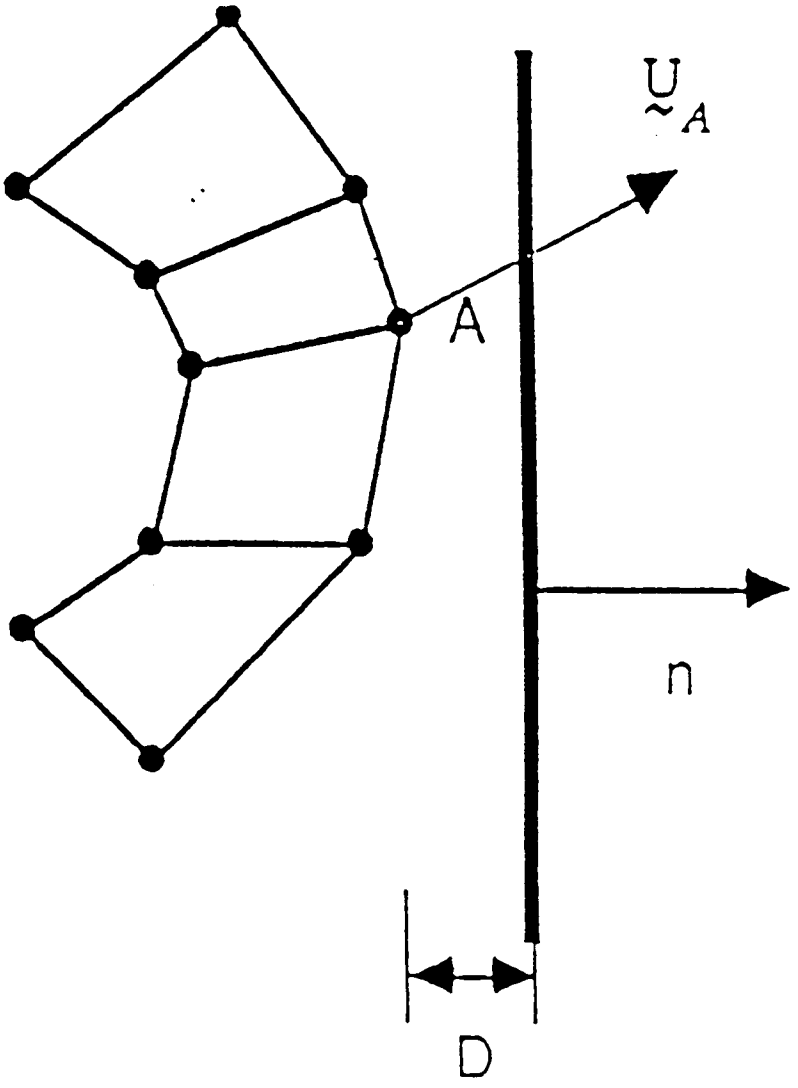

Figure 3.3 The Non-penetration constraint in CONTACT

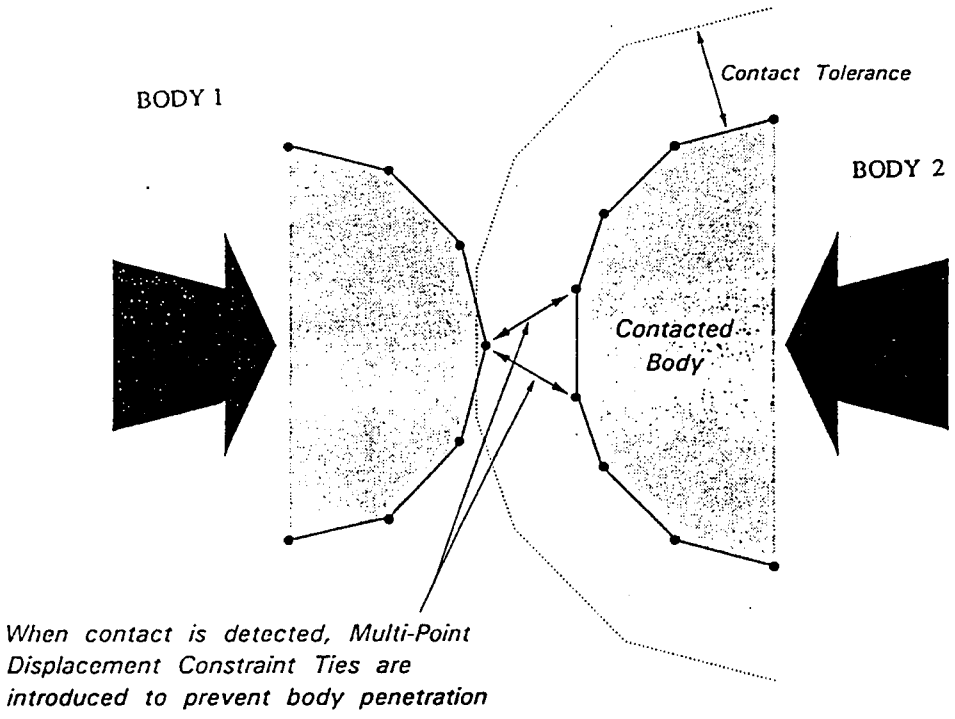

Figure 3.4 Contact Algorithm

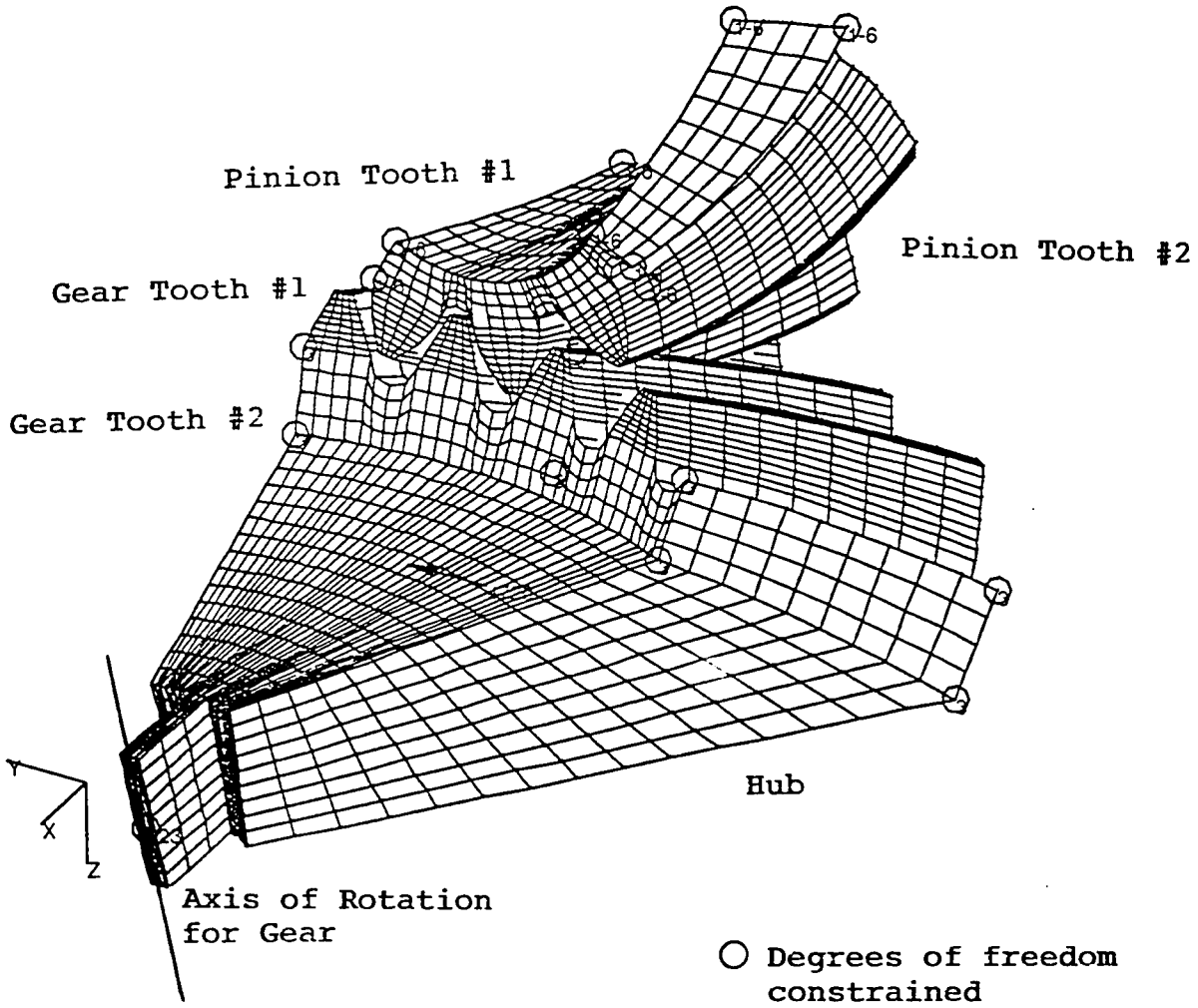

Figure 4.1 Seven tooth model with boundary conditions

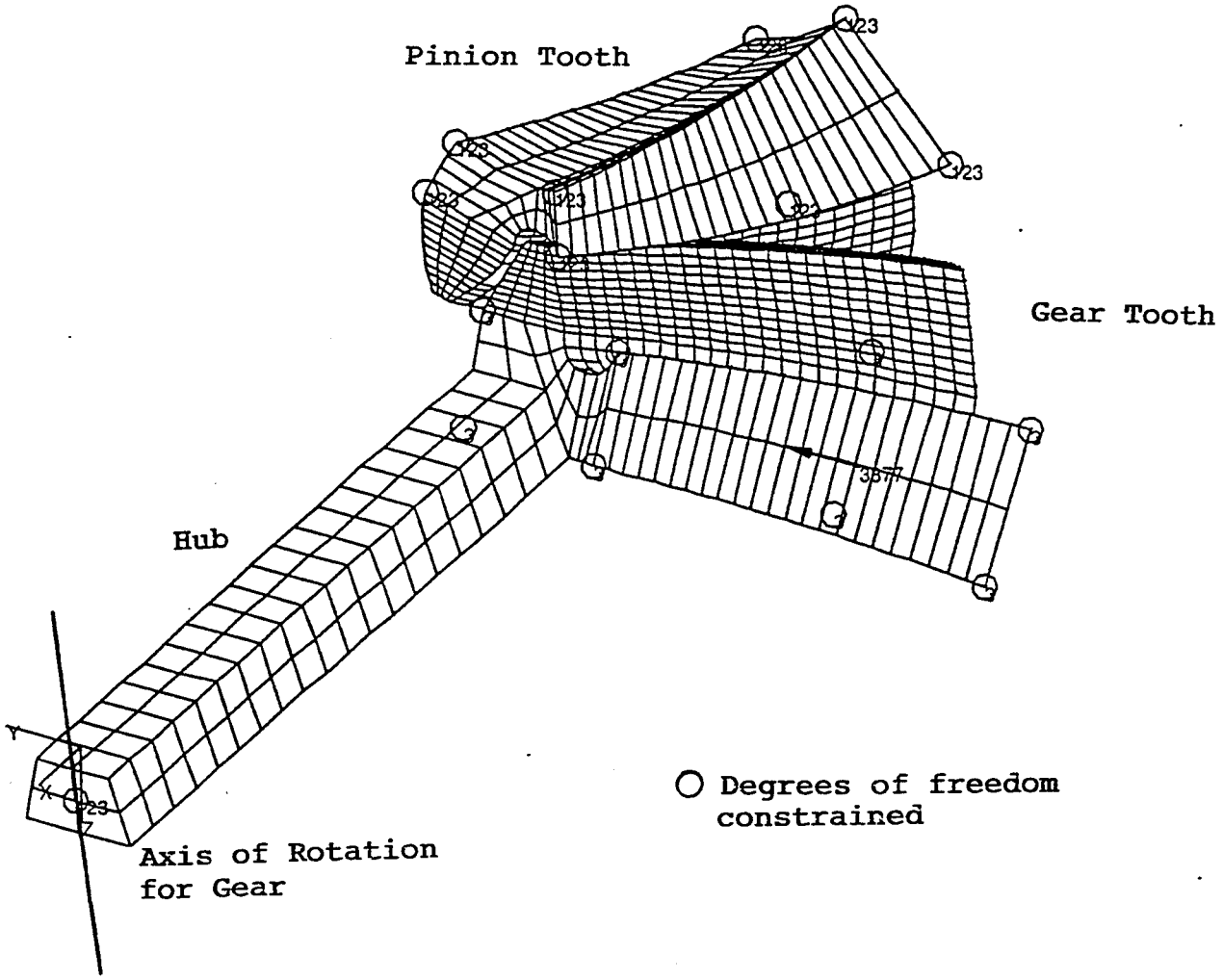

Figure 4.2 Two tooth model with boundary conditions

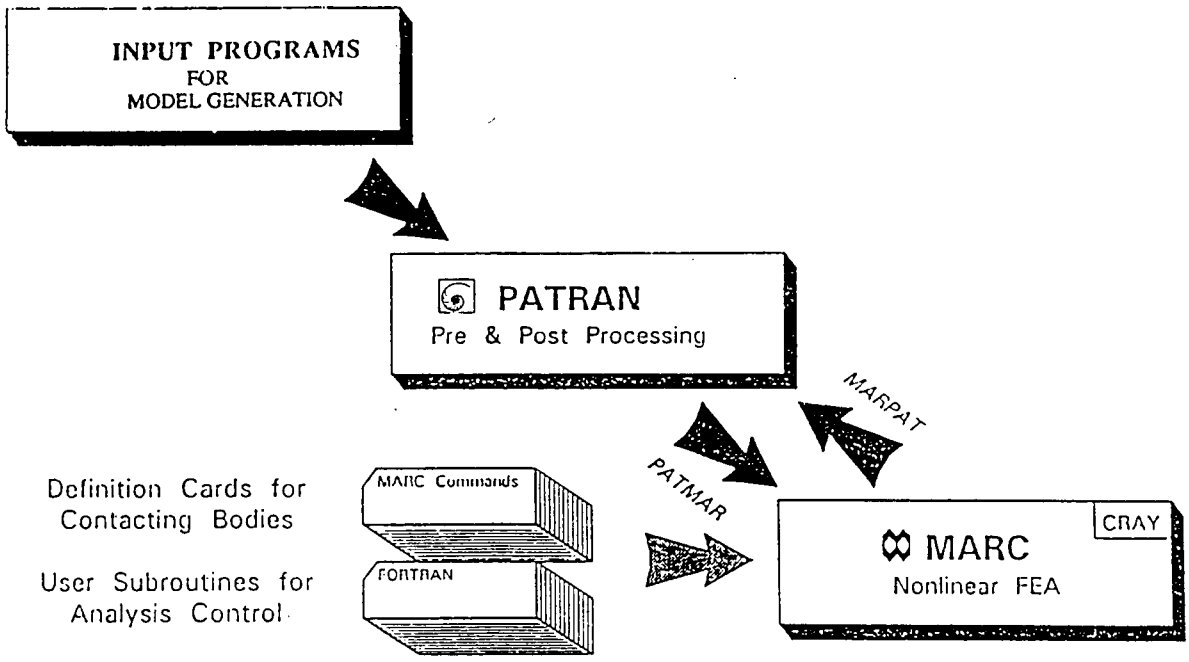

Figure 4.3 Flow diagram for the MARC analysis

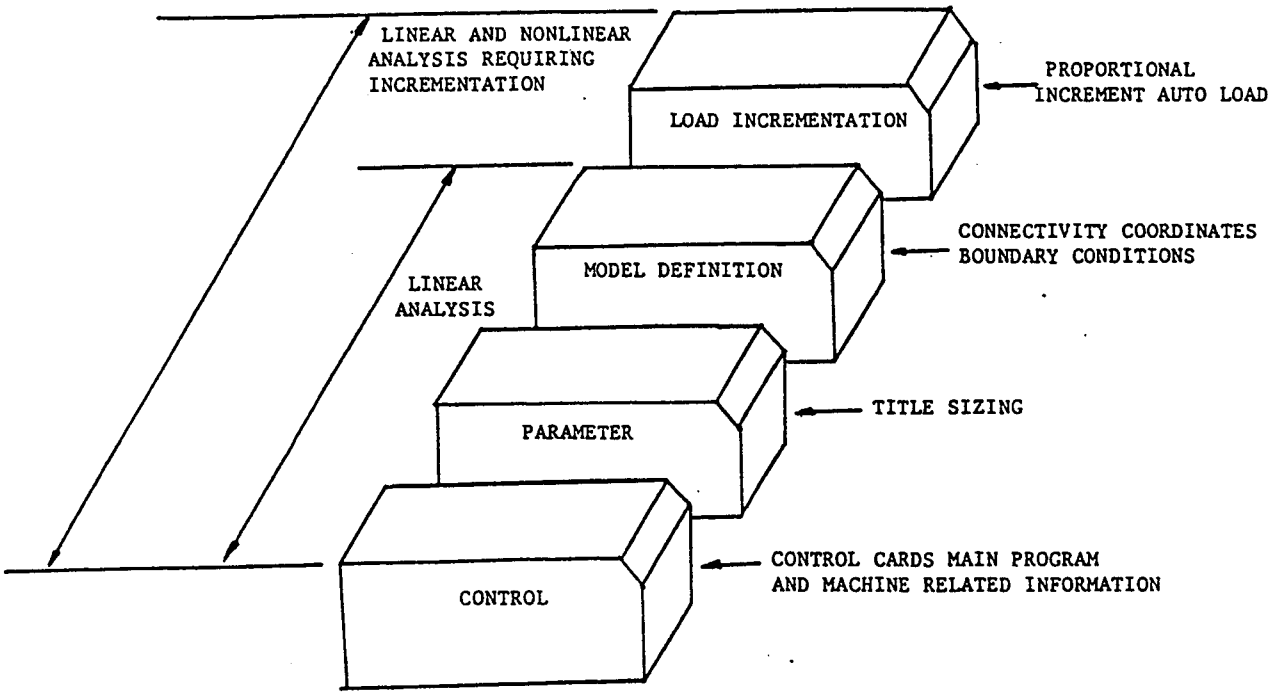

Figure 4.4 MARC Input Deck

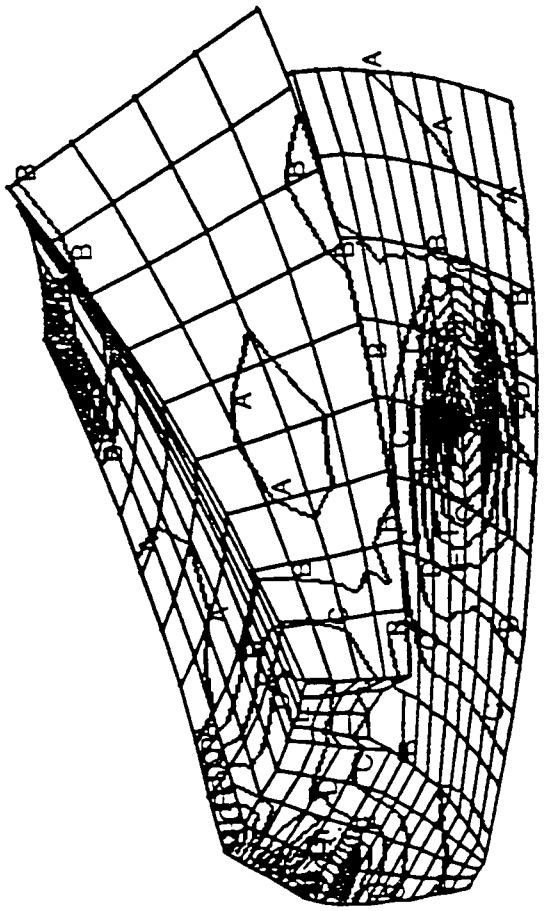

	PSI
A	-6664.
B	-18543.
C	-30422.
D	-42302.
E	-54181.
F	-66060.
G	-77939.
H	-89819.
I	-101698.
J	-113577.
K	-125457.
L	-137336.
M	-149215.
N	-161094.
O	-172974.

Figure 5.1 A typical elliptical contour in the pinion tooth with elemental stresses in seven tooth model (PSI)

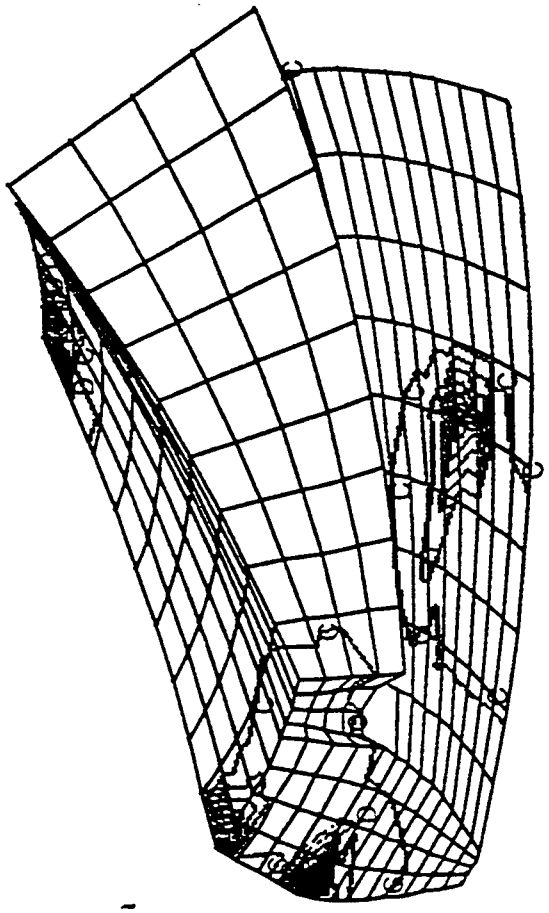

Figure 5.2 A typical elliptical contour in the pinion tooth with nodal stresses in seven tooth model

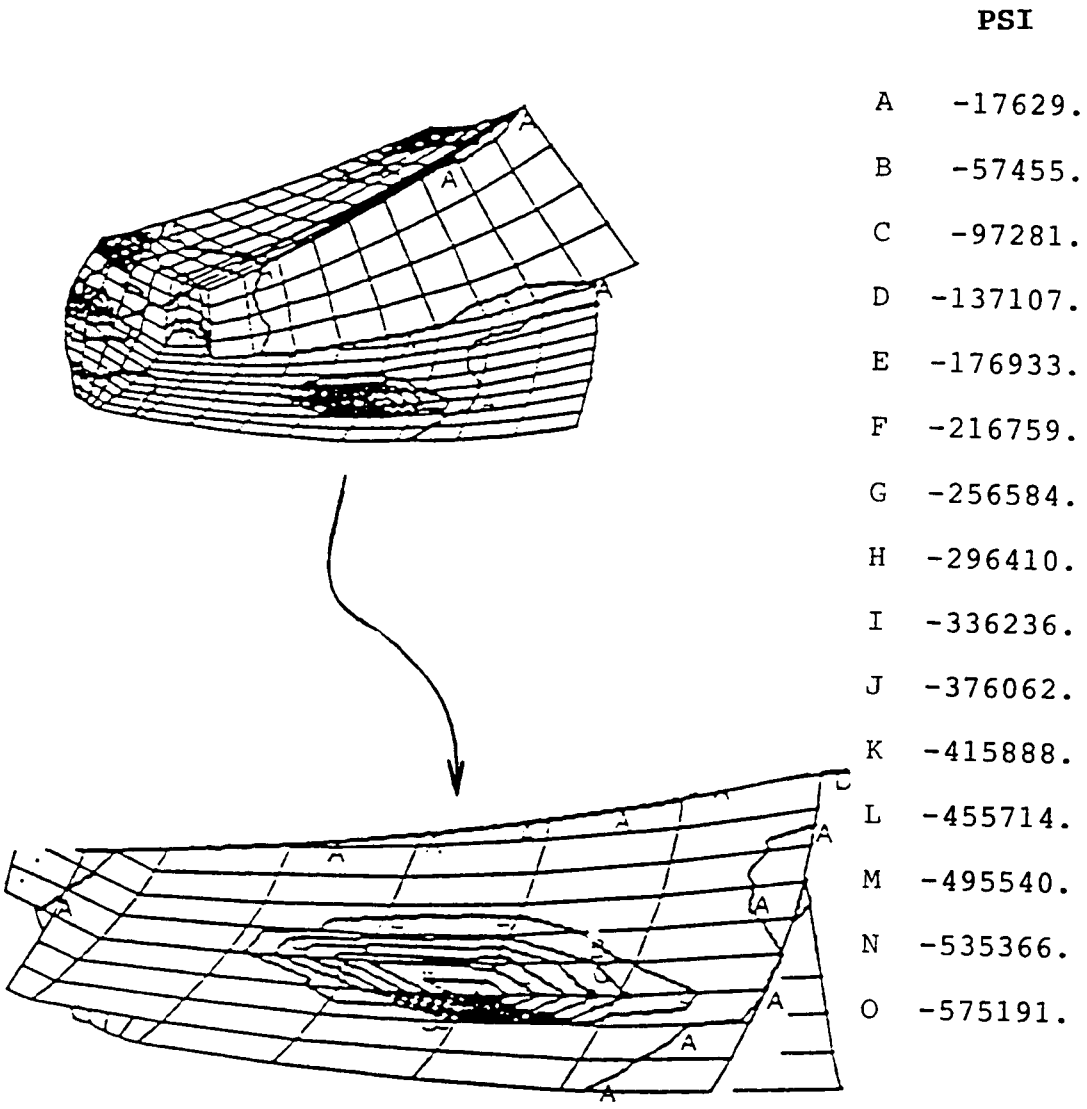

Figure 5.3 Nodal Stress Result on Pinion Obtained From the Gap Element Solution and Seven Tooth Model

PSI

A 85251.

B 22459.

C -40334.

D -103126.

E -165918.

F -228711.

G -291503.

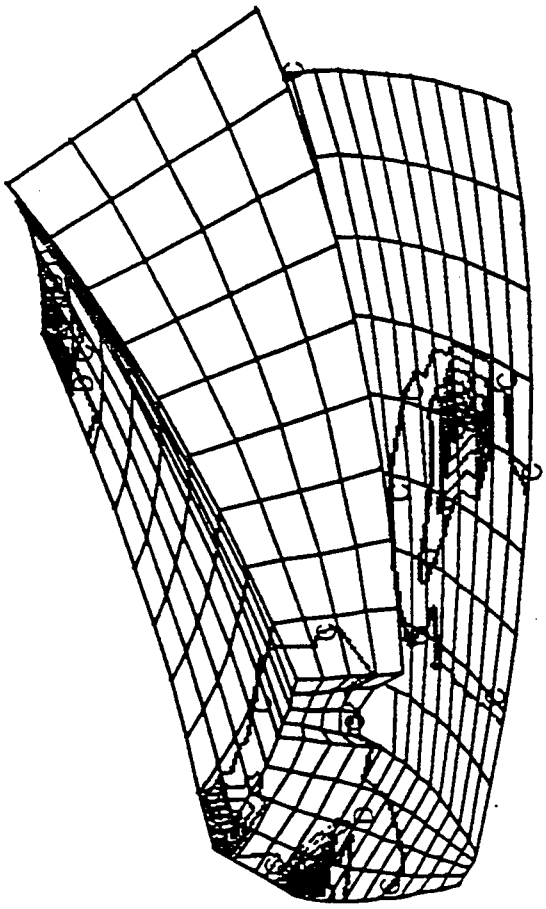

Figure 5.4 Nodal stress result on pinion obtained from automated contact analysis in seven tooth model

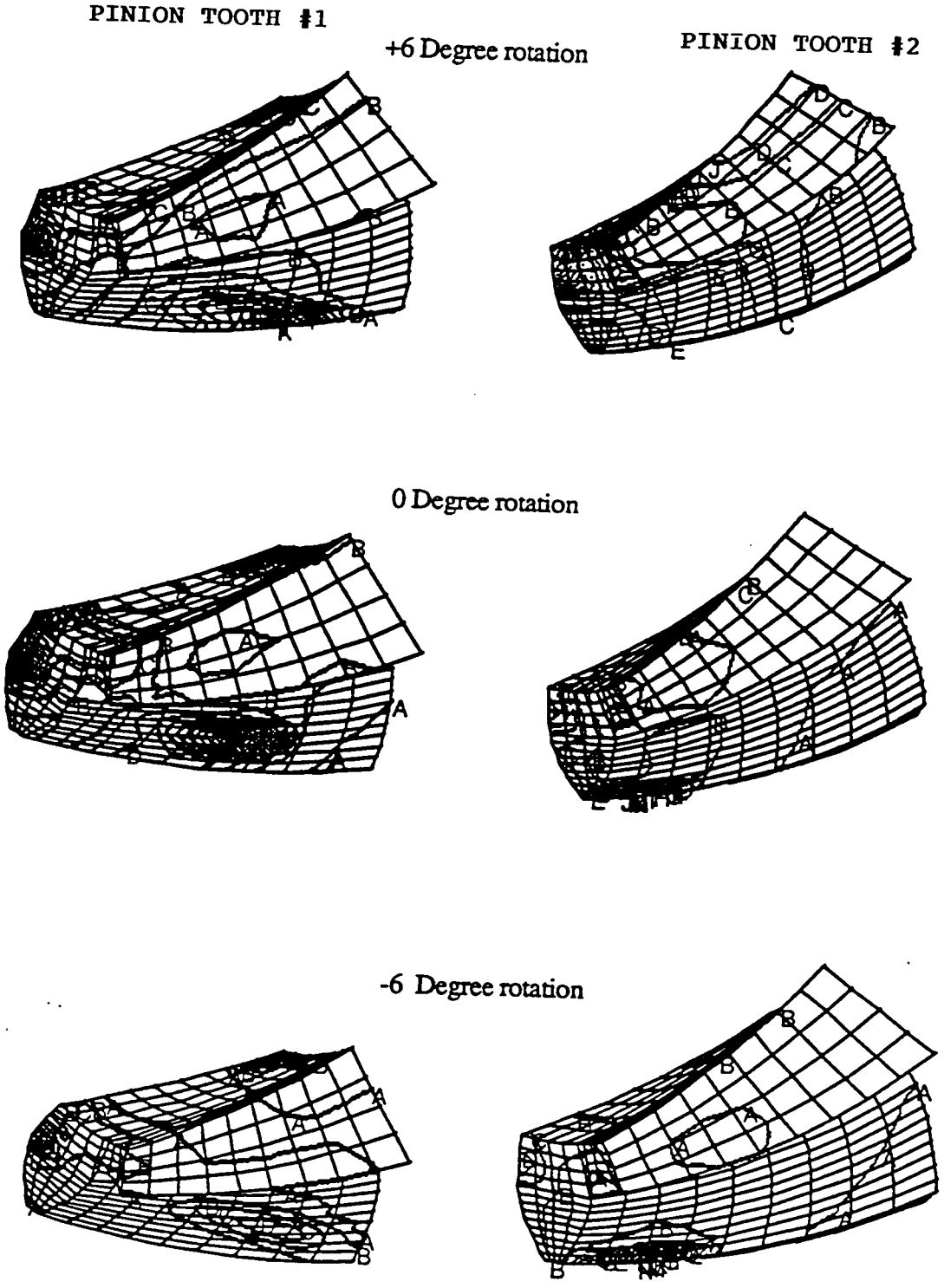

Figure 5.5 Elemental Stresses for Pinion Tooth #1 and Pinion Tooth #2 as They Roll In and Out of Mesh for Rotations from +6 to -30 Degrees in Seven Tooth Model.

Pinion Tooth #1

-12 Degree rotation

Pinion Tooth #2

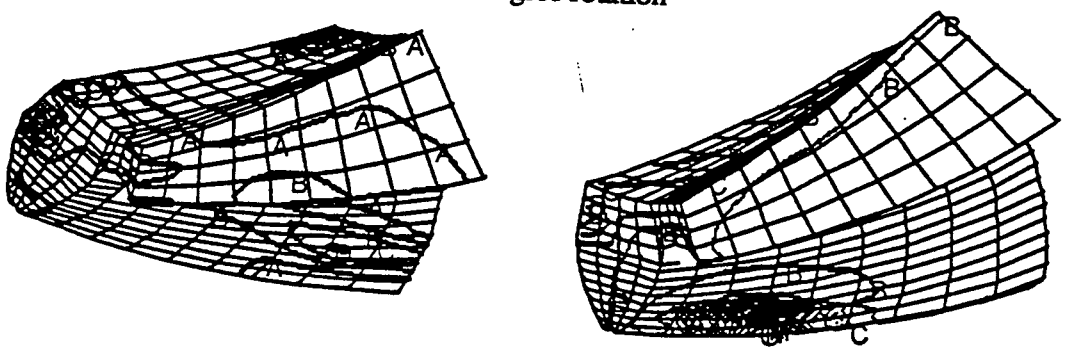

-18 Degree rotation

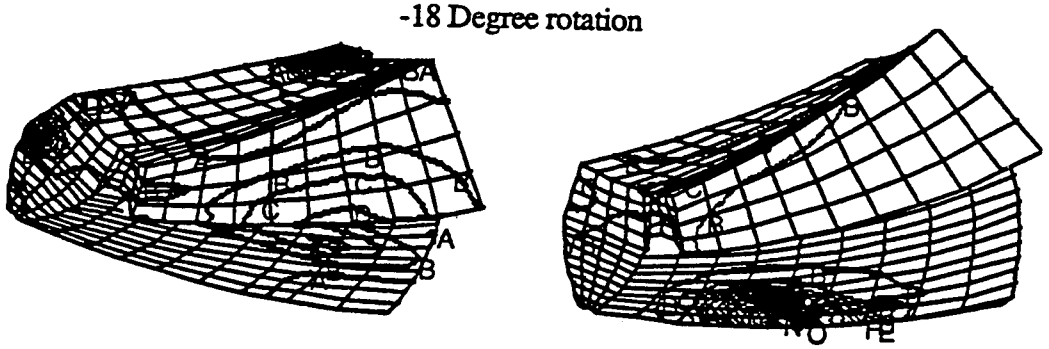

-24 Degree rotation

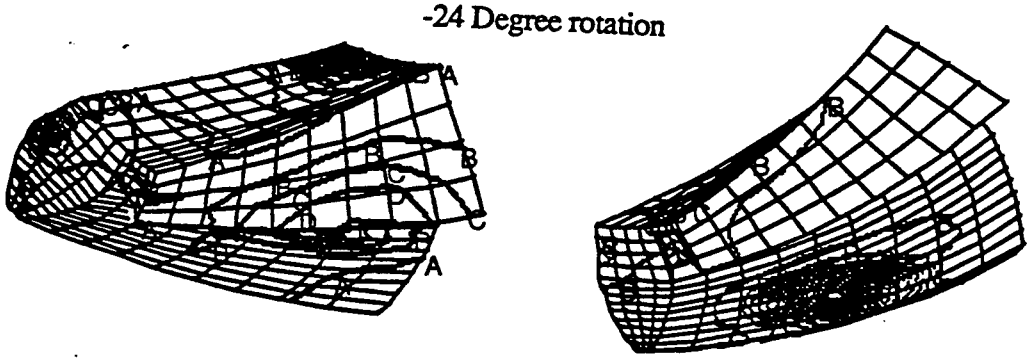

-30 Degree rotation

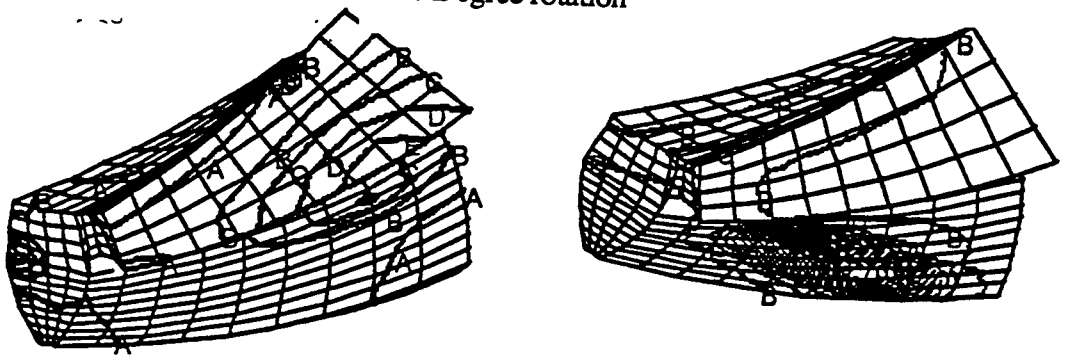

Figure 5.5 (continued)

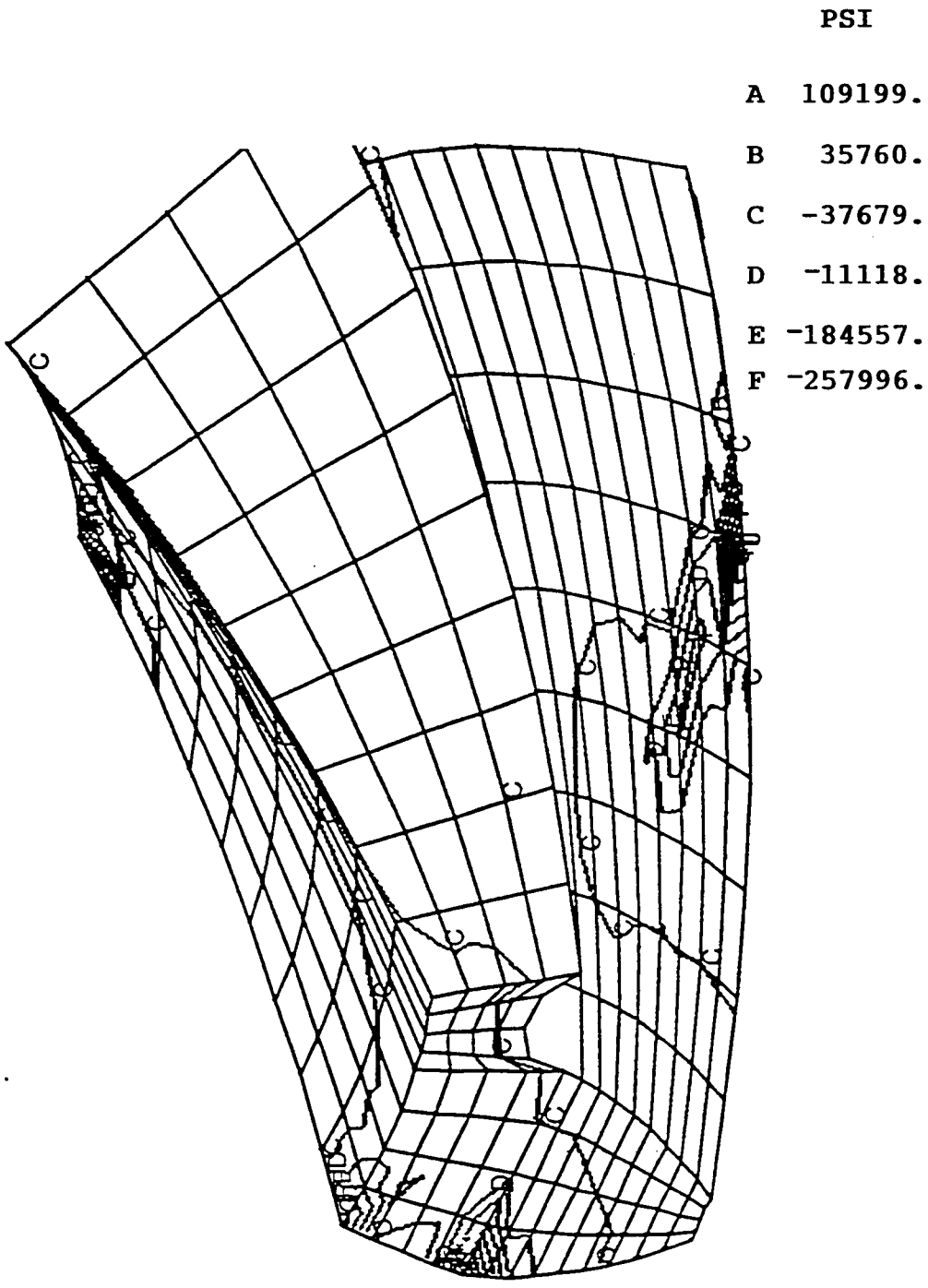

Figure 5.6 Nodal stresses on pinion tooth #1 after it is rotated by +6 degrees in the seven tooth model

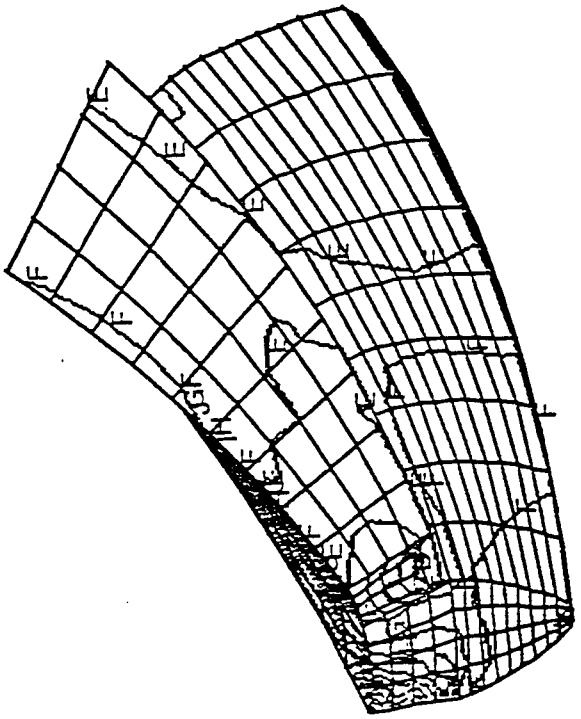

Figure 5.7 Nodal stresses on pinion tooth #2 after it is rotated by +6 degrees in the seven tooth model (No Contact)

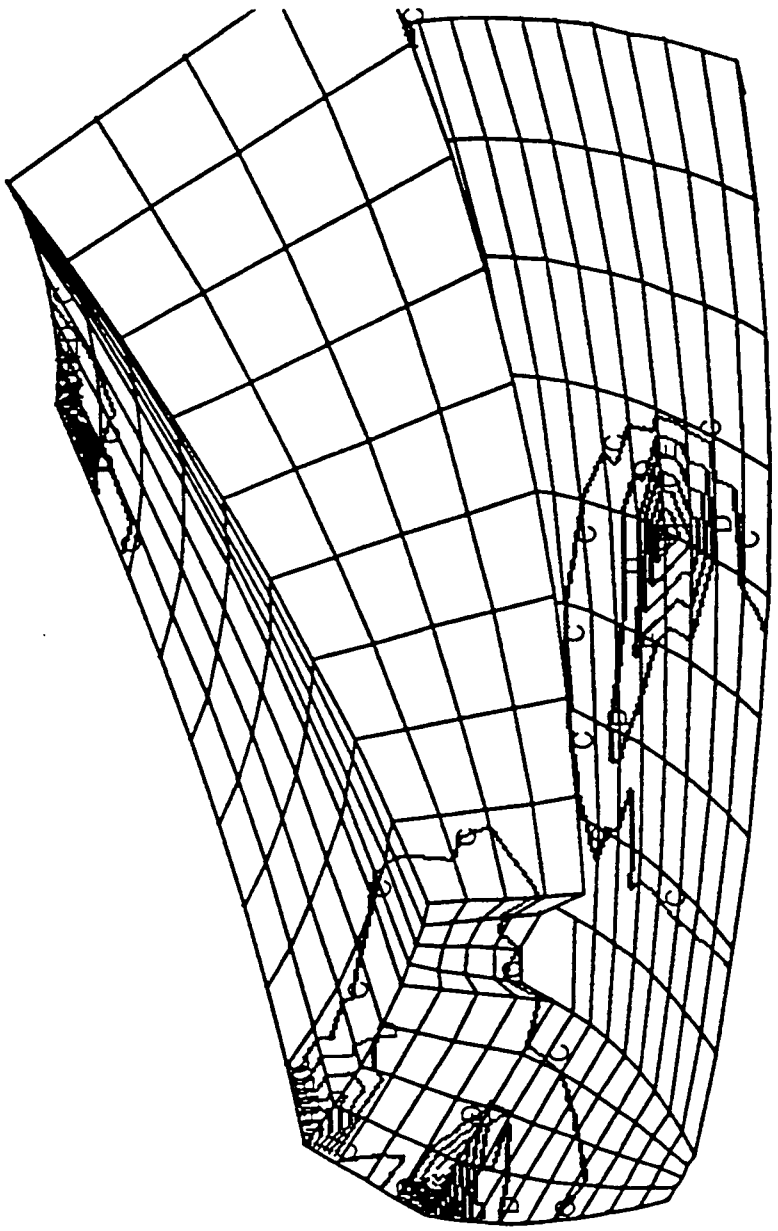

Figure 5.8 Nodal stresses on pinion tooth #1 after it is rotated by 0 degrees in the seven tooth model

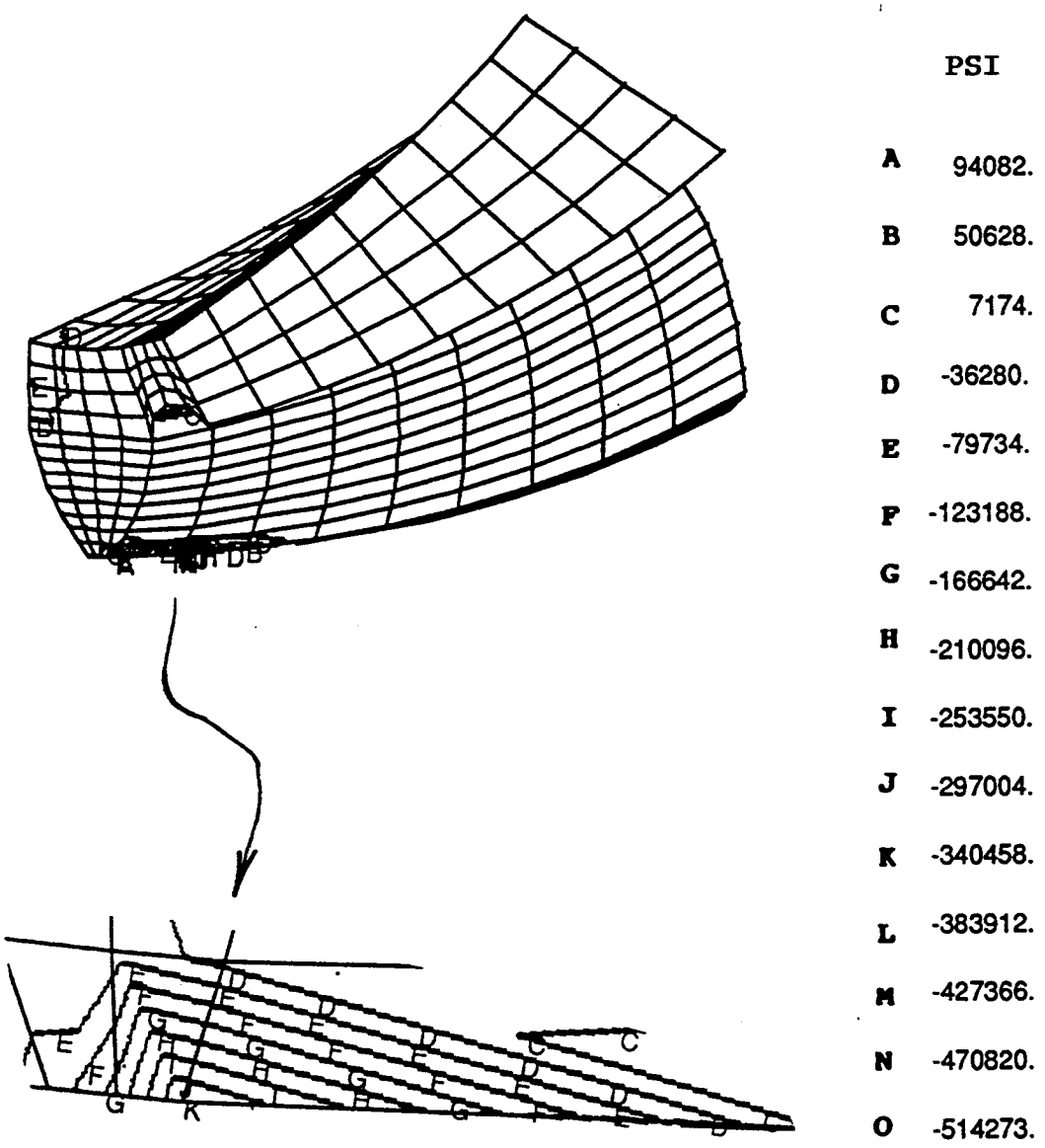

Figure 5.9 Nodal Stress on Pinion Tooth #2 after it is rotated 0 Degrees in the Seven Tooth Model

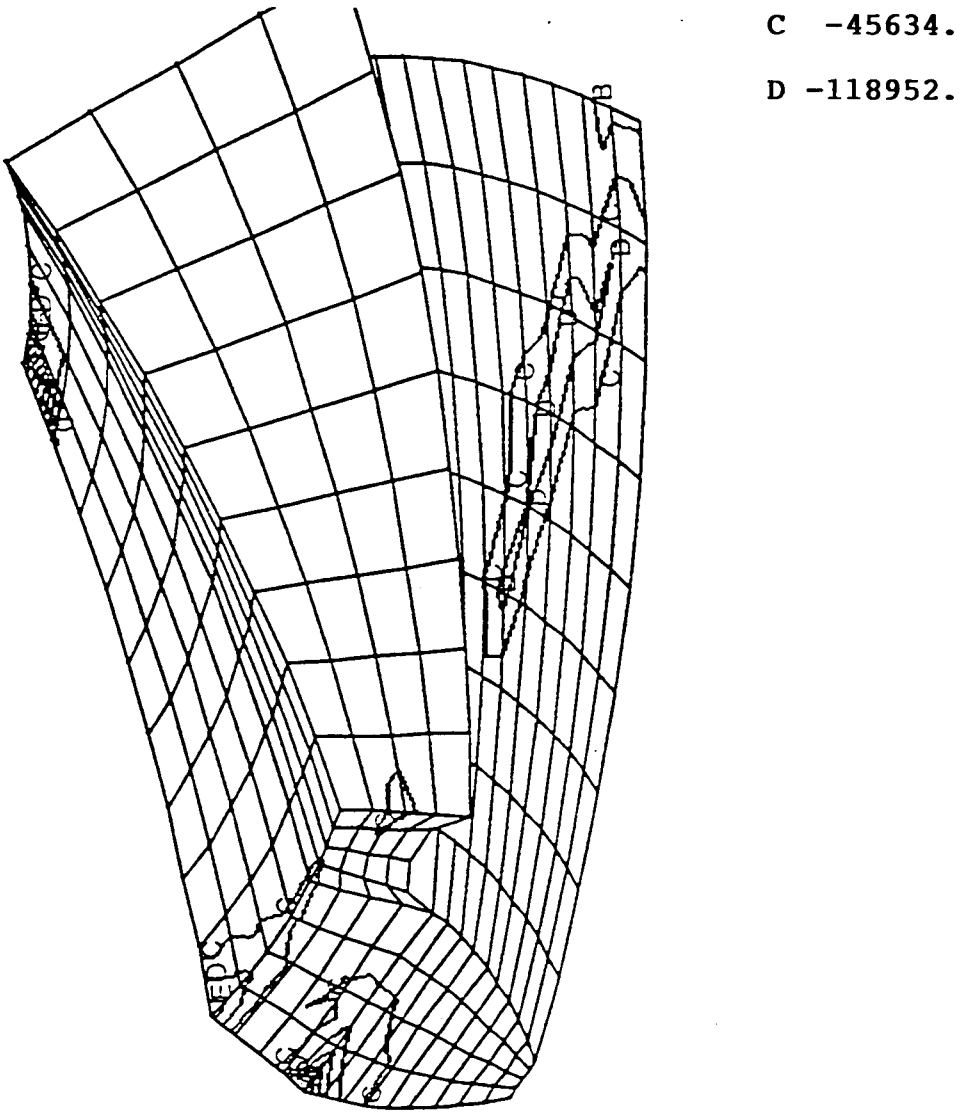

Figure 5.10 Nodal stresses on pinion tooth #1 after it is rotated by -6 degrees in the seven tooth model

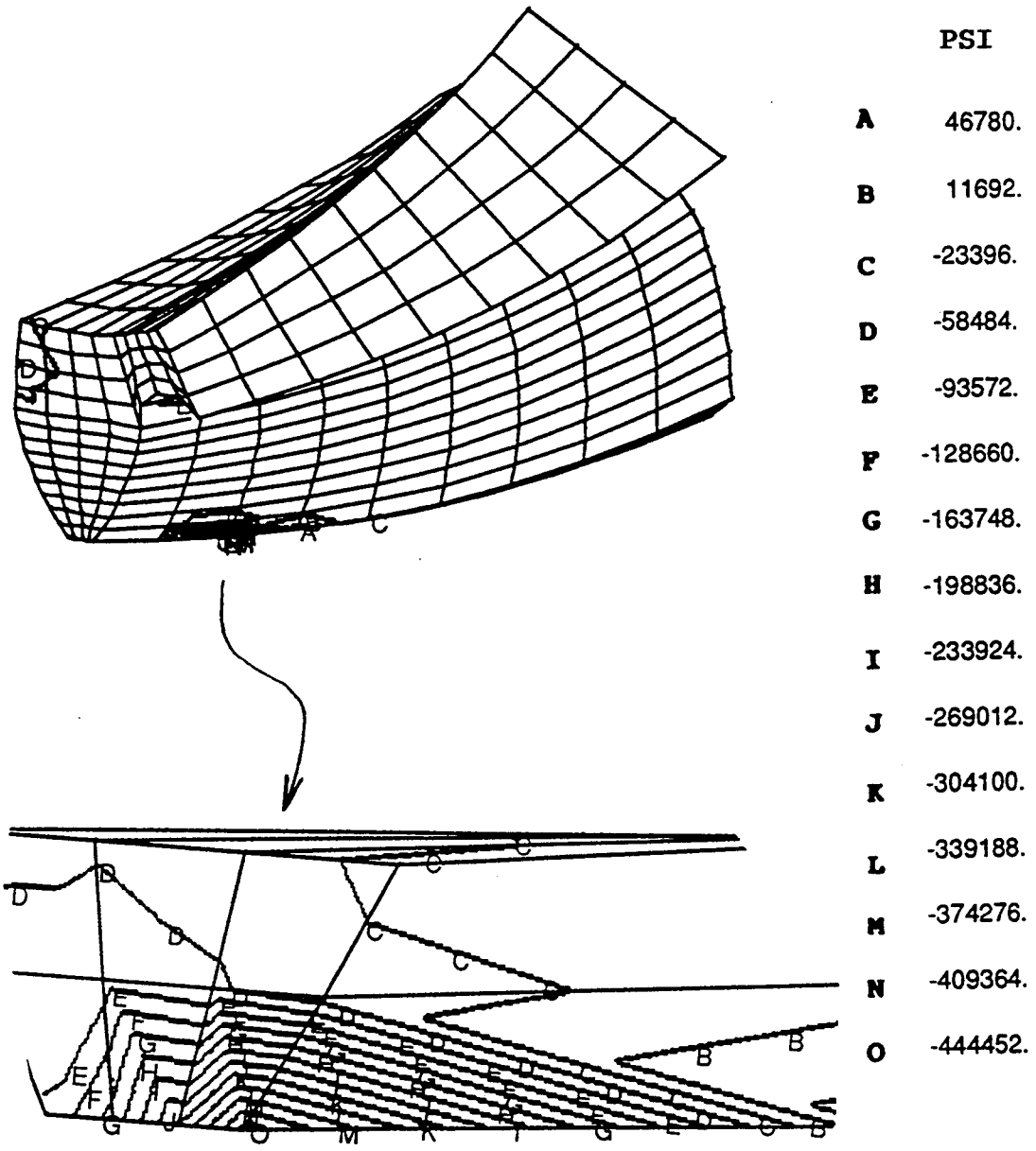

Figure 5.11 Nodal Stress on Pinion Tooth #2 after it is rotated -6 Degrees in the Seven Tooth Model

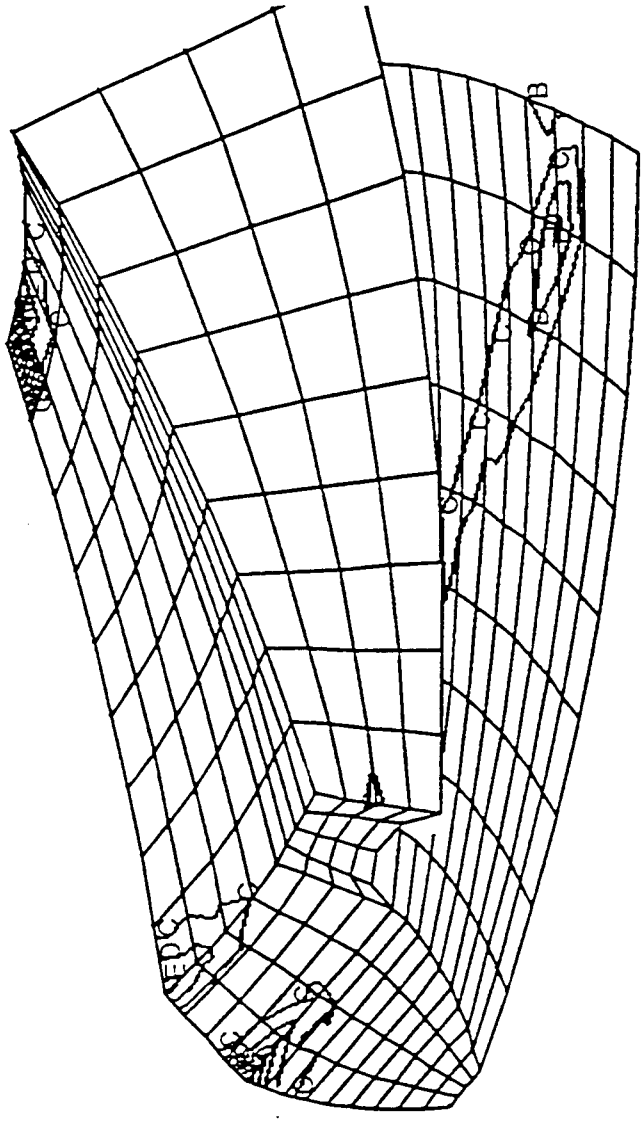

Figure 5.12 Nodal stresses on pinion tooth #1 after it is rotated by -12 degrees in the seven tooth model

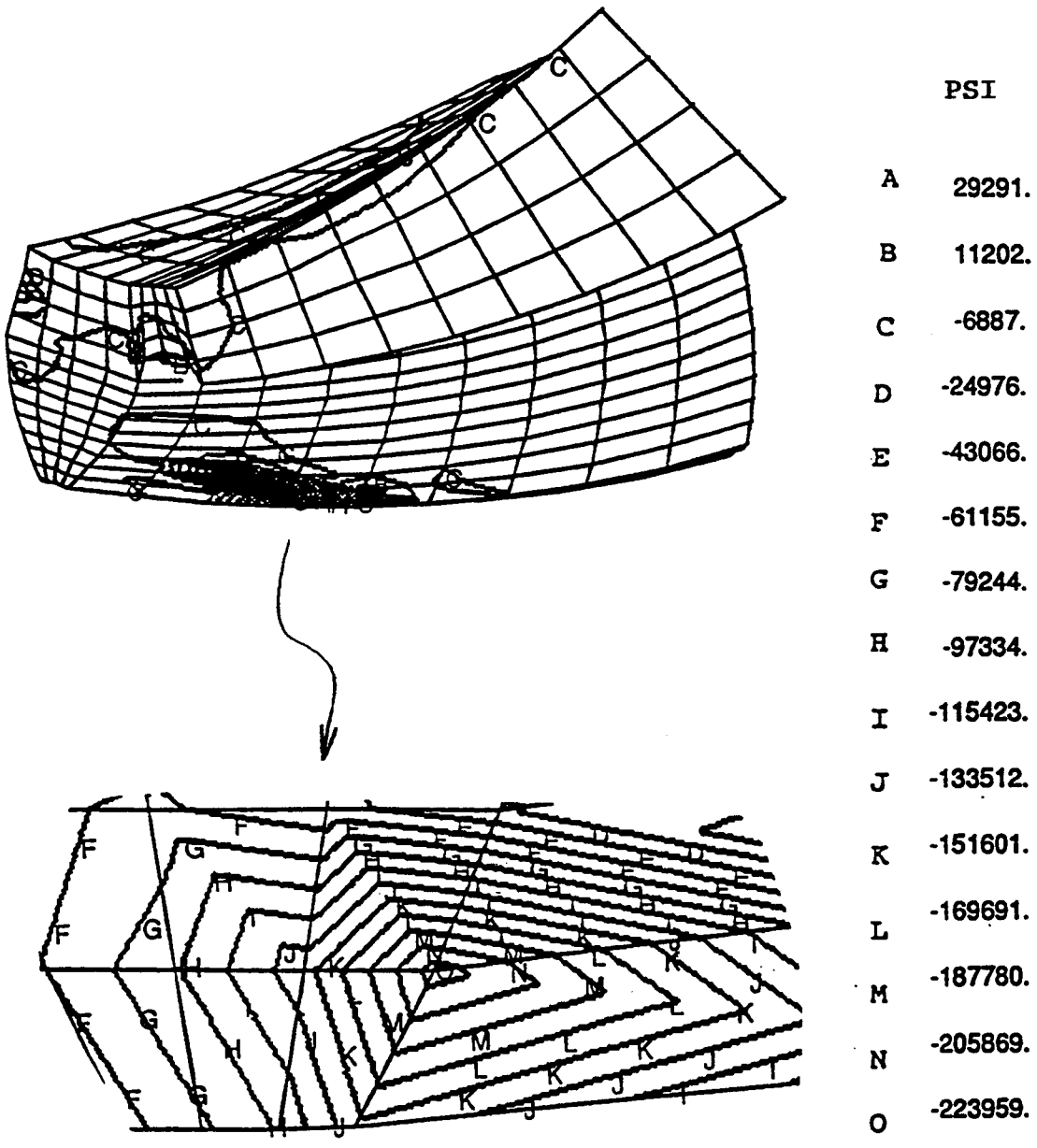

Figure 5.13 Nodal Stress on Pinion Tooth #2 after it is rotated -12 Degrees in the Seven Tooth Model

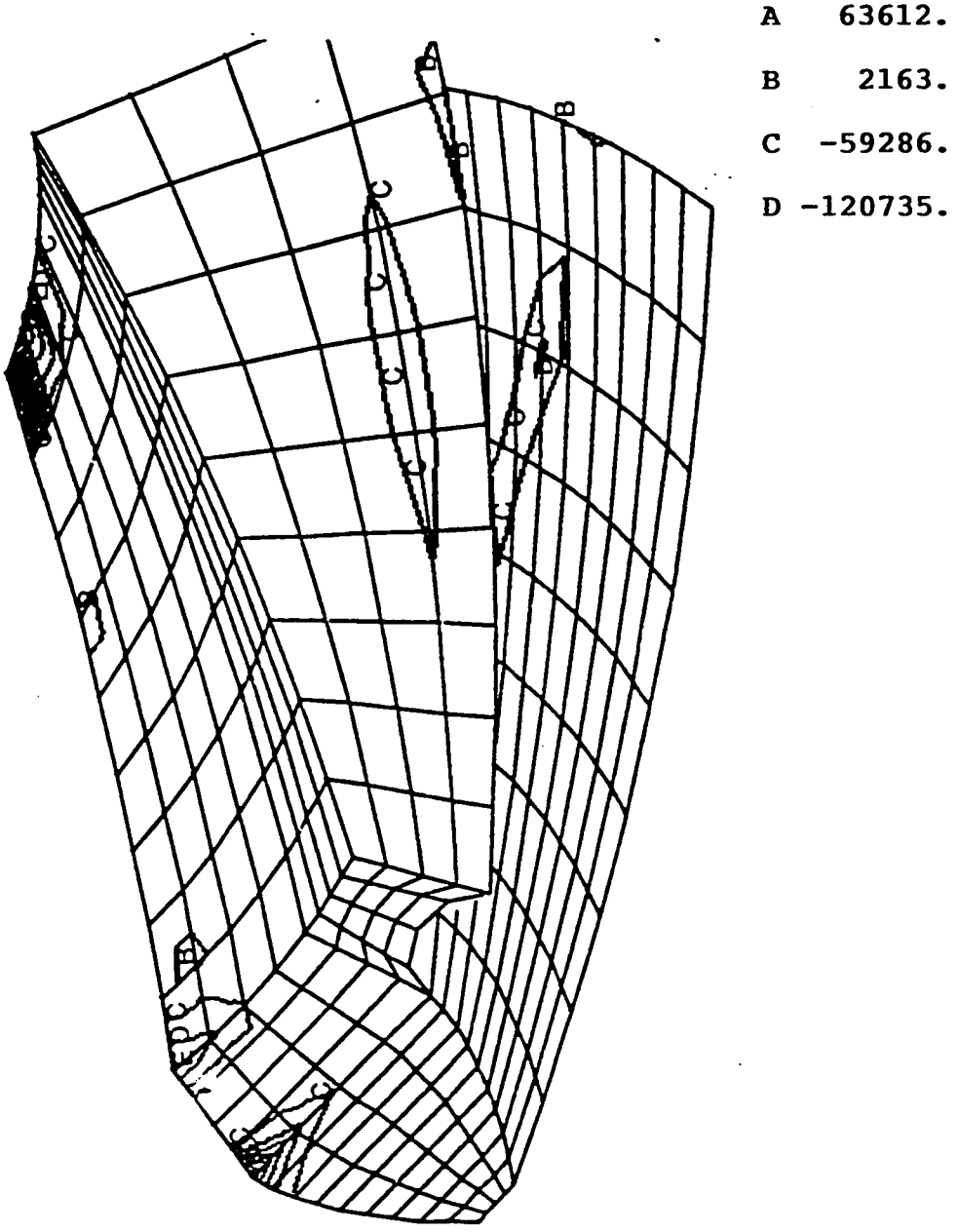

Figure 5.14 Nodal stresses on pinion tooth #1 after it is rotated by -18 degrees in the seven tooth model

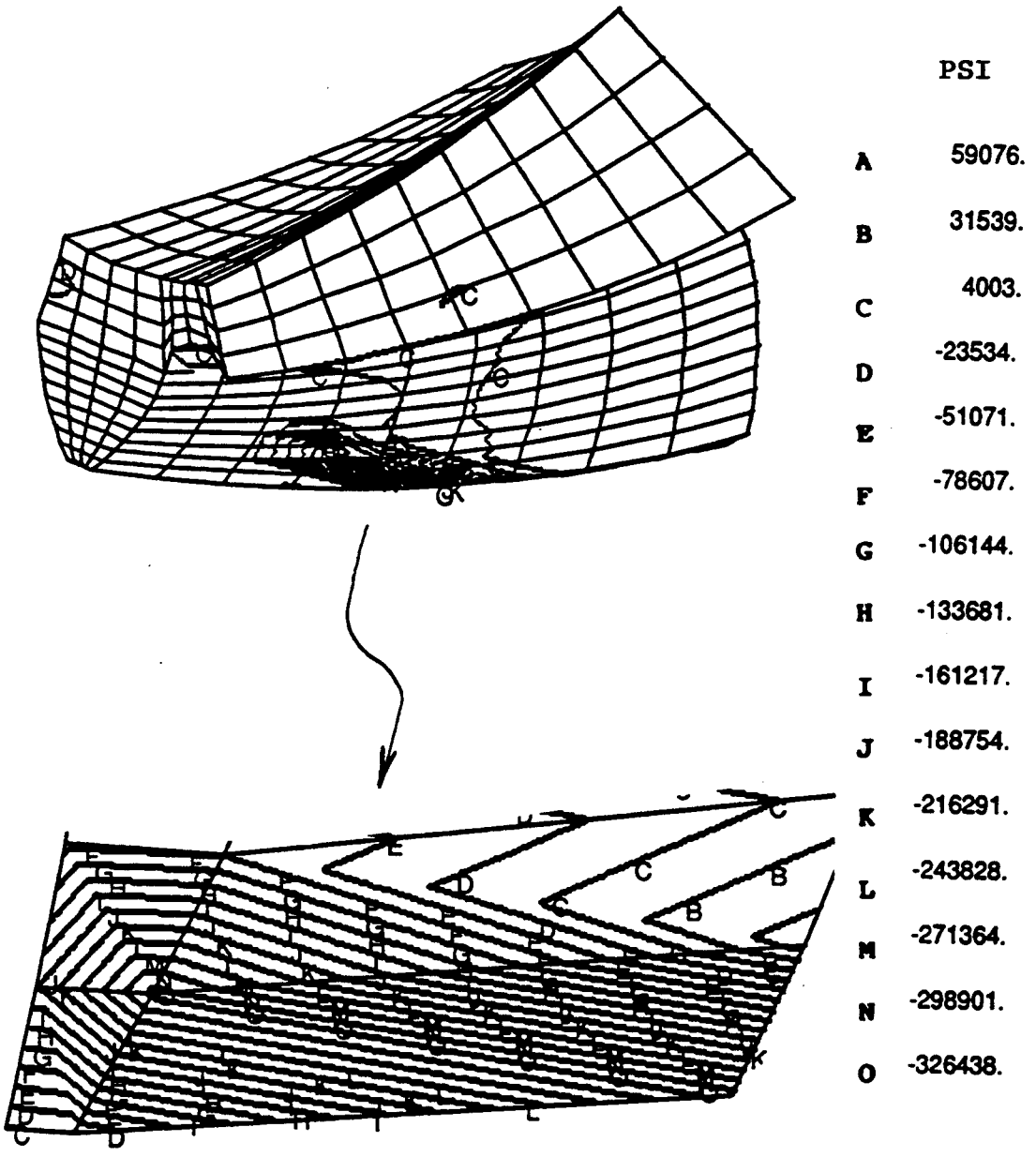

Figure 5.15 Nodal Stress on Pinion Tooth #2 after it is rotated -18 Degrees in the Seven Tooth Model

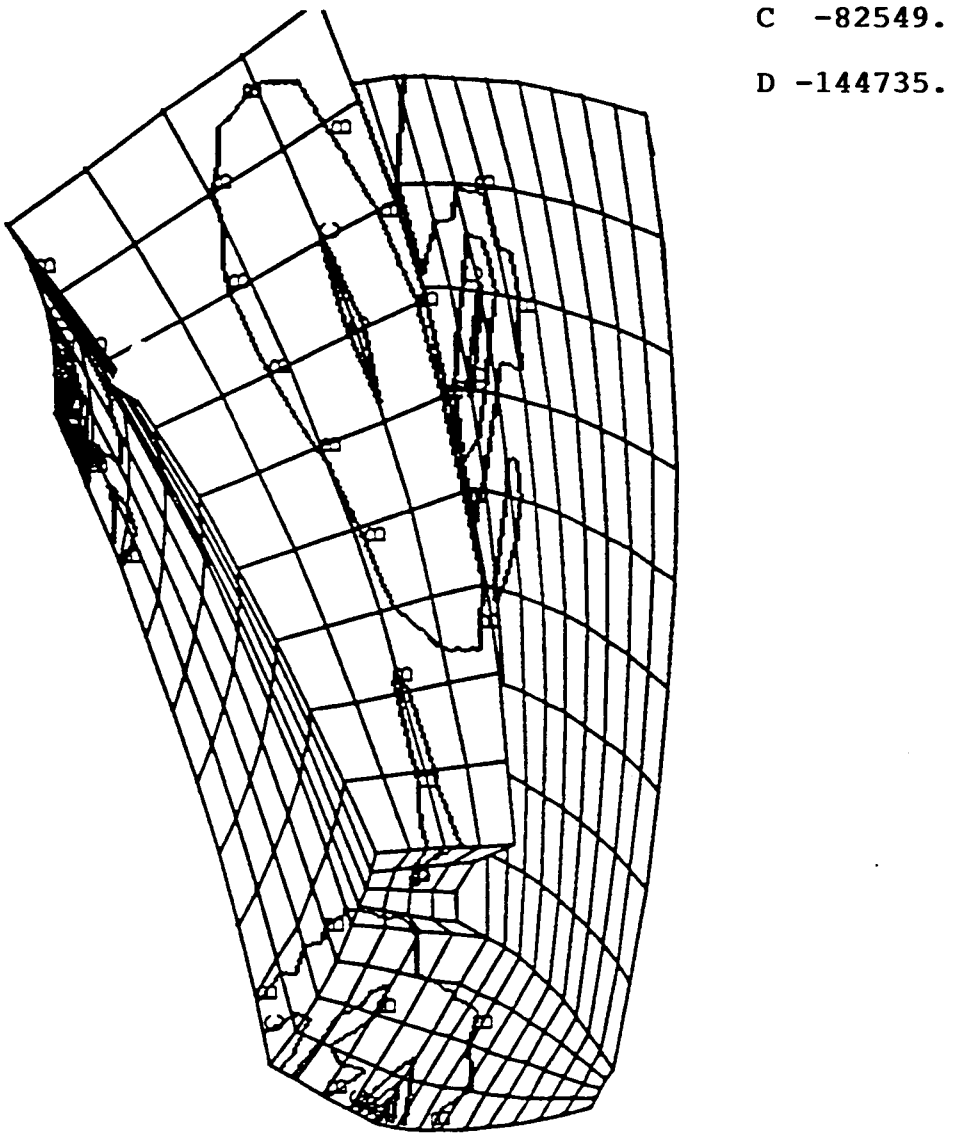

Figure 5.16 Nodal stresses on pinion tooth #1 after it is rotated by -24 degrees in the seven tooth model

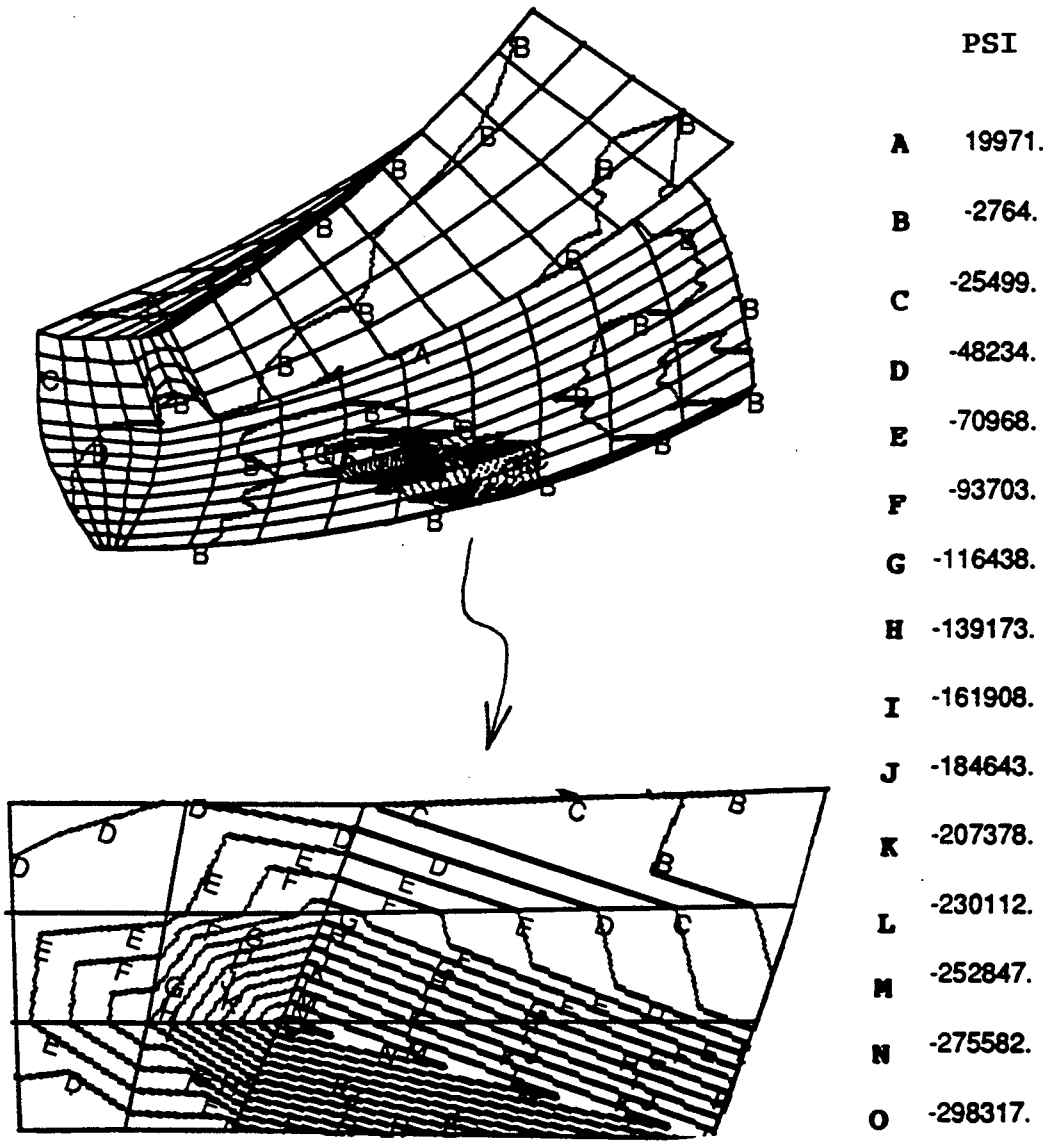

Figure 5.17 Nodal Stress on Pinion Tooth #2 after it is rotated -24 Degrees in the Seven Tooth Model

PSI

A 21750.

B -40817.

C-103384.

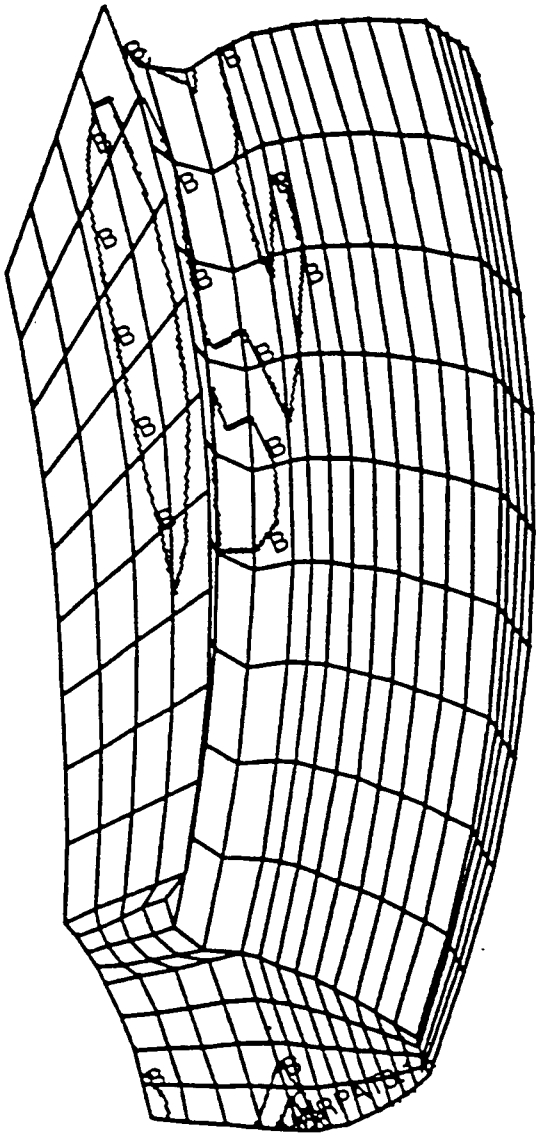

Figure 5.18 Nodal stresses on pinion tooth #1 after it is rotated by -30 degrees in the seven tooth model

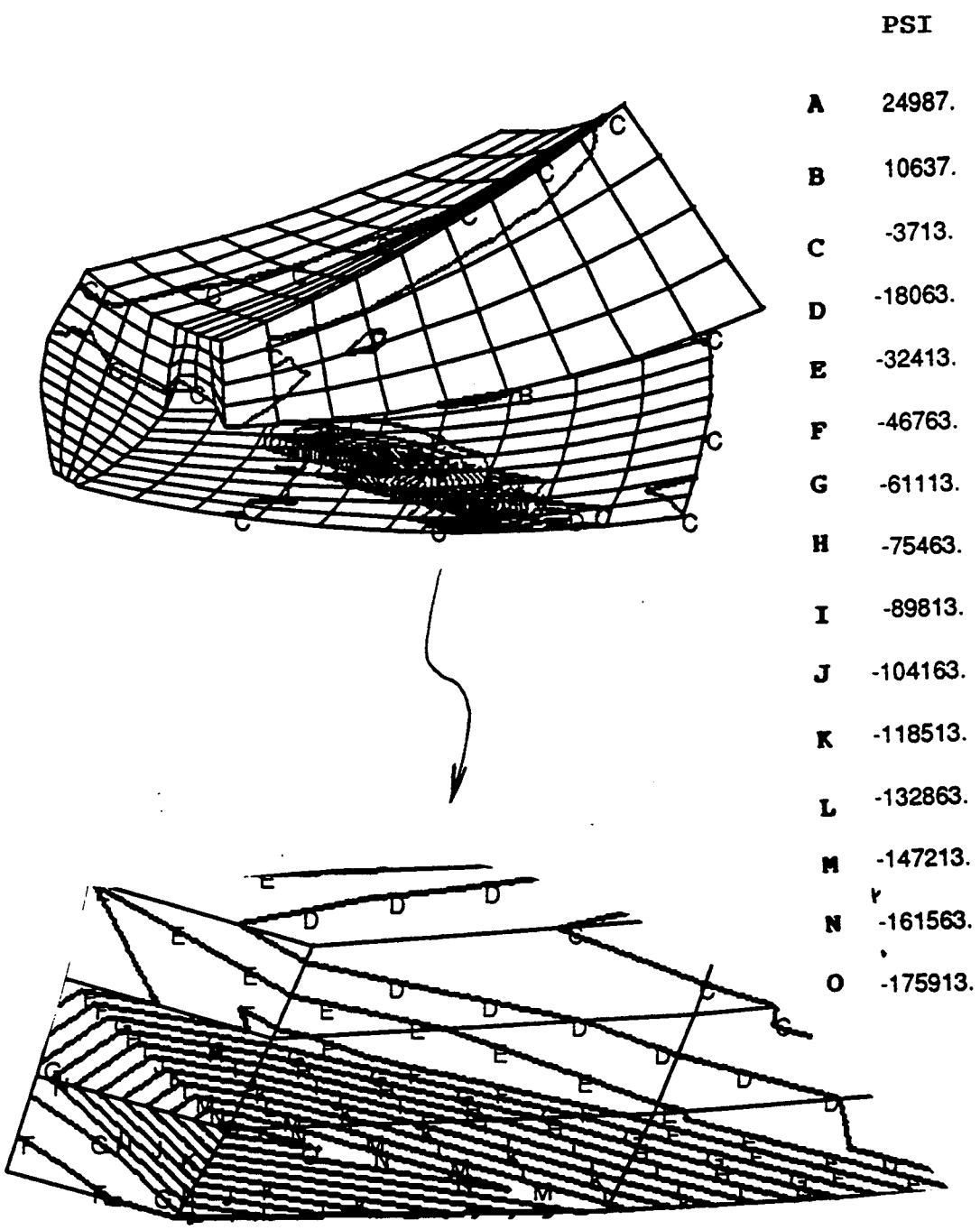

Figure 5.19 Nodal Stress on Pinion Tooth #2 after it is rotated -30 Degrees in the Seven Tooth Model

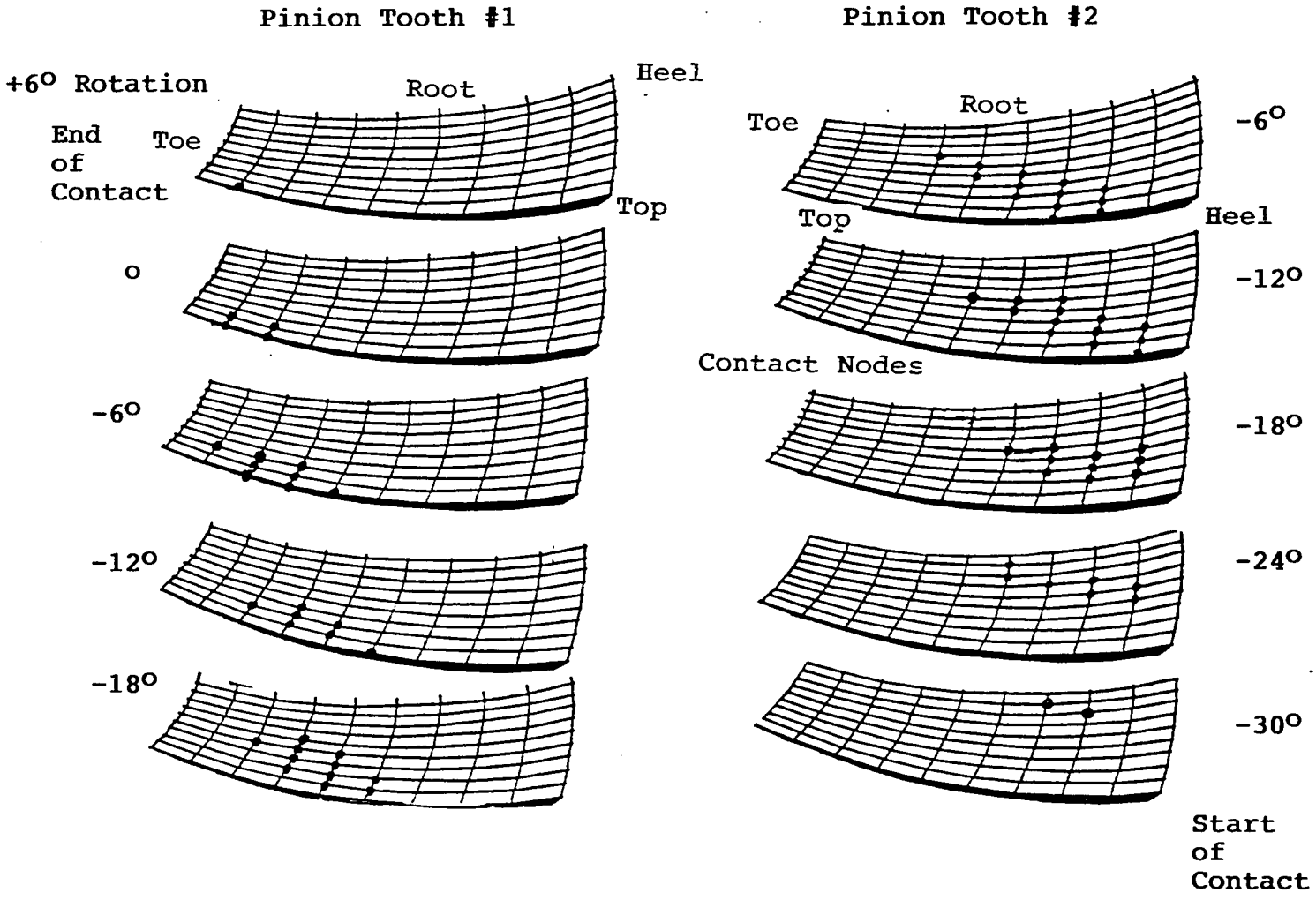

Figure 5.20 Nodal contact points on pinion. Shift in the contact nodes on pinion teeth at selected rotations during meshing for the seven tooth model

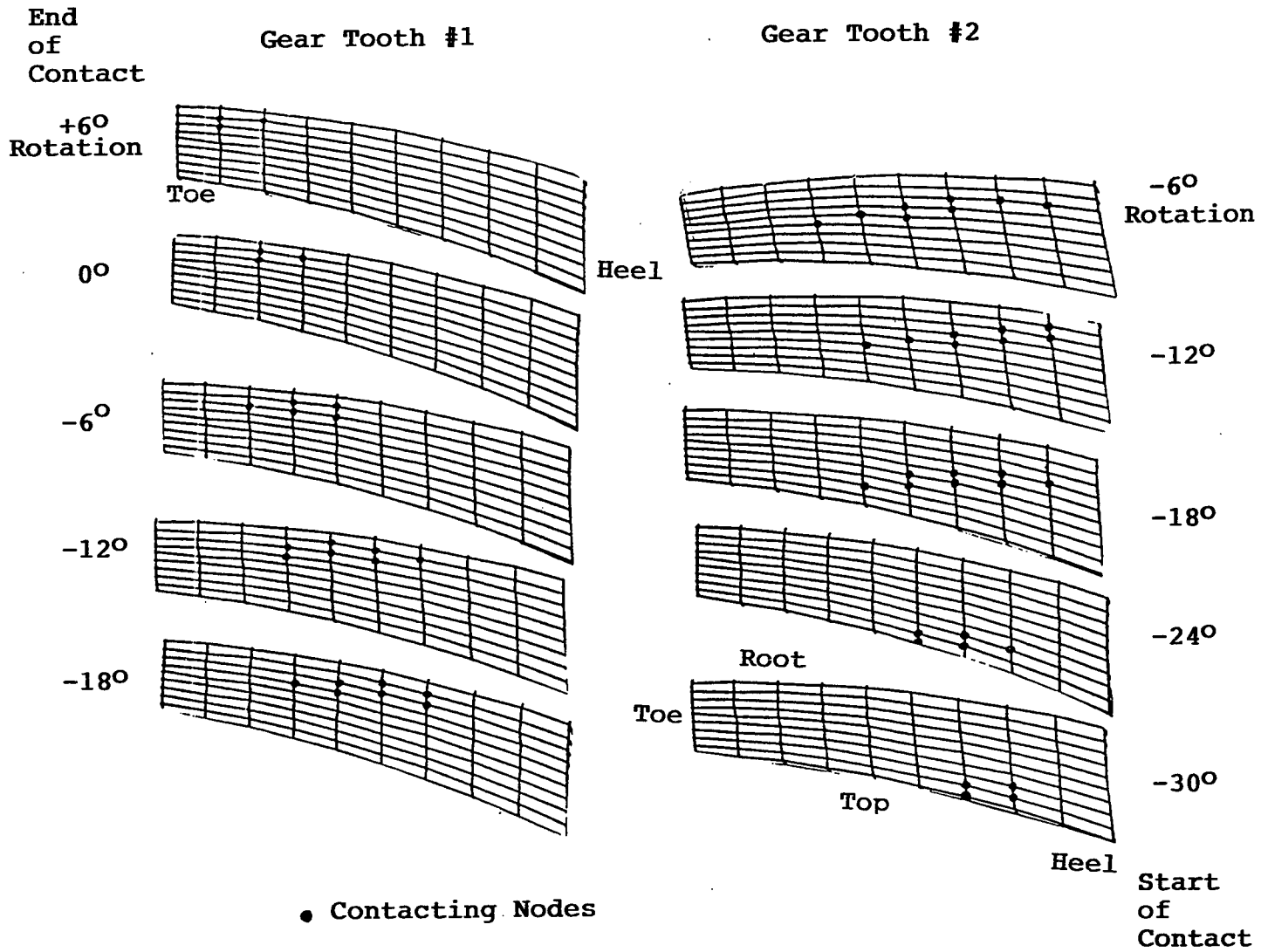

Figure 5.21 Nodal Contact Points on Gear. Shift in the contact nodes on gear teeth at selected rotations during meshing for the seven tooth model

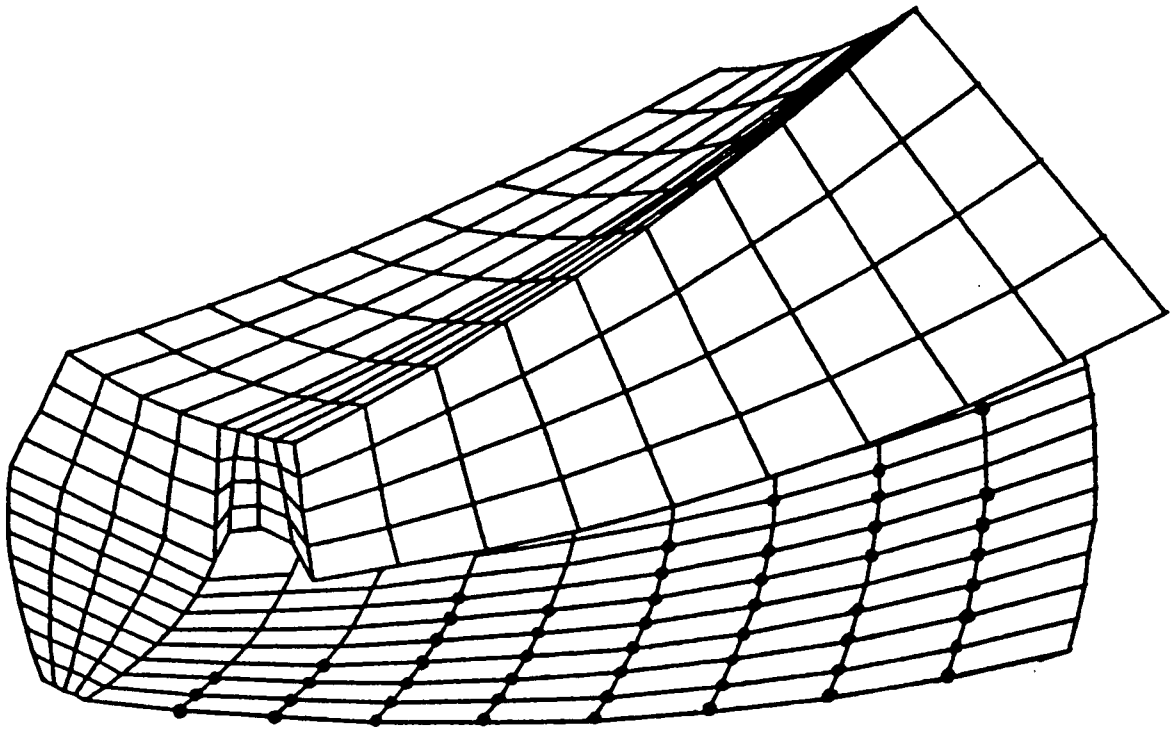

Figure 5.22 Contact Node Density for the Seven Tooth Model

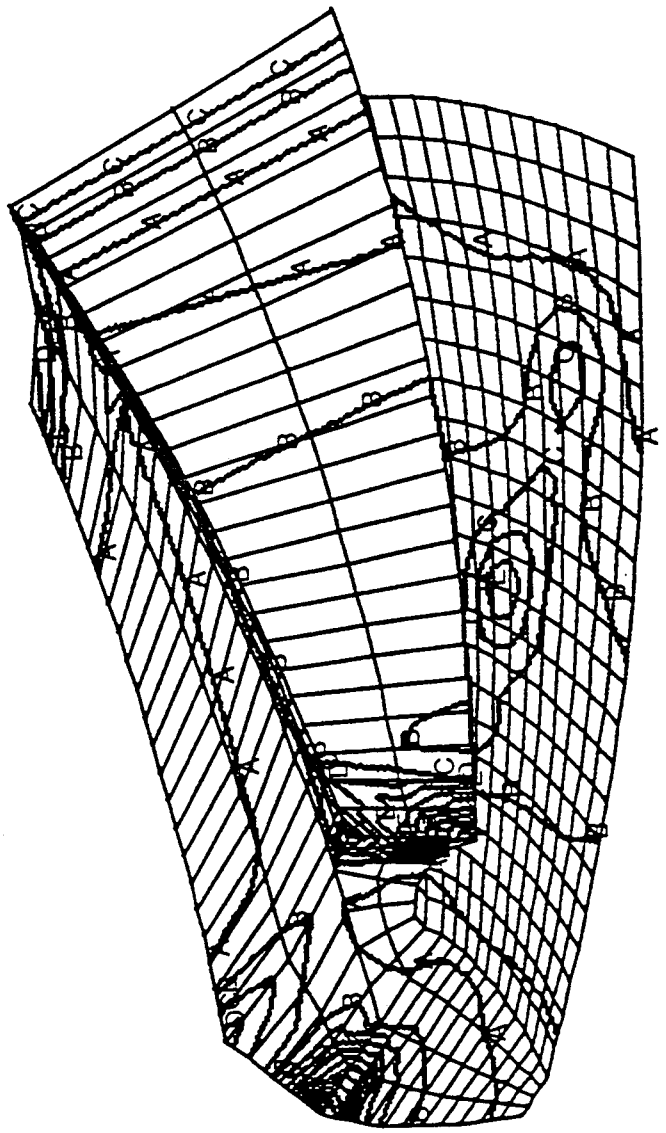

Figure 5.23 Elemental stress results for two tooth model at -6 degree rotation

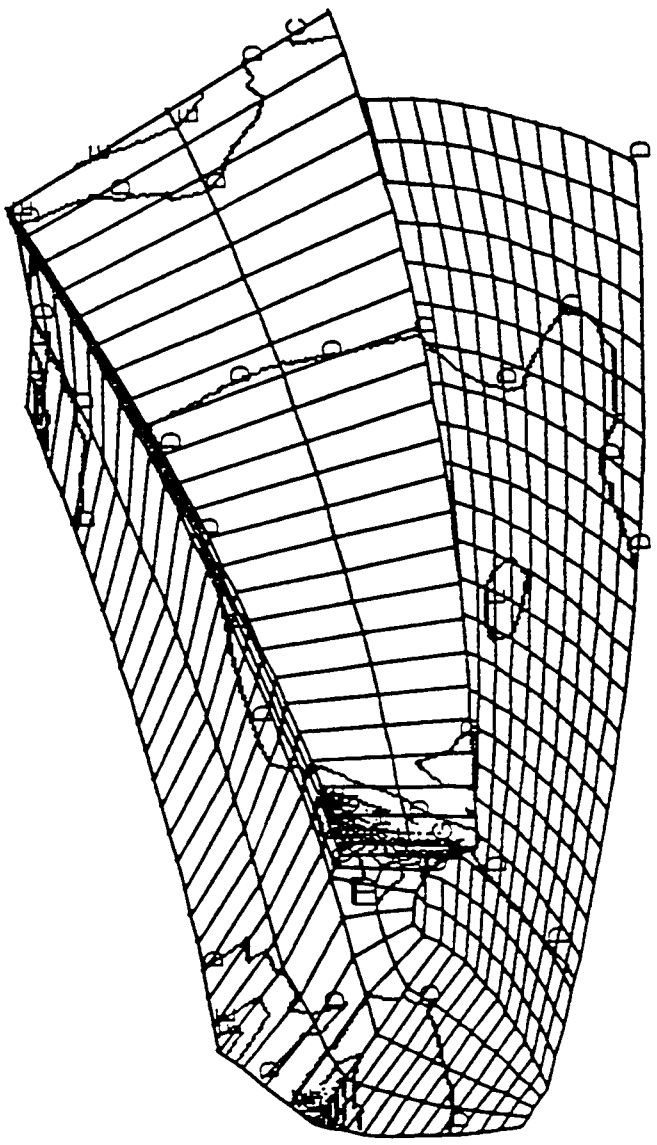

Figure 5.24 Nodal stress results for two tooth model at -6 degree rotation

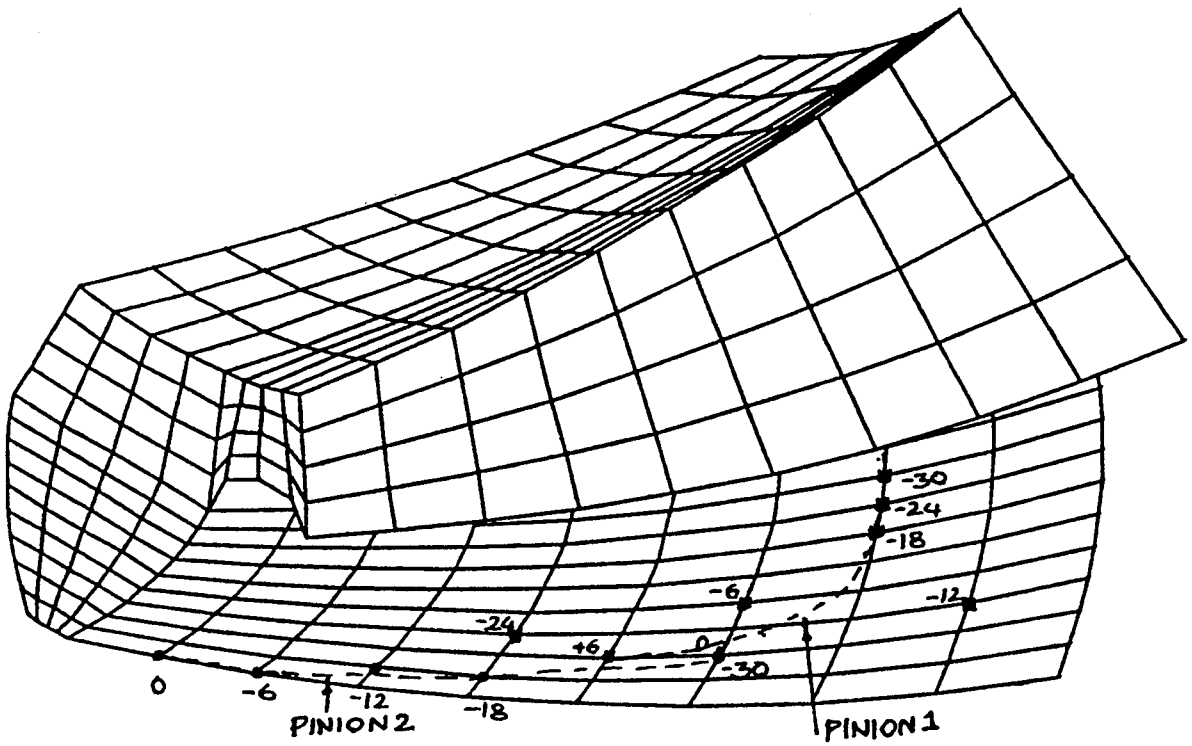

Figure 5.25 Contact Path of Seven Tooth Model in Pinion Tooth #1 and Pinion Tooth #2. Shown is the Location of the Highest Contact Force For Each Rotation Indicated.

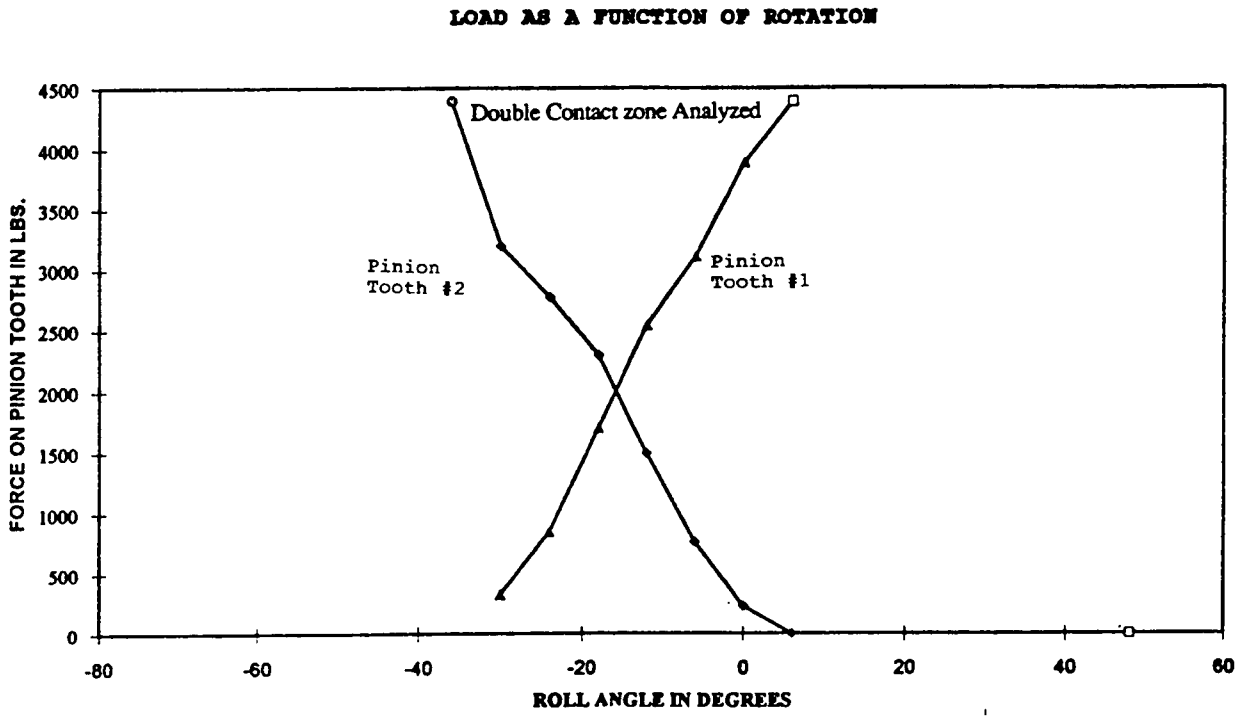

Figure 5.26 Load on Tooth as a Function of Rotation

Figure 5.26 Load on Tooth as a Function of Rotation

Pinion Tooth #1

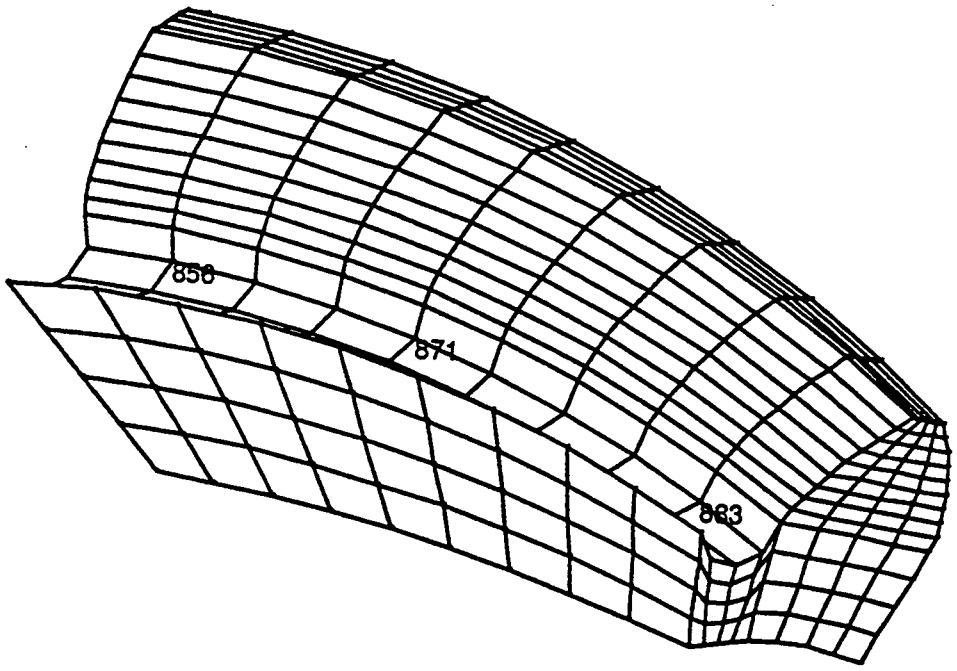

Pinion Tooth #2

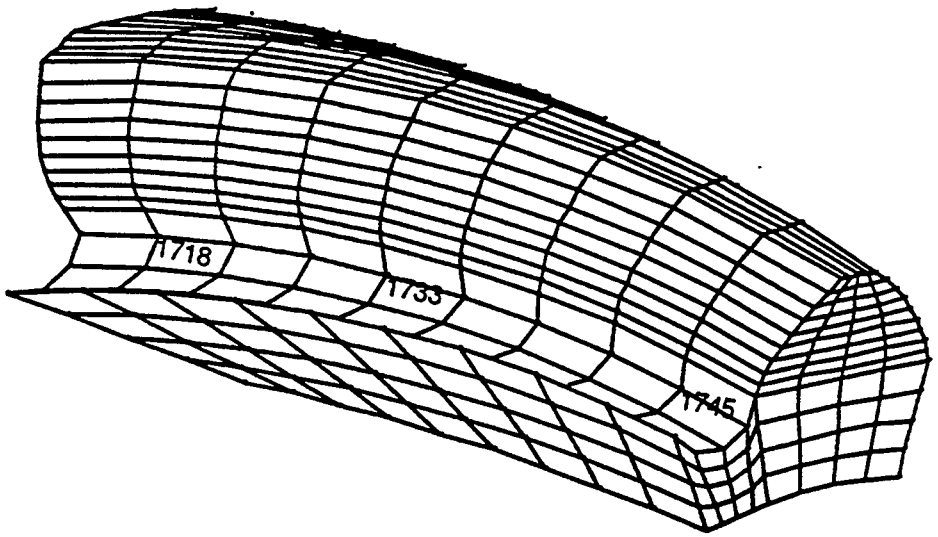

Figure 5.27 Location of Nodes Identified in Table VII.

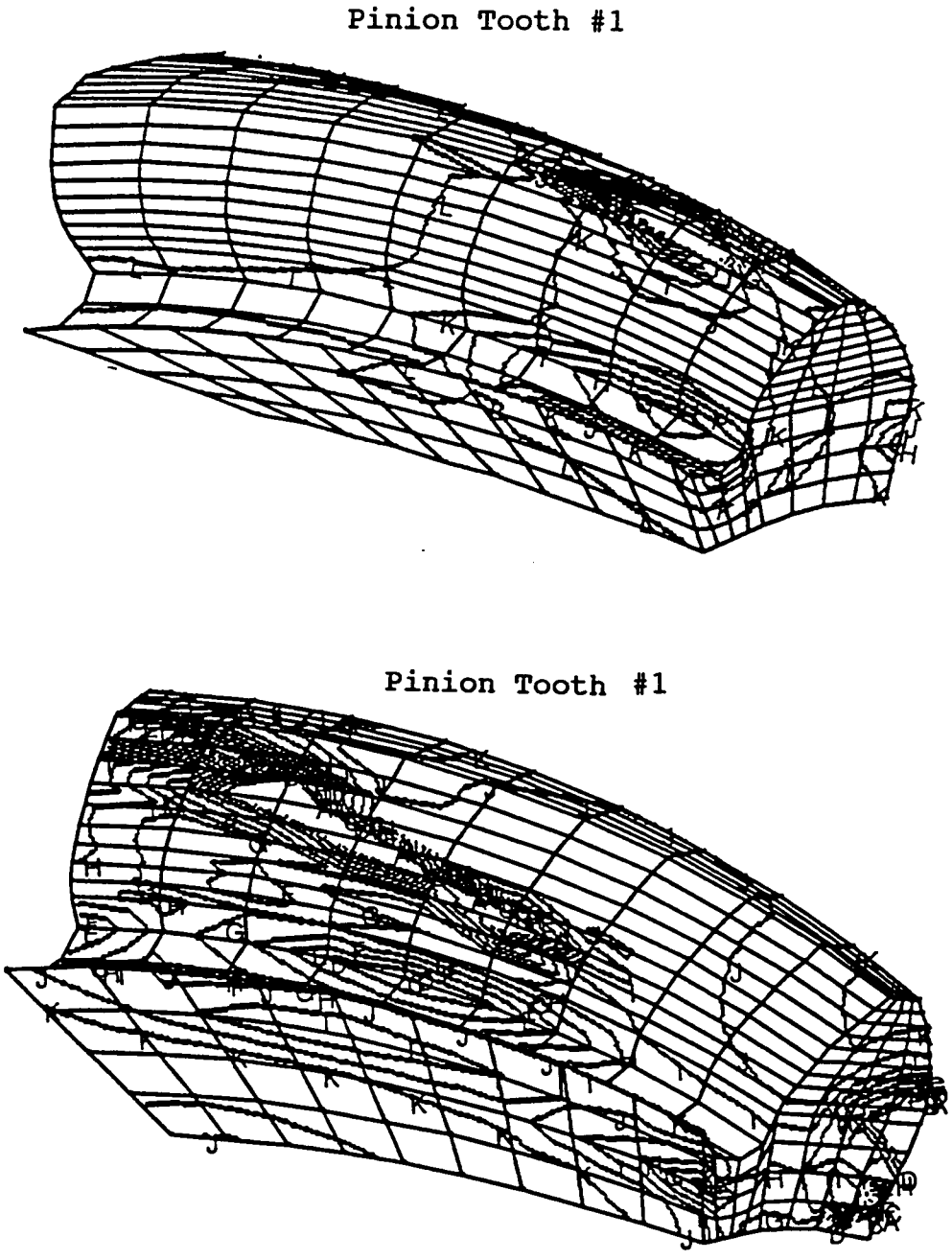

Figure 5.28 Typical fillet stress contours.
Shown for -6 degree rotation of pinion

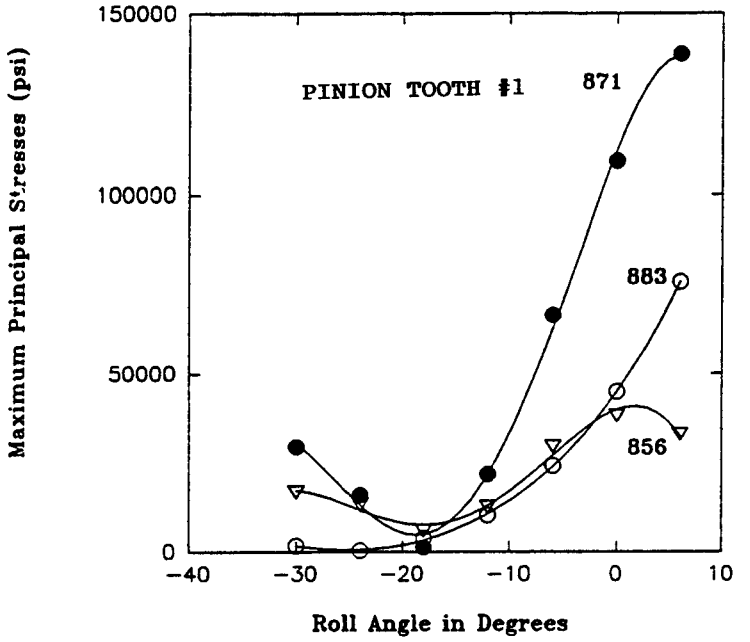

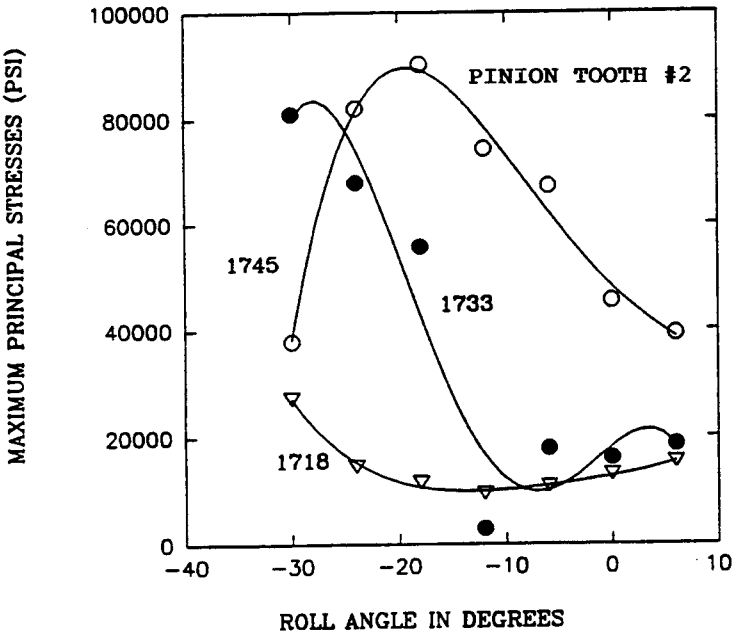

Figure 5.29 Fillet Stresses as a Function of Rotation

APPENDIX A

MARC INPUT DATA

```
TITLE      BULK DATA CARDS PRODUCED BY PATMAR RELEASE 3.1A
TITLE      20-Jul-93    15:14
TITLE      OPTIMIZED 7TEETH MODEL
$ *** PARAMETER CARDS ***
$...!....1....!....2....!....3....!....4....!....5....!....6....!....7....!....8
SIZING      28500000     ...     this allocates workspace storage memory
SETNAME     200          ...     defines max. no of items in DEFINE sets
ELEMENTS      7          ...     element type is 8 noded hexahedral
PRINT,5                  ...     gives extra information about contact nodes
ELSTO                    ...     reduces in-core memory by storing elements out-of-core
END                      ...     signifies end of parameter cards
$ *** CONTROL CARDS FOR POST-PROCESSOR TAPE ***
$ --- SPECIFY POST CODES AND LABELS FOR EACH ELEMENT VARIABLE.
$...!....1....!....2....!....3....!....4....!....5....!....6....!....7....!....8
POST
$ 1 in 20th column gives formatted post file which is readable on different m/c's
$ 4 shows the frequency at which POST data is written
    3              1    1                    4
   17     VON MISES STRESS
  131     MAXIMUM PRINCIPAL STRESS
  133     MINIMUM PRINCIPAL STRESS
$ *** MODEL DEFINITION CARDS ***
$ --- SPECIFY DISPLACEMENTS AND THE ASSOCIATED DOFS AND NODES FOR EACH SET.
$...!....1....!....2....!....3....!....4....!....5....!....6....!....7....!....8
FIXED DISP
    3                                    ...     three sets of displacement data
      0.0                                ...     prescribed displacement
    3                                    ...     Z direction constrained
 2952 2961 2992 3016 8500 8581 9680 9761         ...     list of nodes on gear
      0.0       0.0       0.0
    1    2    3                          ...     X/Y/Z directions constrained
 7872                                    ...     pivot node on hub
      0.0       0.0       0.0
    1    2    3
  259  263  364  380 2317 2333 2528 2561         ...     list of pinion nodes
$
$ --- A NAMED SET MUST BE DEFINED BEFORE ITS NAME IS USED IN THE INPUT DECK.
$...!....1....!....2....!....3....!....4....!....5....!....6....!....7....!....8
$Element set GEARE is th list of elements of named component GEAR in PATRAN
DEFINE    ELEMENT   SET          GEARE
 1837 1838 1839 1840 1841 1842 1843 1844 1845 1846 1847 1848 1849 1850 1851    C
 7426 7427 7428 7429 7430 7431 7432 7433 7434 7435 7436 7437 7438 7439 7440    C
 7441 7442 7443
$Defines PINION elements
DEFINE    ELEMENT   SET        PINIONE
    1    2    3    4    5    6    7    8    9   10   11   12   13   14   15    C
 1831 1832 1833 1834 1835 1836
DEFINE    ELEMENT   SET         PROJ2E
 5023 5024 5025 5026 5027 5028 5029 5030 5031 5032 5033 5050 5051 5052 5053    C
 6679 6680 6681 6682 6683 6684 6685 6686 6687
DEFINE    ELEMENT   SET           RIME
 2116 2117 2118 2119 2120 2121 2122 2123 2124 2125 2126 2127 2128 2129 2130    C
 8779 8780 8781 8782 8783 8784 8785 8786 8787 8788 8789 8790 8791 8792 8793
$ --- SPECIFY CONNECTIVITY FOR EACH ELEMENT.
$...!....1....!....2....!....3....!....4....!....5....!....6....!....7....!....8
CONNECTIVITY
$shows total no. of elements in the model, 1 suppresses connectivity printout
 8793         1
```

```
    3    7   54   53    3    4   59   58    8    9
    4    7   55   54    4    5   60   59    9   10
    5    7   57   56    6    7   62   61   11   12
 8791    711246112481125811252112471124911260112 56
 8792    711251112571125411250112551126111259112 53
 8793    711252112581125711251112561126011261112 55
$ --- SPECIFY COORDINATES FOR EACH NODE.
$...!....1....!....2....!....3....!....4....!....5....!....6....!....7....!....8
COORDINATES
$# of directions per node, total no. of nodes, suppression of coordinate listing
    611261         1
    1 -3.429364 -0.538929  1.299387
    2 -3.429364 -0.553653  1.292881
    3 -3.429364 -0.568376  1.286376
    4 -3.429364 -0.583099  1.279870
    5 -3.429364 -0.597823  1.273365
11261 -1.094289 -0.899709  1.786157
$defines material properties
ISOTROPIC
3                          ...     three sets of material properties
1,VON MISES
3.0000E+07,0.3             ...     defines Young's modulus, poisson ratio
$list of elements not nodes...
$LIST OF GEAR AND PINION ELEMENTS...
GEARE AND PINIONE          ...elements defined by ELEMENT SET names
2,VON MISES
3.0000E+10,0.3
$RIM ELEMENTS...
RIME
3,VON MISES
6.0000E+13,0.3
$PRJECTION IN FRONT OF THE HUB..
PROJ2E
SPRINGS
258,1,2671,1,100           ...     1st node, dof, 2nd node, dof, stiffnes
258,2,2671,2,100
258,3,2671,3,100
364,1,2626,1,100
364,2,2626,2,100
364,3,2626,3,100
2528,1,5512,1,100
2528,2,5512,2,100
2528,3,5512,3,100
2317,1,5541,1,100
2317,2,5541,2,100
2317,3,5541,3,100
CONTACT
2,450,450                  ...no. of contacting bodies and entities on their surface
,0.0002,,                  ...contact tolerance defined
1,0                        ...definition of 1st body
,,,
0:,
$list of gear elements not nodes on the contacting surface.......
$GE_4 BACK FACE ELEMENTS..
2902 TO 2904 BY 1 AND 3109 TO 3111 BY 1 AND 3316 TO 3318 BY 4 AND C
3523 TO 3525 BY 1 AND 3730 TO 3732 BY 1 AND C
2666,2670, AND 2673 TO 2685 BY 4 AND 2686 TO 2688 BY 1 AND C
2881 TO 2901 BY 4 AND 3088 TO 3108 BY 4 AND C
3295 TO 3315 BY 4 AND 3502 TO 3522 BY 4 AND C
3709 TO 3729 BY 4 AND 3745 TO 3771 BY 1 AND C
```

```
$GE_5 BACK FACE ELEMENTS...
4180 TO 4182 BY 1 AND 4450 TO 4452 BY 1 AND C
4702 TO 4704 BY 1 AND 4945 TO 4947 BY 1 AND C
5215 TO 5217 BY 1 AND 5485 TO 5487 BY 1 AND C
4159 TO 4179 BY 4 AND 4429 TO 4449 BY 4 AND C
4681 TO 4701 BY 4 AND 4924 TO 4944 BY 4 AND C
5194 TO 5214 BY 4 AND 5464 TO 5484 BY 4 AND C
5734 TO 5739 BY 1 AND 5806 TO 5811 BY 1 AND C
5740 TO 5742 BY 1 AND 5815 TO 5820 BY 1
2,0                        ...defintion of 2nd body
,,,
0.,
$list of pinion elements not nodes on the contacting surface.......
$PI_1 FRONT FACE ELEMENTS..
4 TO 16 BY 4 AND 40 TO 52 BY 4 AND 76 TO 88 BY 4 AND C
112 TO 124 BY 4 AND 148 TO 160 BY 4 AND 184,195,199,203,C
282,291,300,303,362,369,376,383,460,465,470,475,C
20,27,32,35,36,56,63,68,71,72,92,99,104,107,108, AND C
128,135,140,143,144,164,171,176,179,180,AND C
207,214,219,222,223,306,309,314,317,318,AND C
385,387,389,392,393, AND 480 TO 484 BY 1 AND C
$PI_2 FRONT FACE ELEMENTS...
508 TO 520 BY 4 AND 580 TO 592 BY 4 AND 652 TO 664 BY 4 AND C
726 TO 738 BY 4 AND 796,807,811,815,903,912,915,988,995,C
443,450,455,458,459,524,531,536,539,540, AND C
596,603,608,611,612,668,675,680,683,684, AND C
742,749,754,757,758,819,826,831,834,835, AND C
918,921,928,929,930,997,999,1001,1004,1005, AND C
1092 TO 1096 BY 1
CONTACT TABLE
1                          ...one set of bodies defined
1                          ...body1 is contacting
2                          ...body2 is contacted
OPTIMIZE,2,,,,1            ...Cuthill Mckeee bandwidth optimizer is used
20,
CONTROL                    ...sets controls for iterations
$# of increments, max. # of recycles, min. # of recycles, residual checking invoked,..
,5,0,1,0,,
.15
RESTART                    ...optional restart command
1,2
PRINT ELEM
1,2
STRAIN,STRESS
1 TO 8793

PRINT NODE
1,2
LOAD,REAC,TOTA,STRESS
$CONSTRAINT POINTS...
7872,2952,2961,2992,3016,8500,8581,9680,9761, C
259,263,364,380,2317,2333,2528,2561, AND C
$PI_1 FRONT FACE NODES...
5 TO 20 BY 5 AND 55 TO 70 BY 5 AND 105 TO 120 BY 5 AND C
155 TO 170 BY 5 AND 205 TO 220 BY 5 AND 255,268,273,278,C
384,395,406,410,493,502,511,520,632,639,646,653,751,AND C
25 TO 225 BY 50 AND 34 TO 234 BY 50 AND C
41 TO 241 BY 50 AND 46 TO 246 BY 50 AND C
49 TO 249 BY 50 AND 50 TO 250 BY 50 AND C
283,292,299,304,307,308,414,418,425,430,433,434,761,756,C
```

```
523,526,529,534,537,538, AND 660 TO 670 BY 2 AND C
770 TO 780 BY 2 AND C
$PI_2 FRONT FACE NODES...
585 TO 605 BY 5 AND 614,621,626,629,630, AND C
705 TO 725 BY 5 AND C
805 TO 825 BY 5 AND C
905 TO 925 BY 5 AND C
734 TO 934 BY 100 AND C
741 TO 941 BY 100 AND C
746 TO 946 BY 100 AND C
749 TO 949 BY 100 AND C
750 TO 950 BY 100 AND C
1009 TO 1029 BY 5 AND C
1038,1045,1050,1053,1054,1117, AND C
1130 TO 1145 BY 5,AND 1154,1161,1166,1169,1170, AND C
1246,1257,AND 1268 TO 1280 BY 4 AND 1287,1292,1295,1296, AND C
1355,1364,1373,1382,1385,1388,1391,1396,1399,1400, AND C
1494,1501,1508,1515,AND 1522 TO 1528 BY 2 AND 1531,1532, AND C
1613,1618,AND 1623 TO 1638 BY 5 AND 1639 TO 1642 BY 1 AND C
$GE_4 BACK FACE NODES...
3678 TO 3681 BY 1 AND 3948 TO 3951 BY 1 AND C
4198 TO 4201 BY 1 AND 4448 TO 4451 BY 1 AND C
4698 TO 4701 BY 1 AND 4948 TO 4951 BY 1 AND C
3652 TO 3677 BY 5 AND 3922 TO 3947 BY 5 AND C
4172 TO 4197 BY 5 AND 4422 TO 4447 BY 5 AND C
4672 TO 4697 BY 5 AND 4922 TO 4947 BY 5 AND C
4972 TO 5011 BY 1 AND C
$GE_5 BACK FACE NODES...
5488 TO 5491 BY 1 AND 5828 TO 5831 BY 1 AND C
6148 TO 6151 BY 1 AND 6448 TO 6451 BY 1 AND C
6778 TO 6781 BY 1 AND 7108 TO 7111 BY 1 AND C
5462 TO 5487 BY 5 AND 5802 TO 5827 BY 5 AND C
6122 TO 6147 BY 5 AND 6422 TO 6447 BY 5 AND C
6752 TO 6777 BY 5 AND 7082 TO 7107 BY 5 AND C
7412 TO 7421 BY 1 AND 7512 TO 7541 BY 1
ERROR ESTIMATE
1,1
END OPTION                ....terminates model definition cards
$History or Load Definition Cards.....
POINT LOAD

0.0,12.0,0.0
5141
AUTO LOAD
1
TIME STEP
10.0
CONTINUE
POINT LOAD

0.0,2.0,0.0
5141
AUTO LOAD
1
TIME STEP
10.0
CONTINUE
POINT LOAD

0.0,785.0,0.0
```

```
5141
AUTO LOAD
6
TIME STEP
10.0
CONTINUE

************************END OF INPUT DECK*********************************
```

APPENDIX B

Description of MARC Commands

The MARC input deck consists of three blocks. They are as follows:

Parameter Cards:

TITLE: It gives the title given to the problem. This problem has the title as "7TEETH MODEL".

SIZING: This specifies the size of the workspace buffer in number of words. This size should be 1.7 Mwords less than that specified in the JCL file. This is required for MARC program to run. Here, it is quite a large value.

ELEMENT: This gives the element type used in the model. The one used here is number 7.

PRINT,5: It is a special printing option. "5" means additional contact analysis information regarding nodes touching or separating from surfaces is given.

END: It signals the end of Parameter Card block.

Model Definition Cards:

These cards contain the FE model data for the analysis. The data represents:-

a) The FE mesh topology - element connectivity, nodal coordinates and sheet thickness.

b) Material properties

c) Loading and boundary conditions

d) Nonlinear analysis control

e) Output controls

f) Contact analysis controls

FE mesh topology

It is defined by the following cards:-

CONNECTIVITY: This defines connectivuty for the elements in the model. A typical card is as illustrated:

1 7 1 2 3 4 5 6 7 8

First number denotes element number.

"7" is the element type. It is HEX 8-noded element.

The last 8 numbers define the connectivity of the element in the counter clockwise direction.

COORDINATES: This gives the coordinates for the nodes in the model. A typical card is:

1 0.0 0.0 0.0

"1" means 1st node number

The other three numbers give the X, Y and Z coordinates of that particular node.

The 2nd card is

6 111 1

"6" means max. number of coordinate directions to be read in per node.

"111" means the total number nodes in the model

"1" in the 20th column suppresses printout of the nodal coordinates in the output file.

ISOTROPIC: This lets one define material properties, a yield criteria,etc.

2nd card:

no. of sets of isotropic material data to follow.

3rd card:

1,VON MISES

"1" is material identification set no.

"VON MISES" is the selected yield criteria

4th card:

3.00E+07,0.3 gives Young's Modulus and poisson ratio

5th card:

1 TO # gives list of elements associated with this material

SPRINGS: They are used to input any simple linear springs.

2nd card:

103,1,51,1,50

"103" gives the node to which 1st end of spring will be attached

"1" gives the DOF at above node to which spring will be attached

"51" gives node to which the other end of the spring will be attached

"1" gives DOF at above node to which spring will be attached

"50" gives the stiffness of the spring.

Loading and Boundary Conditions

FIXED DISP: It is used to prescribe displacement boundary conditions.

2nd Card: No. of sets of boudary condition cards to be defined.

3rd Card:

"0.0,0.0,0.0" give the prescribed displacements for 1st, 2nd and 3rd DOFs

i.e X, Y and Z directions.

4th Card:

1,2

"1" means the X direction DOF

"2" means the Y direction DOF

5th Card:

76,78,82 to 200 by 5..

This gives the list of nodes to which above boundary condition are applied.

These above 3 Cards are repeated as required to define displacement at various nodes.

POINT LOAD:

2nd Card: no. of sets of point loads to be entered. It can be left blank.

Here, it is left blank.

3rd Card:

0.0,10.0,0.0

"0.0" gives nodal load associated with 1st DOF i.e X direction

"10.0" gives nodal load associated with 2nd DOF i.e Y direction

"0.0" gives nodal load associated with 3rd DOF i.e Z direction

4th Card: Gives list of nodes having the point load given above.

"5141" is the node at which load is applied.

Non-linear Analysis Control

CONTROL: It lets one input parameters which control the convergence and accuracy of the non-linear analysis.

2nd Card:

20,5,0,1,0,

"20" means max. no. of load steps

"5" means max. no. of recycles during an increment

"0" min. no. of recycles during an increment

"1" this flags the convergence testing on displacements

"0.0" flags for relative error testing

"blank" default Full Newton Raphson iterative scheme is used

3rd Card:

".15" gives a relative error of 15%

Output Controls

POST: It creates a post processing tape for PATRAN.

2nd Card:

7 1 1 1

"7" is no. of element variable to be written

"1" is in 16-20 column for formatted POST TAPE

"1" in 20-25 column is to write connectivity and coordinates on POST TAPE

"1" in 45 column is to write post data every increment

3rd Card: Gives various post codes

11-16 give components of generalised stresses

17 gives Equivalent Von Mises stress

PRINT ELEM: Gives elements at which output is to be printed

2nd Card:

1,2

"1" is no. of sets

"2" is increment between printout. Default is every increment printed.

3rd Card:

"STRAIN STRESS" are values to be printed

4th Card:

1 TO 44 is the list of elements to be printed

5th Card: it lists integration points.

PRINT NODE: gives information on nodal printout

2nd Card:

1,2

"1" is no. of sets

"2" is increment between printout. Default is every increment printed.

3rd Card:

"TOTA,LOAD,STRESS" are values to be printed

4th Card:

50 TO 85 is the list of nodes to be printed

ERROR ESTIMATE: It gives error associated with FE discretization. Large values indicate stress gradients are not accurately represented.

2nd Card:

1,1

"1" in 1-5 column is for stress measure to be evaluated

"1" in 6-10 column is for geometric measure to be evaluated

SUMMARY: Gives the summary of output

Contact analysis controls

CONTACT: Allows one to perform automated contact analysis without use of GAP elements for rigid to deformable contact as well as deformable to deformable contact. Here, it is deformable-deformable contact.

2nd Card:

2,60,60

"2" tells two surfaces (bodies) will be defined

"60" shows there are max. of 60 entities to be created for any body

"60" shows max. no. of nodes that lie on the deformable surface

3rd Card:

,0.001, gives the distance below which node is considered touching a surface

04th Card:

1,0

"1" 1st body

"0" implies deformable body

5th Card and 6th Card:

blank

7th Card:

17 TO 32 gives list of elements for body one.

8th TO 11th Card are repeated as above from 6th Card

CONTACT TABLE: It is used for deactivating or activating bodies when the CONTACT option is used.

2nd Card:

"1" no. of sets of bodies to be input

3rd Card:

"1" gives the touching body number

4th Card:

"2" list of bodies for which the above body will detect contact

OPTIMIZE: It allows a choice of bandwidth optimizers to be invoked . Is helpful in reducing the bandwidth

1st Card:

OPTIMIZE,4,,,1

"4" shows that Wavefront algorithm based on connectivity followed by Grooms algorithm is used. It is an effective technique for 3-D (complex) meshes.

2nd Card:

1 TO 44 gives list of elements

3rd Card:

"3" gives acceptable half-bandwidth at which it should exit down the iteration loop.

Load Incrementation Cards:

TIME STEP: Allows user to prescribe time step for static analysis

2nd Card:

"10" means time step of 10 sec

AUTO LOAD: It describes number of equal load steps applied

2nd Card:

"2" shows 2 equal load increments

CONTINUE: This terminates Load Incrementation or History Definition Cards.

APPENDIX C

JCL AND USER SUBROUTINE

The JCL file

```
# USER=tobibel PW=tobibel
# QSUB -r kt7tr0                .....requester's name could be different from user
# QSUB -lT 10800                .....CPU time requested
# QSUB -lM 30.2Mw               .....memory size requested
# QSUB -eo
# QSUB -q systems               .....written only for priority systems queue
set -x
ja
news                            .....gives news about MARC
dir=/hogs/tobibel/7teeth        .....defines where the input file is present
job=7tr0                        .....shows the job name
cd $dir                         .....changes to the directory where input file is present
rm $dir/$job.lst $dir/$job.post .....deletes old output and post files before beginning new run
ls -alp
marc=/wrk/vvmarc/marcK5/marc    .....defines the directory where MARC is accessed from
$
$Accesses MARC, defines input file, output file, and post file
$If RESTART option is used, then output restart file is written
$and also for subsequent restart the input restart file is mentioned
$
$marc  i=$job.marc  o=$job.lst  patran=$job.post  orestart=$job.rest1  usub=$job.f   news=no
ls -alp
ja -st
```

```
      SUBROUTINE INLIST
*****************************************************************************
*                                                                           *
*  MARC USER SUBROUTINE TO DISABLE ECHO PRINTING OF THE INPUT DATA.         *
*                                                                           *
*****************************************************************************
C
      WRITE (6,6000)
C
      RETURN
C
 6000 FORMAT ( 2(/),' ENTRY TO "INLIST" USER SUBROUTINE',6X,90('='),
     &         2(/),5X,'ECHO OF THE INPUT DATA HAS BEEN DISABLED',
     &         2(/),' EXIT FROM "INLIST" USER SUBROUTINE',5X,90('='),/ )
      END
```

APPENDIX F

IMPORTANT OUTPUT LISTING

MARC-CRAY K5-1-L

MARC ANALYSIS RESEARCH CORPORATION

NORTH AMERICAN EUROPE PACIFIC RIM

TRY TO "INLIST" USER SUBROUTINE ==========

ECHO OF THE INPUT DATA HAS BEEN DISABLED

IT FROM "INLIST" USER SUBROUTINE ==========

****
****

program sizing and options requested as follows

element type requested	7
number of elements in mesh	1304
number of nodes in mesh	1980
max number of elements in any dist load list	0
maximum number of boundary conditions	35
load correction flagged or set	
number of lists of distributed loads	3
element out of core storage flagged,buffer size	4096
option for debug print out	1
stresses stored at all integration points	
tape no.for input of coordinates + connectivity	5
no. of simple linear springs	12
no.of different materials 2 max.no of slopes	5
maximum elements variables per point on post tp	33
number of points on shell section	11
option for terminal debug	
new style input format will be used	
maximum number of set names is	10
number of processors used	1
vector length used	1

end of parameters and sizing

****
****

key to stress, strain and displacement output

element type 7

8-node isoparametric brick

stresses and strains in global directions
1=xx
2=yy
3=zz
4=xy
5=yz
6=xz

displacements in global directions
1=u global x direction
2=v global y direction
3=w global z direction

workspace needed for input and stiffness assembly 191452

internal core allocation parameters
degrees of freedom per node (ndeg) 3
coords per node (ncrd) 3
strains per integration point (ngens) 6
max. nodes per element (nnodmx) 8
max.stress components per int. point (nstrmx) 6
max. invariants per int. points (neqst) 1

flag for element storage (ielsto) 1
elems out of core, words per elem (nelsto) 1302
elems per buffer (mxels) 3

out-of-core space needed for element storage = 1699110 based on record size of 3906
vectors in core, total space required 93060

words per track on disk set to 4096

internal element variables

```
                internal element number  1  library code type  7
                number of nodes=  8
                stresses stored per integration point =  6
                direct continuum components stored =  3
                shear continuum components stored =  3
                shell/beam flag = 0
                curvilinear  coord. flag = 0
                int.points for elem. stiffness  8
                number of local inertia directions  3
                int.point for print if all points not flagged  9
                int. points for dist. surface loads (pressure)  4
                library code type =  7
                no local rotation flag = 1
                generalized displ. flag = 0
                large disp. row counts     6    6    6   11   11   11


                residual load correction is invoked

$ *** control cards for post-processor tape ***
$ --- specify post codes and labels for each element variable.
$...!....1....!....2....!....3....!....4....!....5....!....6....!....7....!....8

post
----------


*** note - format of post code cards has changed.
           in k4, enter code in first field and  layer number in second field

elem vars,post tape,prev tape,  type  , conn fl ,post tape, prev tape,  repost ,frequency, k2post
        4        16        17         1         1        19        20         0         3         0
element variables appear on post-processor tape 16 in following order
post variable   1 is post code   17 = von mises stress
post variable   2 is post code  131 = maximum principal stress
post variable   3 is post code  133 = minimum principal stress
$ *** model definition cards ***
$ --- specify components for each load and the nodes where it is applied.
$...!....1....!....2....!....3....!....4....!....5....!....6....!....7....!....8
$point load
$    1
$       0.0    10.000        0.0        0.0        0.0        0.0
$1824
$ --- specify displacements and the associated dofs and nodes for each set.
$...!....1....!....2....!....3....!....4....!....5....!....6....!....7....!....8

***maximum record length on formatted post file=   80     approximate no. of records per increment on file=
```

```
fixed disp
----------

fixed displacement =  0.000E+00  0.000E+00  0.000E+00
a list of degrees of freedom given below
     3
a list of nodes given below
   905   1355   1440   1600   1604   1620   1784   1800
fixed displacement =  0.000E+00  0.000E+00  0.000E+00

a list of degrees of freedom given below
     1      2      3
a list of nodes given below
  1976
fixed displacement =  0.000E+00  0.000E+00  0.000E+00
a list of degrees of freedom given below
     1      2      3
a list of nodes given below
    15    455    520    700    724    740    884    900


fixed boundary condition summary.
total fixed degrees of freedom read so far =   35

 b.c.    node   degree of  magnitude              b.c.    node   degree of  magnitude
number          freedom                        number          freedom

    1     905         3    0.000E+00                2    1355         3    0.000E+00
    3    1440         3    0.000E+00                4    1600         3    0.000E+00
    5    1604         3    0.000E+00                6    1620         3    0.000E+00
    7    1784         3    0.000E+00                8    1800         3    0.000E+00
    9    1976         1    0.000E+00               10    1976         2    0.000E+00
   11    1976         3    0.000E+00               12      15         1    0.000E+00
   13      15         2    0.000E+00               14      15         3    0.000E+00
   15     455         1    0.000E+00               16     455         2    0.000E+00
   17     455         3    0.000E+00               18     520         1    0.000E+00
   19     520         2    0.000E+00               20     520         3    0.000E+00
   21     700         1    0.000E+00               22     700         2    0.000E+00
   23     700         3    0.000E+00               24     724         1    0.000E+00
   25     724         2    0.000E+00               26     724         3    0.000E+00
   27     740         1    0.000E+00               28     740         2    0.000E+00
   29     740         3    0.000E+00               30     884         1    0.000E+00
   31     884         2    0.000E+00               32     884         3    0.000E+00
   33     900         1    0.000E+00               34     900         2    0.000E+00
   35     900         3    0.000E+00
$ --- specify connectivity for each element.
$...!....1....!....2....!....3....!....4....!....5....!....6....!....7....!....8
```

```
connectivity
----------

meshrl,iprnt
     5       1
elem no., type,        nodes
$ --- specify coordinates for each node.
$...!....1....!....2....!....3....!....4....!....5....!....6....!....7....!....8

coordinates
----------

ncrdl ,meshrl,iprnt
     3       5       1
 node       coordinates

isotropic
----------

isotropic material  material id =      1
 von mises  yield criteria
 isotropic  hardening rule
    e            nu          rho         alpha         yield        yield2
  0.300E+08  0.300E+00  0.000E+00  0.000E+00  0.100E+21  0.100E+21
from element      1 to element  1224 by      1

isotropic material  material id =      2
 von mises  yield criteria
 isotropic  hardening rule
    e            nu          rho         alpha         yield        yield2
  0.300E+11  0.300E+00  0.000E+00  0.000E+00  0.100E+21  0.100E+21
from element   1225 to element  1304 by      1

springs
----------


spring  node    degree   node    degree    spring   damping
number          freedom          freedom   force     force

   1      11       1      995       1     1.000E+02 0.000E+00
   2      11       2      995       2     1.000E+02 0.000E+00
   3      11       3      995       3     1.000E+02 0.000E+00
   4      96       1      905       1     1.000E+02 0.000E+00
   5      96       2      905       2     1.000E+02 0.000E+00
   6      96       3      905       3     1.000E+02 0.000E+00
   7     451       1     1400       1     1.000E+02 0.000E+00
   8     451       2     1400       2     1.000E+02 0.000E+00
   9     451       3     1400       3     1.000E+02 0.000E+00
  10     496       1     1355       1     1.000E+02 0.000E+00
  11     496       2     1355       2     1.000E+02 0.000E+00
  12     496       3     1355       3     1.000E+02 0.000E+00
```

contact
---

number of bodies	=	2
max number of entities per body	=	250
bound on number of boundary nodes	=	250
friction type(1-m , 2-coulomb)	=	0
distrib-0 or nodal-1 coul. frict	=	0
relative velocity below which a node is considered sticking	=	0.00000E+00
distance below which a node is considered touching a surface	=	0.00000E+00
nodal reaction above which a node separates from a body	=	0.00000E+00
body number	=	1
number of sets of data	=	0

body positioning data

1st coordinate of center of rotation	0.00000
2nd coordinate of center of rotation	0.00000
3rd coordinate of center of rotation	0.00000
1st component of velocity	0.00000
2nd component of velocity	0.00000
3rd component of velocity	0.00000

body positioning data continue

angular velocity	0.00000
total angle rotated around axis	0.00000
1st component of directional cosine	0.00000
2nd component of directional cosine	0.00000
3rd component of directional cosine	0.00000
friction coefficient	0.00000

from element 616 to element 936 by 4

body number	=	2
number of sets of data	=	0

body positioning data

1st coordinate of center of rotation	0.00000
2nd coordinate of center of rotation	0.00000
3rd coordinate of center of rotation	0.00000
1st component of velocity	0.00000
2nd component of velocity	0.00000
3rd component of velocity	0.00000

body positioning data continue

angular velocity	0.00000
total angle rotated around axis	0.00000
1st component of directional cosine	0.00000
2nd component of directional cosine	0.00000
3rd component of directional cosine	0.00000
friction coefficient	0.00000

```
from element     1 to element   321 by     4
      and
a list of elements given below
   325    341    351    373    389    405
   421    437    597

contact table
----------

     2

flexible body number    1 and flexible body number    2 will be detected by each other

optimize,2,,,,1
----------


cuthill-mckee algorithm

control
----------

max.     max.     min.
incs   recycles recycles
  240        5        0

maximum allowed relative error in residual forces      0.15000E+00

full newton-raphson technique chosen

restart
----------

iwhich,incbrs,incrs,out no.,in no.,itri,ireprt,ilasti,incsur,ilasts
    1     4     0     8        9     0      0      0      0      0

print elem
----------

values will be printed at integration points

element quantities printed every    4 increments

strain,stress
from element   616 to element   936 by     4
      and
from element     1 to element   321 by     4
      and
a list of elements given below
   325    341    351    373    389    405
   421    437    597
```

```
print node
----------

number of sets used for selective print of nodal quantities is    1

nodal quantities printed every    4 increments

reac,tota,stress
from node     1 to node   491 by    10
       and
from node     6 to node   496 by    10
       and
from node   701 to node   781 by    20
       and
from node   801 to node   881 by    20
       and
from node   905 to node  1400 by     5

error estimate
----------

stress discontinuity will be evaluated
geometric distortion will be evaluated

end option
----------

                maximum connectivity is   18  at node  745

                workspace needed for optimizing =    248979

                maximum connectivity is   24  at node 1980


                maximum half-bandwidth is  222  between nodes 1500  and 1721
                 number of profile entries including fill-in is     224672
                 number of profile entries excluding fill-in is      21392
* * * * * * * * * * *

 distance below which a node is considered
 touching a surface is                      2.51180E-03

* * * * * * * * * * *

                total workspace needed with in-core matrix storage =   2246772
```

restart information

...file 8-- maximum record length= 83160
approximate no. of words on file per increment= 1867308

sliding velocity below which sticking is considered 0.10000E+05

warning: input data was not enough for this value to be calculated.
results may be wrong if friction calculations are being made.

load increments associated with each degree of freedom
summed over the whole model

distributed loads
0.000E+00 0.000E+00 0.000E+00

point loads
0.000E+00 0.000E+00 0.000E+00

increment zero is a null step

worst original aspect ratio is 10.003 at element 324
worst original warpage ratio is 2.050 at element 289

worst current aspect ratio is 10.003 at element 324
worst current warpage ratio is 2.050 at element 289

largest change in aspect ratio is 1.000 at element 20
largest change in warpage ratio is 1.000 at element 13

g e n e r a l i z e d s t r e s s e s

1	0.00000E+00	0.00000E+00	0.00000E+00	0.00000E+00	0.00000E+00	0.00000E+00
6	0.00000E+00	0.00000E+00	0.00000E+00	0.00000E+00	0.00000E+00	0.00000E+00
11	0.00000E+00	0.00000E+00	0.00000E+00	0.00000E+00	0.00000E+00	0.00000E+00

forces in linear springs

spring no.	node1	dof1	node2	dof2	force
1	11	1	995	1	0.0000E+00
2	11	2	995	2	0.0000E+00
3	11	3	995	3	0.0000E+00
4	96	1	905	1	0.0000E+00
5	96	2	905	2	0.0000E+00
6	96	3	905	3	0.0000E+00
7	451	1	1400	1	0.0000E+00
8	451	2	1400	2	0.0000E+00
9	451	3	1400	3	0.0000E+00
10	496	1	1355	1	0.0000E+00
11	496	2	1355	2	0.0000E+00
12	496	3	1355	3	0.0000E+00

e n d o f i n c r e m e n t 0

restart data at increment 0. 0 on tape 8

formatted post data at increment 0. 0 on tape 19
time = 15.67

point load
---

read from unit 5
0.000E+00 0.600E+01 0.000E+00
a list of nodes given below
1732

auto load
---

iotnum,incasm
1 0

time step
---

time increment = 10.00000

continue
---

equal load incs specified for 1 increments

s t a r t o f i n c r e m e n t 1

load increments associated with each degree of freedom
summed over the whole model

distributed loads
0.000E+00 0.000E+00 0.000E+00

point loads
0.000E+00 6.000E+00 0.000E+00

start of assembly
 time =   16.04

start of matrix solution
 time =   21.51

singularity ratio   6.3282E-04

end of matrix solution
 time =   33.11

maximum residual force at node 1805 degree of freedom   2 is equal to   0.112E-04
maximum reaction force at node 455 degree of freedom   2 is equal to   0.263E+01
convergence ratio   0.426E-05

separation force required is   0.11210E-04

MARC-CRAY K5-1, 08/13/93, output for increment   1.   with 2 prop.ids

total transient time = 1.00000E+01

```
worst  current aspect  ratio is 10.004 at element   324
worst  current warpage ratio is  2.050 at element   289

largest change in aspect  ratio is  1.000 at element   936
largest change in warpage ratio is  1.000 at element   940

largest normalized stress jump is  0.79283E+12 at node  1442 component     4 mean value is  0.48236E-10

          largest stress jump is  0.25036E+04 at node   479 component     1 mean value is -0.10067E+04

               e n d   o f   i n c r e m e n t   1
                time =      41.53

point load
----------

read from unit     5
 0.000E+00 0.200E+01 0.000E+00
a list of nodes given below
  1732

auto load
----------


iotnum,incasm
    3    0

time step
----------

time increment =     10.00000

continue
----------


equal load incs specified for   3  increments


                    s t a r t   o f   i n c r e m e n t   2


  node 1260 is touching body   2 patch   149
          the patch it touches is    149
          the internal node numbers for it are    391   396   346   341
the normal vectors are          -0.73027        0.67742        -0.08839
  node 1210 is touching body   2 patch   126
          the patch it touches is    126
          the internal node numbers for it are    336   341   291   286
the normal vectors are          -0.70847        0.69556        -0.11947
```

3	11	3	995	3	-0.1869
4	96	1	905	1	0.2886
5	96	2	905	2	1.800
6	96	3	905	3	-6.9383E-03
7	451	1	1400	1	-2.7481E-02
8	451	2	1400	2	2.121
9	451	3	1400	3	-6.1306E-02
10	496	1	1355	1	-0.1154
11	496	2	1355	2	2.109
12	496	3	1355	3	-0.1131

e n d o f i n c r e m e n t 8

restart data at increment 8. 0 on tape 8
time = 352.85

*** end of input deck - job ends

marc exit number 3004

REPORT DOCUMENTATION PAGE

Form Approved
OMB No. 0704-0188

1. AGENCY USE ONLY (*Leave blank*)	2. REPORT DATE	3. REPORT TYPE AND DATES COVERED
	April 1994	Final Contractor Report

4. TITLE AND SUBTITLE

Prediction of Contact Path and Load Sharing in Spiral Bevel Gears

5. FUNDING NUMBERS

WU–505–62–36
1L162211A47A

6. AUTHOR(S)

George D. Bibel, Karuna Tiku, and Ashok Kumar

7. PERFORMING ORGANIZATION NAME(S) AND ADDRESS(ES)

University of North Dakota
Grand Forks, North Dakota 58201

8. PERFORMING ORGANIZATION REPORT NUMBER

E–8711

9. SPONSORING/MONITORING AGENCY NAME(S) AND ADDRESS(ES)

Vehicle Propulsion Directorate
U.S. Army Research Laboratory
Cleveland, Ohio 44135–3191
and
NASA Lewis Research Center
Cleveland, Ohio 44135–3191

10. SPONSORING/MONITORING AGENCY REPORT NUMBER

NASA CR–195305
ARL–CR–146

11. SUPPLEMENTARY NOTES

George D. Bibel, University of North Dakota; and Karuna Tiku and Ashok Kumar, University of Akron, Akron, Ohio 44325 (work funded by NAG3–1476). Project Manager, Robert F. Handschuh, Propulsion Systems Division, organization code 2730, (216) 433–3969.

12a. DISTRIBUTION/AVAILABILITY STATEMENT

12a. DISTRIBUTION/AVAILABILITY STATEMENT

Unclassified - Unlimited
Subject Category 37

12b. DISTRIBUTION CODE

13. ABSTRACT ***(Maximum 200 words)***

A procedure is presented to perform a contact analysis of spiral bevel gears in order to predict the contact path and the load sharing as the gears roll through mesh. The approach utilizes recent advances in automated contact methods for nonlinear finite element analysis. A sector of the pinion and gear is modeled consisting of three pinion teeth and four gear teeth in mesh. Calculation of the contact force and stresses through the gear meshing cycle are demonstrated. Summary of the results are presented using 3-dimensional plots and tables. Issues relating to solution convergence and requirements for running large finite element analysis on a supercomputer are discussed.

14. SUBJECT TERMS

Gears; Transmission; Finite element

15. NUMBER OF PAGES

117

16. PRICE CODE

A06

17. SECURITY CLASSIFICATION OF REPORT	18. SECURITY CLASSIFICATION OF THIS PAGE	19. SECURITY CLASSIFICATION OF ABSTRACT	20. LIMITATION OF ABSTRACT
Unclassified	Unclassified		